Water Masses in the Atlantic Ocean based on GLODAPv2 dataset: Overview of Characteristics, Distributions and Estimation of mean Transport Time

Dissertation

zur Erlangung des Doktorgrades
der Mathematisch-Naturwissenschaftlichen Fakultät
der Christian-Albrechts-Universität zu Kiel

vorgelegt von

Mian LIU

Kiel, März 2019

Erste Gutachter: Prof. Dr. rer. nat. Arne Körtzinger

Zweiter Gutachter: Prof. Dr. rer. nat. Hermann Bange

Tag der mündlichen Prüfung: 08.05.2019

Zum Druck genehmigt:

08.05.2019

gez.

Eidesstattliche Erklärung:

Hiermit erkläre ich, Mian Liu, dass ich diese Doktorarbeit, abgesehen durch die Beratung meiner Betreuer, selbstständig verfasst, sowie alle wörtlichen und inhaltlichen Zitate als solche gekennzeichnet habe.

Die Arbeit wurde unter Einhaltung der Regeln guter wissenschaftlicher Praxis der Deutschen Forschungsgemeinschaft verfasst.

Sie hat weder ganz, noch in Teilen, einer anderen Stelle im Rahmen eines Prüfungsverfahrens vorgelegen, ist nicht veröffentlicht und auch nicht zur Veröffentlichung eingereicht. Und Kein akademischer Titel von mir wurde jemals annulliert.

Kiel, März 2019

gez. Mian Liu

Zusammenfassung:

Die Eigenschaften des Meerwassers im Ozean sind nicht gleichmäßig verteilt. Merkmale in verschiedenen Regionen und Tiefen unterscheiden sich erheblich. Das Verständnis der Verteilung und Variation von Meerwasser spielt eine wichtige Rolle bei der Untersuchung der thermohalinen Zirkulation des Weltmeers oder der Vorhersage von Klimaänderungen. Ein Meerwasserkörper, der aus einem bestimmten Gebiet stammt und eine gemeinsame Formationsgeschichte aufweist, hat immer ähnliche Eigenschaften, und ein solcher Wasserkörper wird als Wassermasse definiert. Der Quellwassertyp definiert die Eigenschaften der ursprünglichen Wassermasse im Formationsbereich. Die Eigenschaften der Wassermassen bleiben nicht konstant, sondern verändern sich entlang des Fließweges aufgrund biogeochemischer Änderungen und auch aufgrund der Vermischung mit umgebenden Wassermassen, so dass die Optimal Multiparameter (OMP)-Methode zur Untersuchung der Verteilung der Wassermassen erforderlich ist. Bei der OMP-Methode werden die besten Komponenten und Anteile von mehr Wassermassen berechnet, indem die Wassereigenschaften (potentielle Temperatur, Salzgehalt, Sauerstoff, Phosphatnitrat und Silicat in dieser Studie) analysiert und die Gleichungen des linearen Mischens ohne Annahmen gelöst werden. Mit den Anwendungen von transienten Tracern (wie: CFC-12 und SF_6) können Wassermassen markiert und ihr mittleres Alter (Zeitaufwand während des Pfads vom Formationsbereich) berechnet werden. Durch die Kombination der Verteilungen und des Durchschnittsalters können die Transportzeit und die Geschwindigkeiten der Wassermassen geschätzt werden.

Das Hauptziel dieser Arbeit ist es, die Verteilungen und Transporte der Hauptwassermassen im Atlantik in den letzten Jahrzehnten auf der Grundlage der Beobachtungsdaten aus dem Global Ocean Data Analysis Project version 2 (GLODAPv2) Datensatz abzubilden und so den hydrologischen Hintergrund und die theoretische Grundlage für weitere biogeochemische Forschung (z. B.) zu schaffen : der Lüftungsprozess oder der anthropogene Kohlenstoffkreislauf) im gesamten atlantischen Maßstab.

Im Allgemeinen sind die Wassersäulen im Atlantik in vier vertikale Schichten unterteilt, basierend auf der potentiellen Dichte. Die obere Schicht hat die niedrigste potentielle Dichte von weniger als 27,0 $kg \cdot m^{-3}$ und enthält vier zentrale Wassermassen, darunter East North Atlantic Central Water (ENACW), West North Atlantic Central Water (WNACW), East South Atlantic Central Water (ESACW) und West South Atlantic Central Water (WSACW). Die zentralen Gewässer werden während der Subduktion im Winter gebildet und dominieren die obere Schicht mit der linearen T-S-Beziehung als gemeinsames bemerkenswertes Merkmal. Ihre Formationen und Transporte werden von den Strömungen in der flachen Schicht beeinflusst und bilden schließlich innerhalb von 1200 m ein relativ ausgeprägtes Gewässer. Im Allgemeinen sind zentrale Gewässer in den Regionen näher an ihren Formationsgebieten verteilt, und in der vertikalen Skala haben östliche zentrale Gewässer

(ENACW und ESACW) eine relativ höhere potentielle Dichte und liegen unterhalb der westlichen zentralen Gewässer (WNACW und WSACW). In Bezug auf die Zeit haben Zentralgewässer auch das niedrigste Durchschnittsalter innerhalb von 50 Jahren. Das bedeutet, dass sie während ihrer Formationen und Transporte keine komplizierten Ausbreitungsprozesse durchmachen mussten.

Die Zwischenschicht befindet sich unter der oberen Schicht mit potentiellen Dichten zwischen 27,0 und 27,7 kg · m^{-3}. Ähnlich wie bei zentralen Wassermassen stammen auch die intermediären Wassermassen aus den Subduktionen, aber tiefer in die Tiefe zwischen 1000-1500 m und Strömungen in dieser Schicht haben offensichtliche Auswirkungen auf die Verteilung und den Transport. Im Atlantik werden zwei Hauptzwischenwassermassen definiert: Subarctic Intermediate Water (SAIW) aus dem Norden und Antarctic Inter Mediater Water (AAIW) aus dem Süden. Beide Wassermassen bilden sich in der Oberfläche der subpolaren Region und sinken auf ihrem Weg in die unteren Breiten. Neben AAIW und SAIW wird Mediterranean Overflow Water (MOW) aufgrund der ähnlichen Dichte und Tiefe auch als intermediäre Wassermasse definiert. Die MOW stammt aus dem Osten des Golfs von Cádiz und breitet sich sowohl nach Norden in das westeuropäische Becken als auch nach Westen aus, um den Mittelatlantikkamm zu passieren. Im Vergleich zu den zentralen Gewässern weisen Zwischengewässer mit ~ 400 Jahren ein viel höheres Durchschnittsalter auf. Dies zeigt, dass sie viel länger brauchen, um sich vom Formationsbereich bis zur endgültigen Verteilungsposition zu verbreiten.

Die tiefe und Überlaufschicht liegt unterhalb der Zwischenschicht mit einer Potentialdichte zwischen 27,7 und 27,88 kg · m-3. North Atlantic Deep Water (NADW), die vorherrschende Wassermasse in dieser Schicht, wird hauptsächlich im Labrador-See und im Irminger-Becken gebildet. Die Bildung von NADW ist das Mischen von Labrador Sea Water (LSW), Iceland-Scotland Overflow Water (ISOW) und Denmark Strait Overflow Water (DSOW). In dieser Studie wird zwischen oberen NADW, die von LSW stammen, und unteren NADW, die von ISOW und DSOW stammen, unterschieden. LSW ist in der Mitteltiefe zwischen 1000 und 2500 m in der Labrador-See-Region vorherrschend, während sowohl DSOW als auch ISOW aus dem arktischen Ozean und den nordischen Meeren stammen. Nach der Bildung breiten sich die oberen und unteren NADW-Gebiete entlang des DWBC im Süden und die Wirbel im Osten aus. Der Transport von NADW ist ein langer Prozess mit einem Durchschnittsalter von ~ 500 Jahren.

Die Bodenschicht, die von Bodenwassermassen eingenommen wird, ist die unterste Schicht der Wassersäule und ist mit potentiellen Dichten von mehr als 27,88 kg · m-3 definiert. Die unteren Wassermassen in dieser Schicht haben ihren Ursprung im Südpolarmeer und zeichnen sich auch durch ihre hohen potentiellen Dichten und Silikatkonzentrationen aus. Antarctic Bottom Water (AABW), das in der Weddell Sea Region gebildet wird, ist die Hauptwassermasse des Bodens durch das Mischen von Circumpolar Deep Water (CDW) und Weddell Sea Bottom Water (WSBW). Nach der Formation breitet sich AABW nach Norden aus und leidet nach dem Überqueren des Äquators an

einer starken Abnahme der Silikatkonzentration. Dies ist der Grund, warum AABW, der den Äquator hinter sich hat, als neue Wassermasse Northeast Atlantic Bottom Water (NEABW) definiert wird. AABW und NEABW dominieren die untere Schicht des Atlantiks und bedecken den größten Boden des Süd- und Nordatlantiks. Der Transport von AABW in Richtung Norden sowie von NADW in Richtung Süden ist ein weiterer langjähriger Prozess mit einem Durchschnittsalter von ~ 500 Jahren.

Abstract:

Properties of seawater in the ocean are not uniformly distributed. Characteristics in different regions and depths are significantly different. Understanding of the distribution and variation of seawater plays an important role in investigating the thermohaline circulation of the world ocean or predicting climate changes. A body of seawater that originates in a particular area and shares a common formation history always has similar properties and such a water body is defined as a water mass. Source water type defines the properties of the original water mass in the formation area. The properties of water masses do not stay constant but change along the flow path due to biogeochemical changes and also due to the mixing with surrounding water masses so that the OMP method is required to investigate the distribution of water masses. The OMP method is to calculate the best components and fractions of more water masses by analyzing water properties (potential temperature, salinity, oxygen, phosphate nitrate and silicate in this study) and solving the equations of linear mixing without assumptions. With the applications of transient tracers (such as: CFC-12 and SF_6), water masses can be labeled and their mean ages (consuming time during the pathway from formation area) are calculated. Combining the distributions and mean ages, the transport time and velocities of water masses can be estimated.

The main goal of this work is to map out the distributions and transportations of main water masses in the Atlantic Ocean in the past few decades based on the observational data from Global Ocean Data Analysis Project version 2 (GLODAPv2) dataset thus providing the hydrological background and theoretical basis for further biogeochemical research (for instance: the ventilation process or anthropogenic carbon cycle) in the whole Atlantic scale.

In general, the water columns in the Atlantic Ocean are divided into four vertical layers based on potential density. The upper layer has the lowest potential density lower than 27.0 $kg \cdot m^{-3}$ and contains four central water masses, including East North Atlantic Central Water (ENACW), West North Atlantic Central Water (WNACW), East South Atlantic Central Water (ESACW) und West South Atlantic Central Water (WSACW). The central waters are formed during winter subduction and dominate the upper layer with the linear T-S relationship as a common remarkable characteristic. Their formations and transports are influenced by the currents in the shallow layer and finally form a relative distinct body of water within 1200m. In general, central waters are distributed in the regions closer to their formation areas and in the vertical scale, eastern central waters (ENACW and ESACW), have relative higher potential density and are located below western central waters (WNACW and WSACW). From the time perspective, central waters also have the lowest mean ages within 50 years. That means they did not experience complicate spreading processes during their formations and transports.

The intermediate layer is located below the upper layer with potential densities between 27.0 and 27.7 $kg \cdot m^{-3}$. Similar with central water masses, the intermediate water masses also origins from the

subductions but deeper into intermediate depth between 1000-1500m and currents in this layer also have obvious impacts on the distribution and transport. In the Atlantic Ocean, two main intermediate water masses are defined: Subarctic Intermediate Water (SAIW) from the north and Antarctic Intermediate Water (AAIW) from the south. Both water masses are formed in the surface of sub-polar region and sink during their way towards the lower latitudes. Besides AAIW and SAIW, Mediterranean Overflow Water (MOW) is also defined as an intermediate water mass due to the similar density and depth. The MOW originates from the east in the Gulf of Cadiz and spreads both to the northward into the West European Basin and westward to pass the Mid-Atlantic-Ridge. Compared with the central waters, the intermediate waters have much higher mean ages with ~400 years. This shows that they take a much longer time to spread from formation areas to the final distribution position.

The deep and overflow layer lies below the intermediate layer with potential density between 27.7 and 27.88 $kg \cdot m^{-3}$. North Atlantic Deep Water (NADW), the dominate water mass in this layer, is mainly formed in the Labrador Sea and Irminger Basin. The formation of NADW is the mixing of Labrador Sea Water (LSW), Iceland-Scotland Overflow Water (ISOW) and Denmark Strait Overflow Water (DSOW). In this study, a distinction between upper NADW, which origins from LSW, and lower NADW, which origins from ISOW and DSOW, is taken. LSW is predominant in mid-depth between 1000 and 2500m in the Labrador Sea region while both DSOW and ISOW originate from Arctic Ocean and the Nordic Seas. After formation, upper and lower NADW spread and dominate the most area of the deep Atlantic Ocean along the Deep Western Boundary Current (DWBC) to the south and eddies to the east. The transport of NADW is a long process with mean ages of ~500 years.

The bottom layer that occupied by bottom water masses is the lowest layers of the water column and defined with potential densities higher than 27.88 $kg \cdot m^{-3}$. Bottom water masses in this layer have an origin in the Southern Ocean and are also characterized by their high potential densities and silicate concentrations. Antarctic Bottom Water (AABW) formed in the Weddell Sea region is the main bottom water mass, through the mixing of Circumpolar Deep Water (CDW) and Weddell Sea Bottom Water (WSBW). After the formation, AABW spreads northward and suffers from a sharp decline of silicate concentration after crossing the equator. That is the reason why AABW that past the equator is defined as a new water mass Northeast Atlantic Bottom Water (NEABW). AABW and NEABW dominate the bottom layer of the Atlantic Ocean and cover the most bottom area of south and north Atlantic respectively. The northward transport of AABW, as well as southward NADW, is another long time scale process with mean ages ~500 years.

Acknowledgements:

First of all, I must thank my advisors Dr. Toste Tanhua and Prof. Dr. Arne Körtzinger for always taking interest in my thesis and ensuring the continued progress. In particular, my deepest gratitude goes firstly and foremost to Dr. Toste Tanhua for his constant encouragement and guidance. He has walked me through all the stages of the writing of this thesis and also my entire PhD study in GEOMAR. With their help, it is possible for me to finish my thesis.

I also would like to thank the working groups of GLODAP for their support and information of the collation, quality control and publishing of data. Thanks also to the efforts from all the scientists and crews on cruises, who generated funding and dedicated time on committing the collection of data. Their contributions and selfless sharing are prerequisites for the completion of this work.

I am also grateful to Dr. Marcus Dengler for the information and suggestions on physical oceanography during the writing process, to Dr. Johannes Karstensen for his support and advice in running OMP programs, to Dr. Tim Stöven for his help during the analysis of transient tracers.

Also thank to the technicians for taking water sample on cruise and maintaining instruments for us, to our department secretaries for their help during my staying here, and especially to all the colleagues in our department for giving me so great help in dealing with all of the procedures when I came here initially and thanks for their help and their encouragement to me to study as a foreign student in Kiel.

Thanks to the China Scholarship Council (CSC) for providing funding support to my PhD study in GEOMAR Helmholtz Centre for Ocean Research Kiel. Besides the financial support, CSC and embassy staffs also gave me plenty of warm care from my motherland, so that my study in Germany could be maintained in good condition and completed smoothly.

Contents:

Chapter I: Motivations and Scientific Background

1. Introduction

1.1 Scientific Background of Water Mass

1.1.1 Cognition Progress to Marine Science

The vast and deep ocean is a familiar but still mysterious topic. Throughout the ages, countless seafarers, adventurers and scientists spent their lifelong effort in hoping to conquer the ocean or to experience its mysteries. Early understanding of the ocean can be traced back to the ancient Holy Bible. ‘‘And God called the dry land Earth; and the gathering together of the waters called the Seas: and God saw that it was good’’ (Genesis, Bible). Since then, curiosity to the ocean has never stopped and for a long time, enthusiasm from human for the exploration did not subsided, but grows with each passing day. Throughout the history, development of marine science can be roughly divided into following three periods.

Period 1: Ancient times to the end of the 18th century

The first period can be traced back from ancient times to the end of the 18th century. Human accumulated knowledge and experience to the marine in this time. Due to the limitations of navigation technology, understanding of the marine during this period is confined to only exterior observation and simple logical reasoning. In about the sixth century BC, ancient Greek philosopher Thales of Miletus believed water as a first principle and the earth floats in the vast sea. In the 1st century AD, Wang Chong, philosopher in Han Dynasty of China history, pointed out the correspondence between tidal movement and moon operation scientifically. During the Age of Exploration (from the 15th to the end of the 18th century), with the development of navigation and natural sciences, the accumulation of marine knowledge has been rapidly developed. One of the representative examples is Captain James Cook. From 1768 to 1779, he made the first batch of data on sea surface temperatures (SST), currents and sea depths, and coral reefs during his three Pacific cruises.

Period 2: Beginning of the 19th century and the middle of the 20th century

The second period is between the beginning of the 19th century and the middle of the 20th century when oceanography was established. In this period, navigation and observation

technology have strongly promoted the establishment of oceanography with the development of machine industry. Between 1872 and 1876, Challenger Expedition was considered as the real beginning and the foundation of modern oceanography. The Challenger made a multi-disciplinary and comprehensive ocean observation over more than 120,000 km of voyage and made a great deal of achievements in ocean meteorology, ocean current, seawater temperature, chemical composition, marine organisms and seafloor sediments. Challenger Expedition differentiates oceanography from the traditional field of physical geography and gradually forms itself into an independent discipline. Since then, from 1925 to1927, German research vessel "Meteor" made scientific investigation in the South Atlantic. During this cruise, electronic acoustic sounding method was firstly used and measured more than 70,000 data of ocean depth, and revealing that the bottom of the ocean is not flat, but varied as surface of the continent. Numbers of research achievements and publications also came out during this period. The most classic reference is so-called ‘unsurpassed’ given by Sverdrup (1942) (Warren, 1993). This literature made a comprehensive and profound summary of marine science and is considered as a symbol of oceanography.

Period 3: After middle of the 20th century

The establishments of Scientific Committee on Oceanic Research (SCOR) in 1957 and Intergovernmental Oceanographic Commission (IOC) in 1960 mark a new/the third period in the development of marine science. Simultaneously, maturity of the detection technology provides strong technical support to oceanography. For instance, U.S. nuclear submarine "Nautilus" crossed the North Pole from ice in 1958 and US submersible "Trieste II" dived deep into the depths of 10,919 meters of the sea in 1960, indicate that any part of the ocean could be conquest by human. However, the too many unknown truths of the fact also prove that marine is still impossible to grasp by humans. The development of oceanography in this new period has the following features. Firstly, general research on specific observational phenomena or specific areas develops from traditional static qualitative description and simple causal analysis toward the development of dynamic quantitative analysis. Secondly, the combination and penetration between branches of oceanography, even between other related sciences (such as meteorology or geology), come more frequently and inevitably and finally formed series of interdisciplinary highly integrated research topics. Thirdly, tremendous progress has been made in the modernization of marine survey methods and in the international cooperation in oceanography. Just as GLODAPv2 used in this study, the dataset is composed of huge numbers of expeditions from multiple countries. In the meantime,

the traditional qualitative description is replaced by "simulated" quantitative analysis. The specific and complex natural entities are reflected by simplify and approximate the simulation or numerical model. Simulation increases the uncertainty of the results, but the advantage is that time and cost required by observation are greatly reduced. In this study, we also use the simulation to interpolate values between data at relatively long distances to display the distribution of key parameters in the whole Atlantic Ocean scale.

1.1.2 Classic Investigation to the Water Mass based on Physical Oceanography

With the development of observation technology, we found that properties of seawater in the ocean are not uniformly distributed; waters in different regions and depths are characterized by different properties like temperatures (T) or potential temperatures (θ), salinities and nutrients (for instance Nitrate, Phosphate and Silicate). However, similar properties in a range of variables can be found around particular regions or depths. Water body of similar properties and formation are often referred to as a water mass. Understanding of the distribution and variation of water masses in the ocean play an important role in several disciplines of oceanography. For instance while investigating the thermohaline circulation of the world ocean or predicting the climate changes (e.g. Haine and Hall, 2002; Poole and Tomczak, 1999). Particularly important is the concept of water masses for biogeochemical and biological applications where the transformation of properties over time can be viewed in the water mass frame-work. For instance, the formation of Denmark Strait Overflow water in the Denmark Strait could be described using mixing of a large number of water masses from the Arctic Ocean and the Nordic Seas (Tanhua et al., 2009). In a more recent work, Garcia-Ibanez et al. (2015) considered 14 water masses combined with velocity fields to estimate water mass in the north North Atlantic. Jullion et al. (2017) used water mass analysis in the Mediterranean Sea together with measurements of dissolved Barium to better understand the dynamics of dissolved Barium. In this paper we use the concepts and definitions of water masses as given by Tomczak (1999) that reviews the theoretical and applied aspects of water mass analysis.

The definition of a water mass is the whole body of water that originates in a particular are of the ocean with a common formation history. The T-S diagram invented by Helland-Hansen, was recognized for a long time as the most important tool and the most effective method for analyzing water mass. Seawater from the same water mass shares common properties such as temperature (T) or potential temperature (θ) and salinity (S) that is distinct from surrounding

bodies of water (Helland-Hansen, 1916). And a water mass has a measurable extent both in the vertical and horizontal, and thus a quantifiable volume. Since a water mass is always surrounded by other water masses, there will be mixing (both along and across density surfaces) between them, so that away from the formation regions one tend to find mixtures of water masses with different properties compared to the ones in the formation area. Early work by Jacobsen (1927) and Defant (1929) illustrated the application of T-S relationship in the oceanography. In particular, Defant (1929) further clarified the definition of "water mass" by reference to the definition of "air mass" in meteorology. According to his definition, water mass is a limited or unlimited volume of water that contains clear and constant (or conservative) physical and chemical characteristics (such as, temperature and salinity).

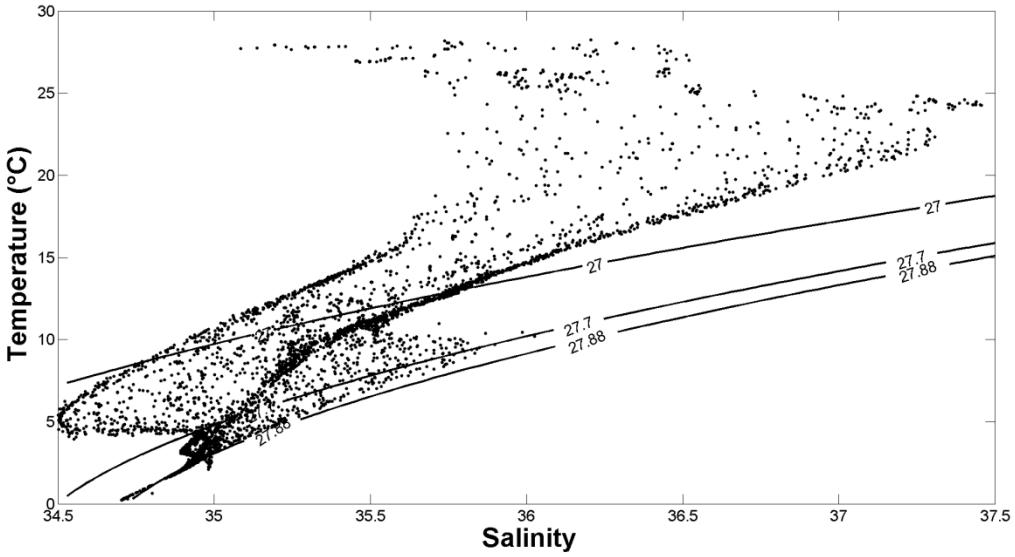

Fig 1.1 T-S diagram of water samples based on cruise from A16 section in 2003 (Expocode: 33RO20030604) in the North Atlantic Ocean

With the continuous deepening of understanding and research, the definition of a water mass is also constantly improving. In the history of research to water mass, the predecessors provided us with many precious experiences and the results those are still of great reference value. For instance, Wüst and Defant (1936) and Wüst and Defant (1936) illustrated the stratification and circulation of water masses in the Atlantic Ocean based on the observational date from Meteor Cruise 1925-1927. In Sverdrup's literature, physical, chemical and biological properties in the ocean are described in detail. Water mass refers to a relative large body of water formed in a defined area (formation area) of the ocean and has unique physical, chemical and biological properties. These properties remain almost constant and continuously distributed for a long period and spread with this water mass as an important feature, and such

properties are defined as the Source Water Type (SWT) of this water mass and play a vital role in the following investigations. The details about relationship between water mass and SWT will be described in the next section.

In the meantime, however, Sverdrup pointed out in his literature that it was still difficult to define surface water masses by applying the above properties even in the relatively stable open ocean area, due to the wide ranges of temperature and salinity in surface seawater. To make up for this regret, plenty of work has been done in the following decades. The concept of water mass has been redefined over time and in Emery and Meincke (1986), for instance, the water masses were divided into upper, intermediate and deep/abyssal layers including the depth to the T-S relationship.

1.1.3 Limitation of Classic Investigation to Water Mass and Combination of Physical and Biogeochemical Parameters

During the last decades, the classic water mass analysis based on physical properties (T and S) formed a complete theoretical system. However, the limitation is also obvious at the same time. When the number of water masses exceeds more than three, or the definition of water mass is a range of values (for instance, Central Waters) rather than a point, this classic analysis method cannot perform accurate analysis. As shown in Fig 1.2, when there are only three water masses, Antarctic Intermediate Water (AAIW), Subarctic Intermediate Water (SAIW) and Mediterranean Overflow Water (MOW), contributions from each water mass can be inferred within the triangle area. However, when more water masses exist, such as NEABW, especially when the water mass is defined by a range of values like East North Atlantic Central Water (ENACW) or East South Atlantic Central Water (ESACW), the composition between them cannot be inferred by the classic Temperature(T)-Salinity(S)-Pressure(P) relationship. In this situation, more additional properties/parameters are required to solve the equations of linear mixing without additional assumptions (Tomczak, 1981).

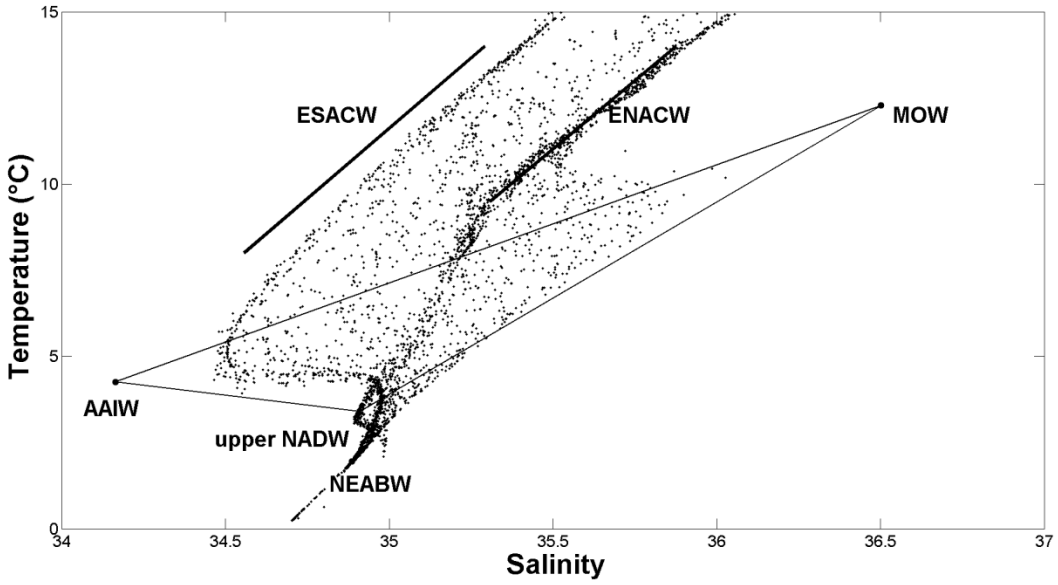

Fig 1.2 T-S diagram based on A10 cruise with definition of water masses

With the development of observational capacities for a range of variables, definition of water masses is not only limited by the T-S-P relationship. New physical and chemical parameters, both conservative and non-conservative, are added in the concept e.g. (Tomczak, 1981; Tomczak and Large, 1989b). These additional variables exhibit different importance in defining a water masses but are complementary to each other and provide a more solid basis for the water mass definition. Based on researches in last decades, Tomczak summarized the history of the water mass research and looked forward to the evolution of researches in water mass in the future (Tomczak, 1999). With the consummation of this theoretical system, the Optimal Multi-parameter (OMP) analysis came into being and was applied to calculate the contribution from each water mass, when multiple water masses (more than three) coexist. Besides abovementioned physical parameters (potential temperature and salinity), more biogeochemical parameters (oxygen, silicate, phosphate and nitrate in this study) are added in OMP analysis, so the number of water masses that can be calculated in one OMP run increases to five. Details of OMP analysis will be displayed in the Data and Method Section.

1.2 Significance of Water Mass to Biogeochemical Oceanography

As described in the last section, early researches on the water mass are mainly done in the physical oceanography and mostly of around the T-S-P relationship. With the development of oceanographic research and the improvement of survey techniques, directions in oceanography (physical, chemical or biological oceanography) have broken their traditional boundaries and have more combination and cooperation. Biogeochemical methods are often

used to investigate and analyze the physical processes in oceanography. Transient tracers (CFCs, SF_6 or helium isotopes) become important tools to measure upwelling velocities (Rhein et al., 2010; Tanhua and Liu, 2015). Physical oceanography, on the other hand, can also provide biogeochemistry with effective support. For instance, during the investigation of nitrogen cycle, physical knowledge about eastern boundary upwelling systems (EBUS) can provide corresponding help. Upwelling brings N_2O, which is a potent greenhouse gas, from intermediate layer, where N_2O is produced, to the surface, influences the emissions to the atmosphere and has further impacts on the nitrification and denitrification processes (Alvarez et al., 2014). The same reasoning, understanding about currents has also significance to the biogeochemical oceanography. One of the typical examples is that the zonal equatorial currents in Pacific Ocean affect the distribution of OMZ and finally change the ventilation of the ocean's interior and biogeochemical cycles (Karstensen et al., 2008).

Recent developments of sensitive, autonomous and environmental friendly measurement techniques have created numerous datasets with large spatial and temporal resolution, which foster inter-disciplinary collaborations among physical, chemical and biological oceanography. Physical processes, such as the variability of coastal upwelling, can be quantified by monitoring the distribution of transient tracers (CFCs, etc…) over time. Likewise, physical and chemical interactions (temperature, nutrients and solar radiation) fundamentally determine the timing and magnitude of spring phytoplankton bloom (Townsend and Spinrad, 1986). These examples highlight the importance of water mass characterization (temperature, salinity and other variables) in understanding the ocean biogeochemistry.

Water mass, traditionally defined by physical oceanography with (potential) temperature and salinity, has also extensive applications in contemporary biogeochemical oceanography. In the Atlantic Ocean, warm water masses in the upper/central layer are transported northward into high latitude region in North Atlantic, where cold deep water is formed. After formation, cold deep water with high density sinks, spreads southward across the equator, into South Atlantic (Zickfeld et al., 2007). During this process, transport of surface water masses has certain impact on Sea-Air carbon exchange, while formation of deep water masses in north Atlantic transports carbon from surface to the deep ocean (e.g. Duplessy et al., 1984; Tanhua et al., 2013). Distribution of oxygen is also influenced. Warm surface water with relative low oxygen spreads to the north, where cold deep water with high oxygen is formed, and further influence the distribution of biogeochemical elements, such as carbon or nitrogen, and biological densities in the Atlantic Ocean (e.g. Keeling et al., 2009; Stramma et al., 2010). All

of these studies show that the study of water masses plays not only an important role in physical oceanography, but also irreplaceable role in biogeochemistry.

1.3 Water Masses and Source Water Types (SWTs)

After we realized the significance of water mass to biogeochemical oceanography, we also found that the ocean is thus composed of a large number of different water masses. Water masses, however, are not simply piled up in the ocean like bricks; in fact there are no clear boundaries between them so that there is a gradual and mixed process between water masses (Castro et al., 1998). In order to quantify how water masses are distributed and how they are being mixed we use the concept of Source Water Types (SWTs). SWTs describe the original properties of water masses in their formation area, and can be considered as the original form of water masses (Tomczak, 1999).

1.3.1 Definition of SWTs

It is important to realize that a water mass has a defined volume and extent, while a Source Water Type is only a mathematical definition that does not have a physical extent. A SWT is defined based on a number of properties and their variance, or standard deviation (Tomczak, 1999). Knowledge of the properties of the SWT is essential in labeling a water masses, tracking their spreading and mixing progresses. In other words, the SWT is just like the fingerprint of a water mass and no matter how a water mass spreads, it can be recognized by its own SWT. So an accurate definition to all the SWTs is an essential step for performing OMP analysis (Tomczak and Large, 1989b), or any other water mass mixing investigation. In practice though, defining source water types is often a difficult and time-consuming part of water mass analysis, particularly when analyzing data from a particular region of the ocean distant from the water mass formation regions. In order to facilitate water mass analysis we, in this paper, use the GLODAPv2 Atlantic data to identify and define source water types for the most prominent water masses in the Atlantic Ocean based on 6 commonly measured variables. The aim of this work is to facilitate water mass analysis and understanding for particularly biogeochemical and biological oceanographic work in a broad sense. We realize that the SWTs that we define here are static, i.e. they do not change with time, and are relatively course so that we do not consider subtle differences between closely related SWTs but rather paint the picture with a rather broad brush. Studies looking at temporal variability of water masses, or water mass formation processes in detail, for instance, may find this study useful

but will certainly want to use a more granular approach to water mass analysis in their particular area.

1.3.2 Water Masses in the Atlantic Ocean

As early as the beginning of 20th century, Bjerknes and Sandström proposed, both theoretically and experimentally, the existence of heat source into the deep Atlantic Ocean and opened up the large scale research on heat transport and water mass in the Atlantic Ocean (Bjerknes, 1920; Sandström, 1908, 1916). With the development of the research, the fact is gradually realized that in the Atlantic Ocean there are four processes, or more specifically, a complete large scale cycle that composed by four parts. 1. Surface waters are transport by surface currents northward until high latitude in the North Atlantic; 2. Deep waters are formed and sink near Labrador and Irminger Sea region, where surface water becomes dense due to low temperature and high salinity. 3. The formed deep water spreads southwards with Deep Western Boundary Currents (DWBC); 4. Upwelling of deep water to the surface takes place in the Southern Ocean. This cycle also constitutes the main part of thermohaline circulation and AMOC (e.g. Bryden et al., 2005; Hall and Bryden, 1982; Kuhlbrodt et al., 2007). Almost all main water masses in the Atlantic Ocean are involved in the above cycle. In order to better define and distinguish water masses, the Atlantic Ocean can be roughly divided into four layers from the vertical direction based on potential density (σ_θ). The shallowest layer is defined as the upper/central layer with σ_θ<27 kg/m^3. There are four main water masses formed in this layer, including East and West North Atlantic Central Water (ENACW and WNACW), East and West South Atlantic Central Water (ESACW and WSACW). Below the upper/central layer, there is the intermediate layer with σ_θ between 27 and 27.7 kg/m^3. Antarctic Intermediate Water (AAIW), Subarctic Intermediate Water (SAIW) and Mediterranean Overflow Water (MOW) are main water masses in this layer. The deep and overflow lies below the intermediate layer with σ_θ between 27.7 and 27.88 kg/m^3. Labrador Sea Water (LSW), Iceland-Scotland Overflow Water (ISOW), Denmark Strait Overflow Water (DSOW), they finally form upper and lower North Atlantic Deep Water (uNADW and lNADW), are located in this layer. The bottom layer with σ_θ>27.88 kg/m^3 contains Antarctic Bottom Water (AABW), Northeast Atlantic Bottom Water (NEABW), Circumpolar Deep Water (CDW) and Weddell Sea Bottom Water (WSBW).

1.4 Transient Tracers and Water Masses

1.4.1 Transient Tracers (CFCs and SF_6)

Concentration of transient tracers in the atmosphere increases (or decreases) monotonously in the history, and their surface concentration depends on time (Fine, 2011). From measuring their concentrations in the water masses, we can calculate that, to which year from the atmospheric history it is equilibrium, and how many years did it take to move from surface into the deep ocean.

CFCs: Chlorofluorocarbon (CFC) is a group of halogenated paraffin compounds composed by carbon, chlorine and fluorine. CFCs are widely used in industry and daily life as refrigerants, propellants or solvents due to their low activity, non-flammability and non-toxicity. As the increasing of atmospheric concentration since early 1950s, the accumulation (or solution) of CFCs in seawater also increase continuously. This situation, although harmful to the ozone layer, provides a new using of CFCs as tracers (e.g. Bullister and Weiss, 1983; Gammon et al., 1982). In Warner and Weiss (1985), measurement and calculation of CFC solubility in seawater are improve and elaborated, and since then, CFCs are more widely used as tracers in the oceanic measurements. Walker et al. (2000) reconstructed the atmospheric history of CFC groups and provides basis for calculation of mixing ratio and transit time distribution (TTD) in the ocean. Since then, CFCs are frequently used as tracers, for instance, to measure East Greenland Current (Olsson et al., 2005) and overflow water from the Greenland to the Labrador Sea (Tanhua et al., 2005a). Dichlorodifluoromethane (CFC-12) is the most common representative of Chlorofluorocarbons (CFCs) and used together with SF_6 to label water masses in this study.

SF_6: As mentioned, the reduction of CFCs in the atmosphere since late 1990s makes the demand for new tracers appear to be concerned. Sulfur hexafluoride (SF_6) is an anthropogenic and extremely stable trace gas produced and released during the development of the electronics industry since 1960s (Maiss et al., 1996). As early as in Watson and Liddicoat (1985), the application of SF_6 as a new tracer was illustrated. In this article, practicality of using SF_6 as tracer was demonstrated and a primary profile decreased with depth in the Atlantic Ocean was displayed. After that, the operability of SF_6 was further elaborated and an experiment in Santa Monica Basin was enumerated as example, furthermore, the prospect of using SF_6 was also predicted (Watson et al., 1988). As a new transient tracer, advantages of SF_6 are obvious. Besides chemical and biological inertness and harmless to the handlers or environment, an important feature different from CFC-12 is that its atmospheric concentration of is still increasing so far (Fig 1.4). And meanwhile, the increase of concentration in seawater and the development of high sensitivity of the electron capture detector (ECD) to SF_6 make

the accuracy of SF_6 measurement greatly increased (Law et al., 1994). This development reduced the original disadvantage (relative higher standard deviation due to low concentration). Since then, SF_6 becomes another significant tracer and measurements in different sea areas are available. SF_6 was used to label the seawater transport in Persian Gulf Water (Law and Watson, 2001), in the Southern Ocean (Tanhua et al., 2004) and in the North Atlantic, from Greenland to Labrador Sea (Tanhua et al., 2005a). And SF_6 was also used to estimate biogeochemical process like anthropogenic CO_2 in the upper ocean (Tanhua et al., 2008). Figure 1.4 provides the basis for the choice of tracers. Concentration of CFC-12 in atmospheric history increased until early 1990s, and decreased from 2000s. The uncertainties of mean ages based on CFC-12 increases for the recently formed water masses (pCFC-12 > 450ppt). For the deeper water masses, the relative error will increase due to the pretty low absolute concentration of SF_6. As a result, mean ages are calculated based of SF_6 for pCFC-12 > 450ppt, while CFC-12 is the better choice for pCFC-12 < 450ppt (Tanhua et al., 2008).

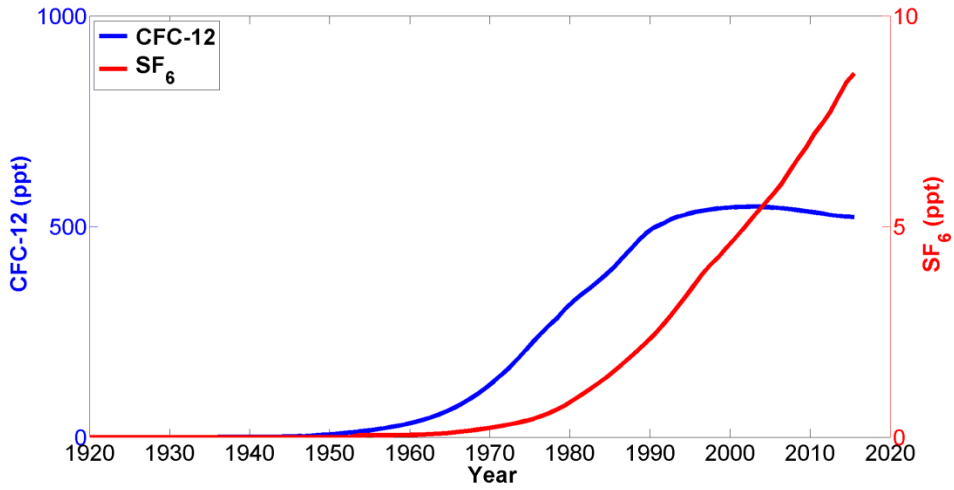

Fig 1.4 Atmospheric history of CFC-12 (blue) and SF_6 (red) in ppt

1.4.2 Application of Transient Tracers in Water Mass Analysis

As mentioned above, distributions of water masses in the Atlantic Ocean are not static, but constantly varying with the passage of time and changes of currents. Key properties are the main basis to find the formation area and SWTs, furthermore, OMP analysis can be used to display the distribution of the water mass. However, there are still many interesting or meaningful information, like the age of water masses or the duration of transports, cannot be measured or quantified directly. In this situation, we need to resort to transient tracers.

In a broad sense, property that can provide signals to reflect the physical or biogeochemical processes in the ocean can all be recognized as tracers. So from this aspect, 6 key properties used to define SWTs are also belongs to tracer category. Tracers with no sources or sinks in the ocean (e.g. T and S) are distinguished as conservative from non-conservative those are involved in biogeochemical actions (oxygen and nutrients). Transient tracers (e.g. CFCs or SF_6) are conservative tracers with a time varying source or sink in the atmosphere. Early use of transient tracers was associated air movements (Lovelock, 1971). With the sea-air exchange and accumulation of tracers in the seawater, use of transient tracers in the oceanography also became extensive. As transient tracers used to label the water masses, following additional features are required. The concentration of them in the atmosphere increases (or decreases) monotonously in the history, and their concentration in the surface (in formation area) depends on time (Fine, 2011). On this basis, by measuring the concentration in each water mass, we can clearly know that, to which year it is equilibrium to the atmospheric history (or in other words, in which year the water mass is formed in the formation area) and how many years were taken to spread to the final distribution location. Among the transient tracers, following two of them are chosen in our study to label water masses in the Atlantic Ocean.

2 Data and Methods

2.1 GLODAPv2 data set

As mentioned in the introduction section, research of marine science has entered a new historical period since the late 1950s, after the establishment of the Scientific Committee for Marine Research (SCOR) under the Council of the International Union of Science in 1957 and the Intergovernmental Oceanographic Commission (IOC) of UNESCO in 1960. Besides the widely using of modern stereoscopic observation technology systems, the other feature of this period is that marine surveys from various countries are actively organized and coordinated, and meanwhile, academic exchanges between world countries and organizations become frequent and popular.

The Geochemical Ocean Sections Program (GEOSECS) during the 1970s is the earliest global data set that included the essential chemical parameters in the ocean especially for studying distribution and cycling of carbon (Craig and Turekian, 1976; Craig and Turekian, 1980; Kroopnick and Craig, 1972; Pearson, 1974). After entering the 1990s, programs in purposes of better understanding of circulation or biogeochemical processes in the ocean, and

air-sea exchange further developed. And meanwhile, numerical models are developed to determine future changes in the ocean and to predict the impacts from changing of parameters or anthropogenic factors. WOCE (World Ocean Circulation Experiment), JGOFS (Joint Global Ocean Flux Study) and OACES (Ocean Atmosphere Carbon Exchange Study) are the three most typical representatives during this period. These programs are often initiated by different countries, and with their respective backgrounds and goals, coordination and collaboration between them are necessary and beneficial. GLODAP (Global Ocean Data Analysis Project) is such a dataset that came into being in this context. In addition to create a global dataset based on above programs, goals of GLODAP include also to describe distribution and biogeochemical processes in the global ocean and to make data publicly available (Key et al., 2004).

GLODAP dataset shows a good start for global data sharing however the shortcomings also cannot be ignored. From the spatial scale, few data in high latitude region, north of 60 °N or in the Arctic region, are collected in this dataset, and meanwhile, data from Mediterranean Sea are also not included. In the term of time, GLODAPv1.1 contains data only until1999. The updated and expanded dataset GLODAPv2 successfully made up for the above disadvantages. In addition to the integration of the other two datasets, CARINA (CARbon dioxide IN the Atlantic Ocean) and PACIFICA (PACIFic ocean Interior CArbon), GLODAPv2 also includes and 168 additional independent cruises those never been collected by any datasets. Thus the coverage of GLODAPv2 is almost global (Lauvset et al., 2016).

2.2 Key variables

In this study six key variables are used to define source water types (SWTs) in Atlantic Ocean, including two conservative variables, potential temperature (θ) and salinity (S), and four non-conservative variables, silicate, oxygen, phosphate and nitrate. We utilize the GLODAPv2 data product (Lauvset et al., 2016) to quantify the properties and related standard deviation of these variables for Atlantic Ocean SWTs. The GLODAPv2 data product is a compilation of interior ocean carbon relevant data from ship-based observations and includes data on oxygen and nutrients. The data in the GLODAPv2 product has passed both a primary quality control (aiming at precision of the data) and a secondary data quality control (aiming at the accuracy of the data). The data product that we use in this work thus uses adjusted values to correct for any biases in data. The methodologies for the QC processes in GLODAPv2 are similar to those used for the CARINA data product and are described in detail in Tanhua and Pérez (2010). Through these QC routines, the GLODAPv2 product is unique in its internal

consistency, and is thus an ideal product to use for this work aiming at definitions of major water masses and source water types in the Atlantic Ocean. Armed with the internally consistent data in GLODAPv2, we utilize previously published studies on water masses and their formation areas to define areas and depth / density ranges that can be considered to be representative samples of a SWT. As a second step we characterize the SWT in a 6 parameter space by quantifying the concentrations of these variables and use the standard deviation as a measure of the variability of each SWT and variable combination.

Source Water Types (SWTs) in the Atlantic Ocean

In line with the results from Emery and Meincke (1986) and from our interpretation of the observational data from GLODAPv2, we consider that the water masses in the Atlantic Ocean are distributed in four main vertical layers (Figure 1) roughly separated by surfaces of equal density. Potential density is the main basis to divide the shallow layers whereas the concentration of silicate is used to distinguish deep and bottom layer. In this concept we do not consider the mixed layer as the properties of that tend to be strongly variable on seasonal time-scales so that other methods to characterize the water masses is needed, mostly based on geographic region. The Upper Layer is the shallowest layer (i.e. lowest density) under consideration is located within upper 500-1000m of the water column but below the mixed layer. The Intermediate Layer is located between ~1000 to 1500/2000m, below the Central Layer. The Deep and Overflow Layer occupies the layer roughly between 2000-4000m of the Atlantic Ocean. The Bottom Layer is the deepest layer distributes and transports below 4000m and is often characterized by high silicate concentrations. In this section we will identify key SWTs in each of the four layers. Table 1 lists the four layers and the water masses that we consider in this study. The table also lists the selection criteria that we used to define a Source Water Type in pressure, potential temperature or density space.

During our narrative of each SWT we will display four figures that will guide us to a more intuitive understanding of the SWTs: 1) maps of all GLODAPv2 station locations marked as light gray dots where stations within the area of formation that we consider are marked in red and stations with any samples within the desired properties as defined by a water mass in blue sampling stations, 2) the T-S relationship with the same color coding, 3) depth profiles of the 6 variables under consideration (same color coding), and 4) bar plots of the distribution of the samples within the criteria for a SWT. In the bar plot we have added a Gaussian curve to the distribution derived from the average and standard deviation of the distribution (the amplitude of the curve defined as 2/3 of the highest bar). The plots of properties vs pressure provides an

intuitive understanding of each STW compared to others in the same region. The properties distribution and the Gaussian curve will help us to visually determine and confirm the SWT property values and associated standard deviation.

2.3 OMP (Optimum Multi-Parameter) Analysis

2.3.1 Development and mathematic background of OMP analysis

Key properties of water masses based on the GLODAPv2 data are helpful to make rough estimation for their distribution. But it is obviously not enough to make accurate positioning for water masses only by displaying key properties. In order to determine the distribution of water masses exactly, we have to resort to more accurate mathematical calculations. Since the first publication of global distributions of water masses (Sverdrup, 1942), early studies on water masses are mainly based on potential temperature and salinity. Emery and Meincke (1986) made on summary and review on this kind of analysis. The limitation of this method is that distribution of more (more than three) water masses cannot be calculated at the same time with only these two parameters. So during the same time as the development of this theory, physical and chemical oceanographers also tried to add more parameters to the calculation and the Optimum Multi-parameter (OMP) analysis is one of the typical products.

Base on above results, Tomczak extended the analysis into more than three water masses by adding more parameters/water properties (such as phosphate and silicate) and solving the equations of linear mixing without assumptions (Tomczak, 1981). In Tomczak and Large (1989a), they successfully applied this method to the analysis of mixing in the thermocline in Eastern Indian Ocean. As a summary and practical use of the above results, OMP analysis is developed by Karstenson and Tomczak (Karstensen and Tomczak, 1998a). Parameters (6 key water properties in this study) from the water samples are extracted and compared with SWTs of each water masses to identify their composition structure and percentage in detail.

Before we start the calculation of OMP analysis, some basic definitions of SWTs need to be reiterated again. SWTs are the origin water masses in their formation area and carry their own properties (Poole and Tomczak, 1999). During transport and mixing on the pathway, the total amount of water properties remains constant. In a mixed product of two water masses, contribution from each SWT can be calculated by using a linear set of mixing equations, if we know one water property (such as salinity) in this mixed product and both SWTs. But only one property/parameter becomes insufficient if there are three or more water masses mix together. As a result, we can tell the percentages of each water mass in a final mixed product

with more water masses, with the essential prerequisite that the number of water masses not larger than the number of key properties plus one.

The theory and formulas in the OMP analysis are described in detail by Karstenson and Tomczak in their articles and website (Karstensen and Tomczak, 1998a; Tomczak, 1981; Tomczak and Large, 1989a) (http://omp.geomar.de/). Here we make a brief introduction to the calculation of OMP calculation that related to our research. OMP calculation is based on a simple model of linear mixing, assuming that all key properties of water masses are affected by the same mixing process, and then to determine the distribution and of water masses through the following linear equations.

Gx - d = R;

Where **G** is a parameter matrix of defined source water types (6 key properties in this study),

x is a vector containing the relative contributions of the source water types to the sample (i.e. solution vector of the source water type fractions),

d is a data vector of water samples (observational data from GLODAPv2 in this study) and **R** is a vector of residual.
The solution is to find out the minimum the residual (**R**) with linear fit of parameters (key properties) for each data point with a non-negative values.

Prerequisites (or restriction) for using classic OMP is that source water types are defined closely enough to the observational water samples with short transport times, so that the mixing can be assumed not influenced by biogeochemical processes (i.e. consider all the parameters as quasi-conservative). Obviously, this prerequisite does not apply to our investigation for the entire Atlantic scale, so we use expand OMP analysis instead. The way of considering biogeochemical processes is to convert non-conservative parameters (phosphate and nitrate) into conservative parameters by introducing the "preformed" nutrients PO and NO (Broecker, 1974; Karstensen and Tomczak, 1998b).

2.3.2 OMP runs in this study

As mentioned in the introduction section, SWT is the origin form of each water masses in formation area and we grasp the properties of main SWTs in the Atlantic Ocean. In this study, we show the distributions of water masses in Atlantic Ocean after their formation based on OMP analysis.

In upper/central layer (σ_θ < 27 kg/m^3 and most with pressure within ~500-1000m), central waters are the dominate water masses in this layer, and we define four SWTs, ENACW, WNACW, ESACW and WSACW. Below upper/central layer lies intermediate layer (σ_θ between 27 and 27.7 kg/m^3 and most with pressures between ~1000 and 2000m). In this layer, we have following SWTs, SAIW from the north AAIW from the south and MOW from the east, in this layer. Deep layer is from ~2000 to 4000m and σ_θ between 27.7 and 27.88 kg/m^3. Upper and lower NADW are two main SWTs in mid and low latitude region in this layer. And their origin, LSW, ISOW and DSOW will also be investigated in relative high latitude region. Both bottom waters lie in the lowest layer below 4000m with σ_θ>27.88 kg/m^3. AABW and NEABW are two main water masses in this layer and have similar properties, especially high silicate. Traced back to the source, NEABW is a branch from AABW after passing the equator. After spanning most Atlantic there is a sharp reduction of silicate concentration this is the reason why we define a new SWT of NEABW.

In this study, we analyze all the GLODAPv2 data in the Atlantic Ocean with OMP method developed by Karstenson and Tomczak. We have in total 6 key properties from each water samples, including two conservative potential temperature and salinity and for non-conservative oxygen silicate phosphate and nitrate. However phosphate and nitrate in some water samples are too similar, so we have to control that in each OMP run we should have less than 6 water masses. Some regional factors should also be considered, as some water masses mix and new SWTs are formed during their mixing process. For example, LSW, ISOW and DSOW mix in the North Atlantic after leaving their formation area, as a result, SWTs of upper and lower NADW are formed. Here we specify some 'mixing regions' for these water masses. Between 40 and 60 °N, we define such a 'mixing region', since already formed three water masses LSW, ISOW and DSOW and newly formed two new water masses upper and lower NADW simultaneously exist. So in this region, all these five SWTs are used simultaneously in OMP runs. In south of 40 °N, only upper and lower NADW are used while north of 60 °N, only LSW, ISOW and DSOW are used. In South Atlantic, the same situation, we consider south of 50 °S as a 'mixing region' of old water masses CDW, WSBW and new water mass AABW. So in this region, all the three SWTs are used in the OMP runs while in north of 50 °S, only AABW is used.

Consolidate the above reasons, and also consider the distribution of all the water masses, we firstly divide into North Atlantic and South Atlantic by the equator, since most water masses distributes within the hemisphere of their SWTs (e.g. Central Waters), except some long

transport water masses such as AAIW. Furthermore, North Atlantic Ocean is divided into three parts. The region north of 60 °N contains the LSW, ISOW and DSOW in the OMP runs. The second part, from 40 to 60 °N, mixing region of LSW, ISOW, and DSOW, all the five SWTs should be contained in the OMP runs. And the third part, from equator to 40 °N, only upper and lower NADW are considered. The situation is similar in South Atlantic. Mixing region south of 50 °S contains CDW, WSBW and AABW, while from 50°S to equator we only use AABW. In addition, for relative special long transport water masses those across the equator, AAIW upper and lower NADW, we do not subject to restrictions of equator in this case when analyzing. Additional OMP runs (from 17 - 22) are set in order to maintain the consistency of distribution.

50 °S	Equator	40 °N	
#13 AAIW AABW CDW WSBW (σ_θ = 27 kg/m^3)	**#6** WSACW ESACW AAIW	**#5** WSACW WNACW ESACW ENACW AAIW	**#1** WNACW ENACW SAIW MOW
(σ_θ = 27.7 kg/m^3)	**#8** ESACW AAIW uNADW	**#7** ENACW ESACW AAIW MOW uNADW	**#2** ENACW SAIW MOW LSW
(σ_θ = 27.88 kg/m^3)	**#10** AAIW uNADW lNADW CDW AABW	**#9** AAIW MOW uNADW lNADW NEABW	**#3** SAIW LSW ISOW DSOW NEABW
	#12 lNADW AABW	**#11** lNADW NEABW	**#4** ISOW DSOW NEABW
50 °S	Equator	40 °N	

Table 2.0 schematic diagram of OMP runs in the Atlantic Ocean

2.3.3 Sensitivity of OMP

As mentioned above, OMP analysis calculates the optimal fraction of water mass configuration (minimum value of the residual R) based on the six key properties. Therefore,

the results are more or less influenced by changes in these properties and the accuracy of measurement. For some water masses a slight change or subtle error can result in a big change in the result, but for some others, the result is not obviously influenced. This mainly depends on whether this property has difference with surrounding water mass. In A16 section (Figure 2.1), comparisons are made by increasing or decreasing key properties, potential temperature with ±0.5 °C salinity with 0.05 oxygen and nutrients with 2% (That is the original oxygen and all nutrients, nitrate phosphate and silicate, × 98% and 102%). Compared with the original result, distribution of AAIW expands or shrinks slightly when the above properties change. This is because more surrounding water is consistent with features of AAIW and is considered as AAIW by OMP.

There is not much error in the measurement of temperature or potential temperature. However, there will be certain change in temperature itself. Due to the certain difference in potential temperature between the water masses, the OMP results will be affected by maximum ±20% when the temperature changes by 0.5 °C, although temperature is one of the most significant properties. Salinity is one iconic property to identify AAIW (low salinity) in the intermediate layer. Similar with potential temperature, there are also certain differences between neighboring water masses (e.g. ~34.05 for AAIW, ~34.9 for upper NADW and ~36.5 for MOW). Therefore, errors or changes of salinity are also not sensitive to the results. As shown in Figure 2.2 changing 0.05 in salinity can lead to a difference result about ±20%. The change of oxygen and nutrients with 2% can lead to impacts on the results of OMP analysis with ±20%.

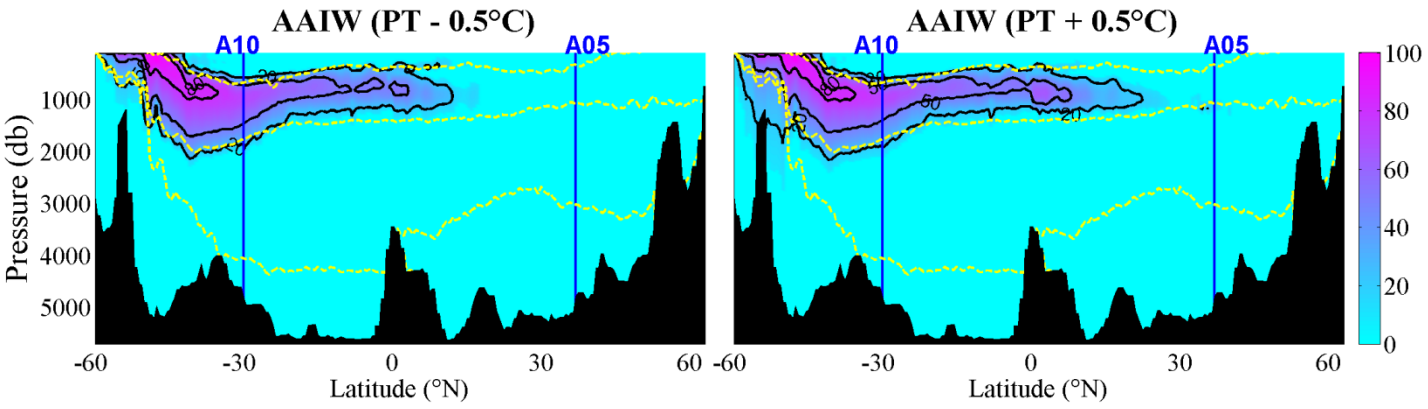

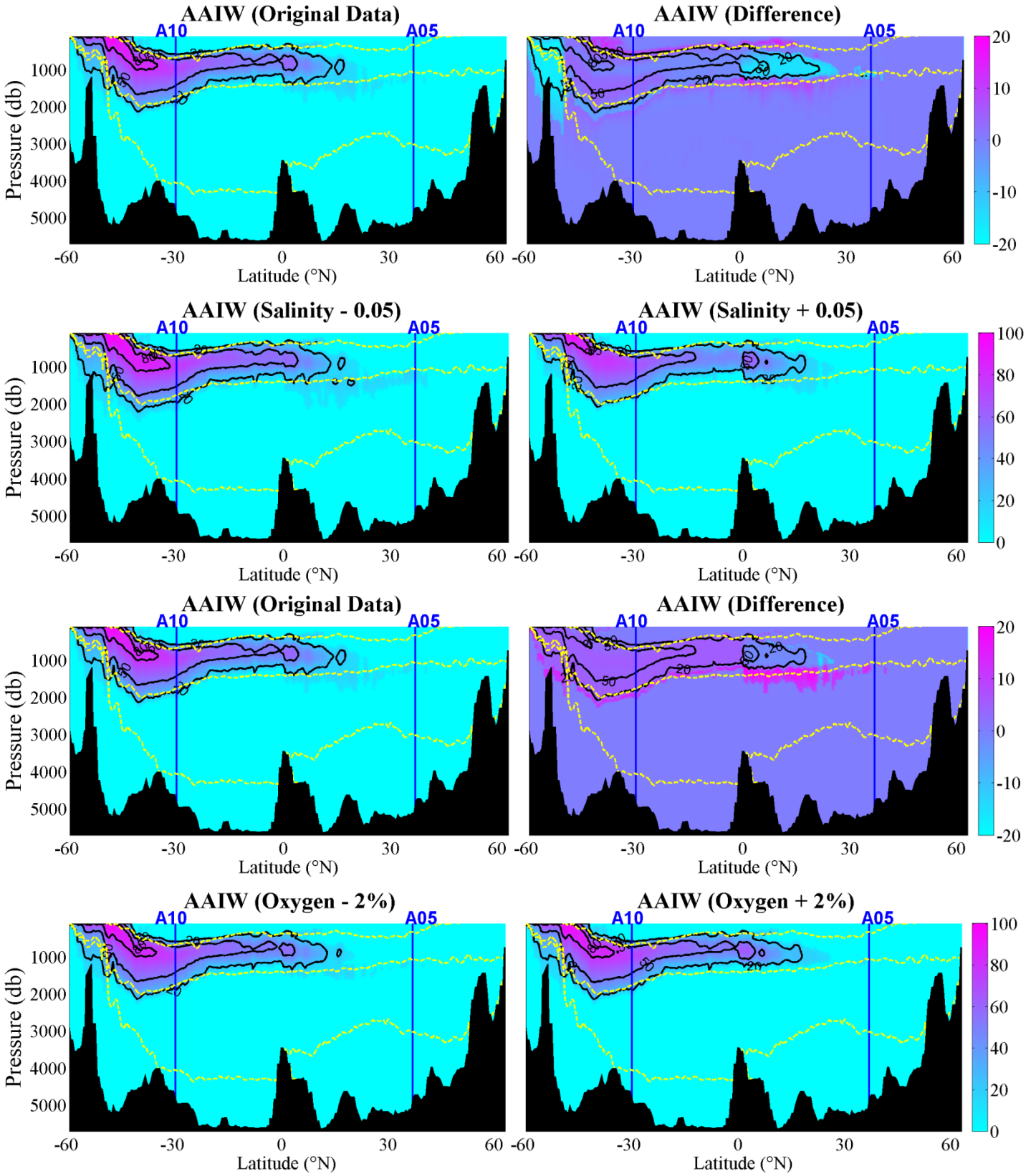
AAIW (Original Data)
AAIW (Difference)
AAIW (Salinity - 0.05)
AAIW (Salinity + 0.05)
AAIW (Original Data)
AAIW (Difference)
AAIW (Oxygen - 2%)
AAIW (Oxygen + 2%)
A10
A05
Pressure (db)
Latitude (°N)

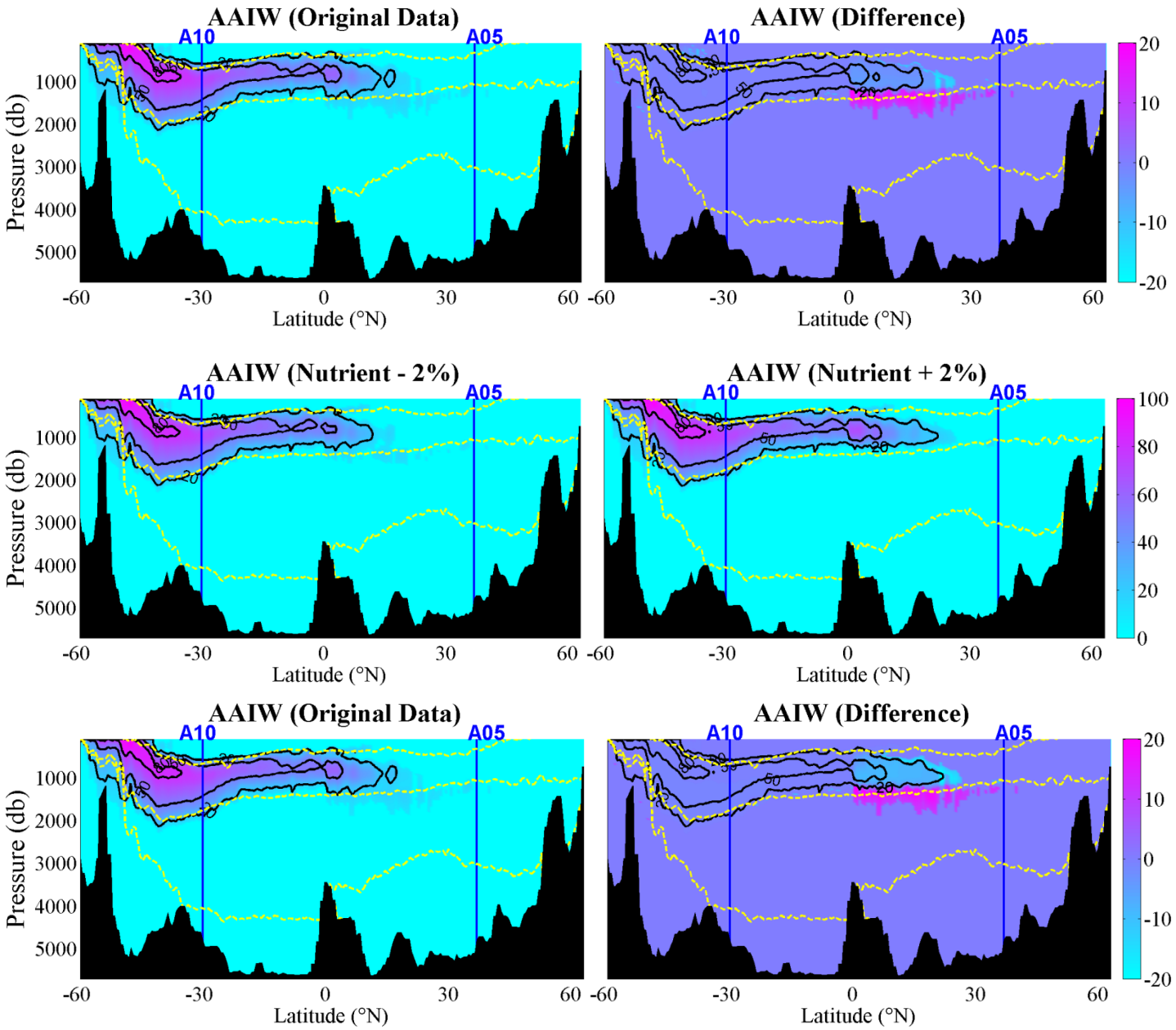

Fig 2.1 Sensitivity of changing Potential Temperature by 0.5 °C Salinity by 0.05 oxygen and nutrients by 2% based on A16 cruise in 2013
Different distributions of AAIW are shown by decreased key propertiy values (upper left), increased (upper right), original data (lower left) and difference in % between increased and decreased values (lower right). The solid contourlines show fractions of AAIW by 20, 50 and 80%; dash yellow lines show four vertial layers of water columns.

2.4 Transient Tracers and Transit Time Distribution

2.4.1 Concentration, Partial Pressure and Saturation

The concentration (solubility) of tracer gas in the seawater is a function of potential temperature (θ), salinity (S). Solubility functions of CFC-12 and SF_6 is described Warner and Weiss (1985) and Bullister et al. (2002) and follow:

$$\ln F = a_1 + a_2 \cdot \left(\frac{100}{T}\right) + a_3 \cdot \ln\left(\frac{T}{100}\right) + a_4 \cdot \left(\frac{T}{100}\right)^2 + \left[b_1 + b_2 \cdot \left(\frac{T}{100}\right) + b_3 \cdot \left(\frac{T}{100}\right)^2\right] \cdot S$$

F is the solubility of the tracers and T is the potential temperature and S is the salinity. And a_1 a_2 a_3 b_1 b_2 b_3 are all constants based on tracers.

Due to the different sampling time, seasons or regions, the potential temperature and salinity of samples are also very different. Concentration of tracers in seawater cannot be compared directly. Partial Pressure is required to remove impacts from different potential temperature and salinity. Partial pressure of tracers (CFC-12 and SF_6 follow (Doney and Bullister, 1992):

$$P_{tracer} = \frac{C_{tracer}}{F(T,S)}$$

P is the partial pressure of tracers in ppt. C is the tracer concentration in mol/kg and F is the solubility function in mol/(kg·atm).

In the long time scale, concentrations of tracers in the can also be very different in the history, it is also meaningless to compare partial pressure, for example in 1980s with 2010s, directly. Therefore, saturation, which equals partial pressure divided by atmospheric concentration, is required to remove the difference in the atmospheric history. Calculation of mean ages is based on saturation of tracers.

$$\textbf{Saturation} = \frac{\textbf{Partial Pressure}}{\textbf{history}}$$

2.4.2 Transit Time Distribution (TTD)

Due to the mixing and diffusion in the ocean, it is difficult to measure the whole process in one timescale and the transit time distribution (TTD) is a required and composed by following parameters (Waugh et al., 2003):

Tracer age (c(t)) describes the time that water particle takes from surface to the deeper layer. For water mass, tracer age means consuming time from formation area to the destination.

$$\mathbf{c(t) = c_0(t - \tau);}$$

Mean age (Γ) shows the year in which the water mass is equilibrium to the atmosphere (i.e. In which year that water mass is formed).

$$\Gamma = \int_0^\infty \xi G(\xi) d\xi;$$

Width (Δ^2) describes the mixing and the diffusion in the ocean.

$$\Delta^2 = \frac{1}{2}\int_0^\infty (\xi - \Gamma)^2 G(\xi) d\xi;$$

The relationship between all the above parameters is often assumed to follow an inverse Gauss distribution:

$$G(t) = \sqrt{\frac{\Gamma^3}{4\pi\Delta^2 t^3}} \exp\left(\frac{-\Gamma(t-\Gamma)^2}{4\Delta^2 t}\right);$$

In this equation t, Γ and Δ describes the tracer age, mean age and the width of TTD. The mixing ratio (Δ/Γ) indicates the advective (low ratio) or diffusive (high ratio) situation in the ocean. In this study, a standard mixing ratio (Δ/Γ = 1) is considered.

3. Conclusion and Outlook

Understanding the characteristics, distributions and transports of water masses in the ocean can provide the support of hydrological background for investigating the thermohaline circulation or biogeochemical process in the world oceans. By analyzing the observational data during the past few decades from GLODAPv2 dataset, this study mapped out the origins, distributions and transportations of main water masses in the Atlantic Ocean.

This study mapped out main water masses in the Atlantic Ocean with 4-layer vertical stratification based on potential density. The upper layer with the lowest potential density lower than 27.0 kg·m^{-3} and contains four central water masses which are formed during winter subduction and with the linear T-S relationship. The intermediate layer is located below the upper layer with potential densities between 27.0 and 27.7 kg·m^{-3}. Two main water masses, SAIW from the North Atlantic and AAIW from the South Atlantic, in this layer are formed in the surface of sub-polar region and subduction deep into intermediate depth during their way towards the lower latitudes. MOW, which is also defined as intermediate water mass due to similar density and pressure, originates from the east in the Gulf of Cadiz and spreads northward and westward. The deep and overflow layer lies below the intermediate layer with potential density between 27.7 and 27.88 kg·m^{-3}. NADW is formed by the mixing

of LSW, ISOW and DSOW in the Labrador Sea and Irminger Basin. A distinction is taken between upper and lower portion based on the origins from LSW or from ISOW and DSOW. NADW spreads and dominates the most area of the deep Atlantic Ocean along the DWBC to the south and eddies to the east. The bottom layer that occupied by bottom water masses is the lowest layers with potential densities higher than 27.88 $kg \cdot m^{-3}$. Bottom water masses in this layer have an origin in the Southern Ocean and are also characterized by their high potential densities and silicate concentrations. AABW formed in the Weddell Sea region is the main bottom water mass, through the mixing of CDW and WSBW. After the formation, AABW spreads northward and suffers from a sharp decline of silicate concentration after crossing the equator and redefined as a new water mass NEABW. To illustrate the situation of water masses in the Atlantic Ocean, the details are split into three chapters. Characteristics (Chapter II), Distribution (Chapter III) and Transport Time (Mean Ages) (Chapter IV) of Water Masses in the Atlantic Ocean based on GLODAPv2 dataset.

The main goal of this study is to map out the distributions and transportations of main water masses in the Atlantic Ocean in the past few decades based on the observational data from GLODAPv2 dataset and furthermore to provide the hydrological background or theoretical basis for further biogeochemical research in the whole Atlantic scale. For instances, understanding of water masses has applications in the following research fields.

Water masses play indispensable role in investigating thermohaline circulation and Atlantic meridional overturning circulation (AMOC).

The heat transport in the Atlantic Ocean is in general northward rather than polarward as in the atmosphere or in the Pacific Ocean. The AMOC, as a significant part that impacts the European and Earth climate, exerts a strong control on heat distribution in the Atlantic Ocean, and the water mass is the main carrier of heat transport. Water masses those participate in the four branches of AMOC have obvious impacts on the heat distribution. 1) The northward heat transport in the shallow Atlantic is achieved by the propagation of central water masses. 2) In the high latitude region of North Atlantic near Labrador and Irminger Sea, surface water becomes dense and due to low temperature and high salinity and NADW is formed and sinks. 3) The formed NADW spreads southwards with Deep Western Boundary Currents (DWBC). 2) and 3) form the cold branch of AMOC and make a southward cold flux of sea water in the deep layer. 4) Upwelling of cold deep water to the surface takes place in the Southern Ocean and closes the cycle. This closed cycle also constitutes the main part of thermohaline circulation in the Atlantic Ocean: the deep southward flow of cold water is matched by a

surface northward warm flow, thus a net heat flux is formed into the North Atlantic which moderates the climate in Europe.

Water mass has impacts on oxygen distribution and ventilation processes in the ocean.

Oxygen concentration in the seawater, as an indispensable element of life activities, plays an extremely important role in biogeochemical processes and can be recognized as a sensitive early warning system for global climate change in the ocean. The oxygen distribution in the ocean is determined by both physical and biological processes. Therefore, changes in the distribution of water masses can also lead to changes in the oxygen distribution. In the shallow layer, oxygen is determined by temperature and salinity as well as currents and mixing, while in the deep ocean is thus determined by circulation of water masses. In meridional scale, the higher oxygen concentrations are found at high latitudes, where the ocean is cold, especially well-mixed and ventilated. In mid-latitude region, oxygen-deficient zones exist especially on the western coasts of the continents due to the sluggish water circulation. In vertical scale, elevated oxygen consumption due to high biological productivity leads to an oxygen-minimum zone in the depth range between 100 and 1000 meters.

Water mass and carbon cycle

Carbon plays important role in the atmospheric regulator of Earth's climate as a fundamental component and the oceans contain ~60 times more carbon than the atmosphere. Besides photosynthesis from phytoplankton, the ocean takes up carbon dioxide also by simply dissolving in seawater. Carbonic acid is created and releases hydrogen ions, which combine with carbonate in seawater to form bicarbonate that doesn't escape into the atmosphere easily. The carbon cycle in the ocean is also closely related to the characteristics and transports of water mass. More carbon would be absorbed by the ocean when more carbon dioxide is released into the atmosphere, for instance by burning fossil fuels. The carbon exchange between the ocean and atmosphere is determined directly from the (temperature-dependent) chemical interaction rates in the mixed layer, using a standard CO_2 flux relation at the air-sea interface. In the surface, carbon dioxide leaks out of seawater when temperatures rise, while in the deep of the ocean, upwelling brings cold waters with high carbonate to the surface. The newly formed surface water masses take up more carbon to match the atmosphere, while the old deep water masses capture carbon into the ocean.

Reference

Alvarez, M., Brea, S., Mercier, H., Alvarez-Salgado, X.A., 2014. Mineralization of biogenic materials in the water masses of the South Atlantic Ocean. I: Assessment and results of an optimum multiparameter analysis. Prog Oceanogr 123, 1-23.

Bjerknes, V., 1920. Über thermodynamische Maschinen die unter Mitwirkung der Schwerkraft arbeiten. BG Teubner.

Broecker, W.S., 1974. No a Conservative Water-Mass Tracer. Earth Planet Sc Lett 23, 100-107.

Bryden, H.L., Longworth, H.R., Cunningham, S.A., 2005. Slowing of the Atlantic meridional overturning circulation at 25 N. Nature 438, 655.

Bullister, J., Weiss, R., 1983. Anthropogenic chlorofluoromethanes in the Greenland and Norwegian Seas. Science 221, 265-268.

Bullister, J.L., Wisegarver, D.P., Menzia, F.A., 2002. The solubility of sulfur hexafluoride in water and seawater. Deep Sea Research Part I: Oceanographic Research Papers 49, 175-187.

Castro, C.G., Perez, F.F., Holley, S.E., Rios, A.F., 1998. Chemical characterisation and modelling of water masses in the Northeast Atlantic. Prog Oceanogr 41, 249-279.

Craig, H., Turekian, K., 1976. The GEOSECS program: 1973-1976. Earth Planet Sc Lett 32, 217-219.

Craig, H., Turekian, K., 1980. The GEOSECS program: 1976-1979. Earth Planet Sc Lett 49, 263-265.

Defant, A., 1929. Dynamische Ozeanographie. Springer.

Doney, S.C., Bullister, J.L., 1992. A chlorofluorocarbon section in the eastern North Atlantic. Deep Sea Research Part A. Oceanographic Research Papers 39, 1857-1883.

Emery, W.J., Meincke, J., 1986. Global Water Masses - Summary and Review. Oceanologica Acta 9, 383-391.

Fine, R.A., 2011. Observations of CFCs and SF6 as ocean tracers. Annual Review of Marine Science 3, 173-195.

Gammon, R., Cline, J., Wisegarver, D., 1982. Chlorofluoromethanes in the northeast Pacific Ocean: Measured vertical distributions and application as transient tracers of upper ocean mixing. Journal of Geophysical Research: Oceans 87, 9441-9454.

Garcia-Ibanez, M.I., Pardo, P.C., Carracedo, L.I., Mercier, H., Lherminier, P., Rios, A.F., Perez, F.F., 2015. Structure, transports and transformations of the water masses in the Atlantic Subpolar Gyre. Prog Oceanogr 135, 18-36.

Haine, T.W.N., Hall, T.M., 2002. A generalized transport theory: Water-mass composition and age. Journal of Physical Oceanography 32, 1932-1946.

Hall, M.M., Bryden, H.L., 1982. Direct estimates and mechanisms of ocean heat transport. Deep Sea Research Part A. Oceanographic Research Papers 29, 339-359.

JACOBSEN, J P. (1927) Line graphische Methode zur Bestimmung des Vermischungskoeffizienten im Meer. Gerlands Beitrdge zur Geophysik, 16, 404-412.

Karstensen, J., Stramma, L., Visbeck, M., 2008. Oxygen minimum zones in the eastern tropical Atlantic and Pacific oceans. Prog Oceanogr 77, 331-350.

Karstensen, J., Tomczak, M., 1998a. Age determination of mixed water masses using CFC and oxygen data. J Geophys Res-Oceans 103, 18599-18609.

Karstensen, J., Tomczak, M., 1998b. Age determination of mixed water masses using CFC and oxygen data. Journal of Geophysical Research: Oceans 103, 18599-18609.

Keeling, R.F., Körtzinger, A., Gruber, N., 2009. Ocean deoxygenation in a warming world.

Key, R.M., Kozyr, A., Sabine, C.L., Lee, K., Wanninkhof, R., Bullister, J.L., Feely, R.A., Millero, F.J., Mordy, C., Peng, T.H., 2004. A global ocean carbon climatology: Results from Global Data Analysis Project (GLODAP). Global biogeochemical cycles 18.

Kroopnick, P., Craig, H., 1972. Atmospheric oxygen: isotopic composition and solubility fractionation. Science 175, 54-55.

Kuhlbrodt, T., Griesel, A., Montoya, M., Levermann, A., Hofmann, M., Rahmstorf, S., 2007. On the driving processes of the Atlantic meridional overturning circulation. Reviews of Geophysics 45.

Lauvset, S.K., Key, R.M., Olsen, A., van Heuven, S., Velo, A., Lin, X., Schirnick, C., Kozyr, A., Tanhua, T., Hoppema, M., Jutterström, S., Steinfeldt, R., Jeansson, E., Ishii, M., Perez, F.F., Suzuki, T., Watelet, S., 2016. A new global interior ocean mapped climatology: the 1° × 1° GLODAP version 2. Earth Syst. Sci. Data 8, 325-340.

Law, C., Watson, A., Liddicoat, M., 1994. Automated vacuum analysis of sulphur hexafluoride in seawater: derivation of the atmospheric trend (1970–1993) and potential as a transient tracer. Marine Chemistry 48, 57-69.

Law, G., Watson, P.R., 2001. Surface tension measurements of N-alkylimidazolium ionic liquids. Langmuir 17, 6138-6141.

Lovelock, J.E., 1971. Atmospheric fluorine compounds as indicators of air movements. Nature 230, 379.

Maiss, M., Steele, P., Francey, R., Fraser, P., Langenfelds, R., Trivett, N., Levin, I., 1996. Sulfur hexafluoride-A powerful new atmospheric tracer. Atmospheric Environment.

Olsson, K.A., Jeansson, E., Tanhua, T., Gascard, J.-C., 2005. The East Greenland Current studied with CFCs and released sulphur hexafluoride. Journal of Marine Systems 55, 77-95.

Pearson, C.J., 1974. Daily changes in carbon-dioxide exchange and photosynthate translocation of leaves of Vicia faba. Planta 119, 59-70.

Poole, R., Tomczak, M., 1999. Optimum multiparameter analysis of the water mass structure in the Atlantic Ocean thermocline. Deep-Sea Research Part I-Oceanographic Research Papers 46, 1895-1921.

Rhein, M., Dengler, M., Sultenfuss, J., Hummels, R., Huttl-Kabus, S., Bourles, B., 2010. Upwelling and associated heat flux in the equatorial Atlantic inferred from helium isotope disequilibrium. J Geophys Res-Oceans 115.

Sandström, J.W., 1908. Dynamische versuche mit meerwasser.

Sandström, J.W., 1916. The hydrodynamics of Canadian Atlantic waters.

Schaffer, A.J., JACOBSEN, A.W., 1927. Mikulicz's syndrome: a report of ten cases. American Journal of Diseases of Children 34, 327-346.

Stramma, L., Schmidtko, S., Levin, L.A., Johnson, G.C., 2010. Ocean oxygen minima expansions and their biological impacts. Deep Sea Research Part I: Oceanographic Research Papers 57, 587-595.

Sverdrup, 1942. The Oceans: Their Physics, Chemistry and General Biology.

Tanhua, T., Bates, N.R., Körtzinger, A., 2013. The marine carbon cycle and ocean carbon inventories, International Geophysics. Elsevier, pp. 787-815.

Tanhua, T., Bulsiewicz, K., Rhein, M., 2005. Spreading of overflow water from the Greenland to the Labrador Sea. Geophysical Research Letters 32.

Tanhua, T., Liu, M., 2015. Upwelling velocity and ventilation in the Mauritanian upwelling system estimated by CFC-12 and SF6 observations. Journal of Marine Systems 151, 57-70.

Tanhua, T., Olsson, K.A., Fogelqvist, E., 2004. A first study of SF6 as a transient tracer in the Southern Ocean. Deep Sea Research Part II: Topical Studies in Oceanography 51, 2683-2699.

Tanhua, T., Pérez, F.F., 2010. Atlantic Ocean CARINA data: overview and salinity adjustments.

Tanhua, T., Waugh, D.W., Wallace, D.W., 2008. Use of SF6 to estimate anthropogenic CO2 in the upper ocean. Journal of Geophysical Research: Oceans 113.

Tomczak, M., 1981. A multi-parameter extension of temperature/salinity diagram techniques for the analysis of non-isopycnal mixing. Prog Oceanogr 10, 147-171.

Tomczak, M., 1999. Some historical, theoretical and applied aspects of quantitative water mass analysis. J Mar Res 57, 275-303.

Tomczak, M., Large, D.G., 1989a. Optimum multiparameter analysis of mixing in the thermocline of the eastern Indian Ocean. Journal of Geophysical Research: Oceans 94, 16141-16149.

Tomczak, M., Large, D.G.B., 1989b. Optimum Multiparameter Analysis of Mixing in the Thermocline of the Eastern Indian-Ocean. J Geophys Res-Oceans 94, 16141-16149.

Townsend, D.W., Spinrad, R.W., 1986. Early spring phytoplankton blooms in the Gulf of Maine. Continental Shelf Research 6, 515-529.

Walker, S., Weiss, R., Salameh, P., 2000. Reconstructed histories of the annual mean atmospheric mole fractions for the halocarbons CFC‐11 CFC‐12, CFC‐113, and carbon tetrachloride. Journal of Geophysical Research: Oceans 105, 14285-14296.

Warner, M., Weiss, R., 1985. Solubilities of chlorofluorocarbons 11 and 12 in water and seawater. Deep Sea Research Part A. Oceanographic Research Papers 32, 1485-1497.

Warren, B., 1993. Circulation of north Indian deep water in the Arabian Sea. Oceanography in the Indian Ocean. AA Balkema, Rotterdam, 575-582.

Watson, A.J., Ledwell, J., Webb, D., Wunsch, C., 1988. Purposefully released tracers. Philosophical Transactions of the Royal Society of London. Series A, Mathematical and Physical Sciences, 189-200.

Watson, A.J., Liddicoat, M., 1985. Recent history of atmospheric trace gas concentrations deduced from measurements in the deep sea: Application to sulphur hexafluoride and carbon tetrachloride. Atmospheric Environment (1967) 19, 1477-1484.

Waugh, D.W., Hall, T.M., Haine, T.W., 2003. Relationships among tracer ages. Journal of Geophysical Research: Oceans 108.

Wüst, G., Defant, A., 1936. Atlas zur Schichtung und Zirkulation des Atlantischen Ozeans: Schnitte und Karten von Temperatur, Salzgehalt und Dichte. W. de Gruyter.

Zickfeld, K., Levermann, A., Morgan, M.G., Kuhlbrodt, T., Rahmstorf, S., Keith, D.W., 2007. Expert judgements on the response of the Atlantic meridional overturning circulation to climate change. Climatic Change 82, 235-265.

Chapter II: Characteristics of Water Masses in the Atlantic Ocean based on GLODAPv2 dataset

Mian Liu

Toste Tanhua

GEOMAR Helmholtz Centre for Ocean Research Kiel,

Marine Biogeochemistry, Chemical Oceanography

Düsternbrooker Weg 20, 24105 Kiel, Germany

Correspondence to: T. Tanhua (ttanhua@geomar.de)

Abstract: The **c**haracteristics of the main water masses in the Atlantic Ocean are investigated and defined as Source Water Types (SWTs) from their formation area by six key properties based on the GLODAPv2 observational data. These include both conservative (potential temperature and salinity) and non-conservative (oxygen, silicate, phosphate and nitrate) variables. For this we divided the Atlantic Ocean into four vertical layers by distinct potential densities in the shallow and intermediate water column, and additionally by concentration of silicate in the deep waters. The SWTs in the upper/central water layer originates from subduction during winter and are defined as central waters, formed in four distinct areas; East North Atlantic Central water (ENACW), West North Atlantic Central Water (WNACW), East South Atlantic Central Water (ESACW) and West South Atlantic Central Water (WSACW). Below the upper/central layer the intermediate layer consist of three main SWTs; Antarctic Intermediate Water (AAIW), Subarctic Intermediate Water (SAIW) and Mediterranean Overflow Water (MOW). The North Atlantic Deep Water (NADW) is the dominating SWT in the deep and overflow layer, and is divided into upper and lower NADW based on the different origins and properties. The origin of both the upper and lower NADW is the Labrador Sea Water (LSW), the Iceland-Scotland Overflow Water (ISOW) and Denmark Strait Overflow Water (DSOW). Antarctic Bottom Water (AABW) is the only natural SWT in the bottom layer and this SWT is redefined as North East Atlantic Bottom Water (NEABW) in the north of equator due to the change of key properties, especial silicate. Similar with NADW, two additional SWTS, Circumpolar Deep Water (CDW) and Weddell Sea Bottom Water (WSBW), are defined in the Weddell Sea in order to understand the origin of AABW. The definition of water masses in biogeochemical space is useful for, in particular, chemical and biological oceanography to understand the origin and mixing history of water samples.

Key Words: Water Mass, Source Water Types, GLODAP, Atlantic Ocean

1. Introduction

Properties of water in the ocean are, obviously, not uniformly distributed so that different regions and depths (or densities) are characterized by different properties. Bodies of water with similar properties often share a common formation history and are referred to as water masses, or, more generally, sea water types. Understanding of the distribution and variation of water masses play an important role in several disciplines of oceanography, for instance while investigating the thermohaline circulation of the world ocean or predicting climate changes (e.g. Haine and Hall, 2002; Tomczak, 1999). Particularly important is the concept of water masses for biogeochemical and biological applications where the transformation of properties over time can be successfully viewed in the water mass frame-work. For instance, the formation of Denmark Strait Overflow water in the Denmark Strait could be described using mixing of a large number of water masses from the Arctic Ocean and the Nordic Seas (Tanhua et al., 2005b). In a more recent work, Garcia-Ibanez et al. (2015) considered 14 water masses combined with velocity fields to estimate transport of water mass, and thus chemical constituents, in the north Atlantic. Similarly, Jullion et al. (2017) used water mass analysis in the Mediterranean Sea to better understand the dynamics of dissolved Barium. Also, Wüst and Defant (1936) illustrated the stratification and circulation of water masses in the Atlantic Ocean based on the observational data from Meteor Cruise 1925-1927. Based on research during last few decades, Tomczak (1999) summarized the history of the water mass research and provided an outlook for the evolution of water mass research. In this paper we use the concepts and definitions of water masses as given by Tomczak (1999).

The definition of a water mass is a body of water that originates in a particular area of the ocean with a common formation history. Water masses share common properties such as temperature, salinity and biogeochemical variables that are distinct from surrounding bodies of water (e.g. Helland-Hansen, 1916; Montgomery, 1958) and have a measurable extent both in the vertical and horizontal, and thus a quantifiable volume. Since water masses are surrounded by other water masses there will be mixing (both along and across density surfaces) between the water masses, so that away from the formation regions one tend to find mixtures of water masses with different properties compared to the ones in the formation area. Early work by Schaffer and JACOBSEN (1927) and Defant (1929) illustrated the application of T-S relationship in the oceanography. This concept has been redefined over time and in Emery and Meincke (1986), for instance, the water masses were divided into upper, intermediate and deep/abyssal layers including the depth to the T-S relationship. With the development of observational capacities for a range of variables, definition of water masses is not only limited by the T-S-P relationship. New physical and chemical parameters, both conservation and non-conservative, are added in the water mass concept e.g. (Tomczak, 1981; Tomczak and Large, 1989b). These additional variables exhibit different importance in defining a water masses but are complementary to each other and provide a more solid basis for the water mass definition.

The ocean is thus composed a large number of water masses, these are however not simply piled up in the ocean like bricks. In fact, there are no clear boundaries between them. Or, in other words, there is a gradual and mixed process between water masses (Castro et al., 1998). As a direct result another concept was introduced: Source Water Types (SWTs). SWTs describe the original properties of water masses in their formation area, and can thus be considered as the original form of water masses (Tomczak, 1999).

It is important to realize that while water masses have a defined volume and extent, a water type is only a mathematical definition that does not have a physical extent. A SWT is defined based on a number of properties and their variance, or standard deviation (Tomczak, 1999). Knowledge of the properties of the SWTs is essential in labeling water masses, tracking their spreading and mixing progresses. Accurate definition and characterization of SWTs is an essential step for performing any water mass mixing analysis, such as the Optimum Multi-parameter (OMP) analysis (Tomczak and Large, 1989b). In practice though, defining properties of source water types and water masses is often a difficult and time-consuming part of water mass analysis, particularly when analyzing data from a region distant from the water mass formation regions. In order to facilitate water mass analysis we use the Atlantic data from the data product GLODAPv2 (Lauvset et al., 2016) to identify and define source water types for the most prominent water masses in the Atlantic Ocean based on 6 commonly measured physical and biogeochemical variables. The aim of this work is to facilitate water mass analysis and in particularly we aim at supporting biogeochemical and biological oceanographic work in a broad sense. We realize that we define the SWTs in a static sense, i.e. we assume that they do not change with time, and that our analysis is relatively course in that we do not consider subtle differences between closely related SWTs but rather paint the picture with a rather broad brush. Studies looking at temporal variability of water masses, or water mass formation processes in detail, for instance, may find this study useful but will certainly want to use a more granular approach to water mass analysis in their particular area.

In a companion paper (Liu and Tanhua, 2018) we will use the here defined Atlantic Ocean SWTs to estimate the distribution of the water masses in the Atlantic Ocean based on the GLODAPv2 data.

2 Data and Methods

In this study we use six key variables to define source water types (SWTs) in Atlantic Ocean, including two conservative variables, potential temperature (θ) and salinity (S), and four non-conservative variables, silicate, oxygen, phosphate and nitrate. We utilize the GLODAPv2 data product (Lauvset et al., 2016) to quantify the properties and related standard deviation of these variables for Atlantic Ocean SWTs. The GLODAPv2 data product is a compilation of interior ocean carbon relevant data from ship-based observations and includes data on oxygen and nutrients. The data in the GLODAPv2 product has passed both a primary quality control (aiming at precision of the data) and a secondary data quality control (aiming at the accuracy of the data). The data product that we use in this work thus uses adjusted values to correct for any biases in data. The methodologies for the QC processes in GLODAPv2 are similar to those used for the CARINA data product and are described in detail in (Key et al., 2010). Through these QC routines, the GLODAPv2 product is unique in its internal consistency, and is thus an ideal product to use for this work aiming at definitions of major water masses and source water types in the Atlantic Ocean. Armed with the internally consistent data in GLODAPv2, we utilize previously published studies on water masses and their formation areas to define areas and depth / density ranges that can be considered to be representative samples of a SWT. As a second step we characterize the SWT in a 6 parameter space by quantifying the concentrations of these variables and use the standard deviation as a measure of the variability of each SWT and variable combination.

3 Source Water Types (SWTs) in the Atlantic Ocean

In line with the results from Emery and Meincke (1986) and from our interpretation of the observational data from GLODAPv2, we consider that the water masses in the Atlantic Ocean are distributed in four main vertical layers (Figure 1) roughly separated by surfaces of equal density. Potential density is the main basis to divide the shallow layers whereas for the deep and bottom layers the concentration of silicate is additionally used to distinguish these layers. In this concept we do not consider the mixed layer as its properties tend to be strongly variable on seasonal time-scales so that other methods to characterize the water masses is needed, mostly based on geographic region. The Upper Layer is the shallowest layer (i.e. lowest density) under consideration and is located within upper 500-1000m of the water column but below the mixed layer. The Intermediate Layer is located between ~1000 to 1500/2000m, below the Upper Layer. The Deep and Overflow layer occupies the layer roughly between 2000-4000m of the Atlantic Ocean. The Bottom Layer is the deepest layer, mostly located below 4000m, and is often characterized by high silicate concentrations. In this section we will identify key SWTs in each of the four layers. Table 1 lists the four layers and the water masses that we consider in this study. The table also lists the selection criteria that we used to define a Source Water Type in pressure, potential temperature or density space, for some SWTs, key properties such as

salinity, oxygen or silicate are also necessary, in order to characterize the biogeochemical properties as well.

During our narrative of each SWT we will display four figures that will guide us to a more intuitive understanding of the SWTs: (a) maps of all GLODAPv2 station locations marked as light gray dots where stations within the area of formation that we consider are marked in red and stations with any samples within the desired properties as defined by Table 1 in blue, (b) the T-S relationship with the same color coding, (c) depth profiles of the 6 variables under consideration (same color coding), and (d) bar plots of the distribution of the samples within the criteria for a SWT. In the bar plot we have added a Gaussian curve to the distribution derived from the average and standard deviation of the distribution (the amplitude of the curve defined as 2/3 of the highest bar). The plots of properties vs pressure provides an intuitive understanding of each STW compared to others in the same region. The properties distribution and the Gaussian curve will help us to visually determine and confirm the SWT property values and associated standard deviation.

3.1 The Upper Layer, Central Waters

The Upper Layer is occupied by four SWTs called central waters that are known to be formed by subducted into the thermocline (Sprintall and Tomczak, 1993; Tomczak and Godfrey, 2013) into the interior of the ocean (Pollard et al., 1996). Figure 2 illustrate a schematic of the main currents in this layer and the main formation regions of the central waters in the Atlantic Ocean. Water masses or SWTs in this layer can be easily recognized by their linear T-S relationship (Pollard et al., 1996; Stramma and England, 1999). In this study, we define upper layer water masses to be located above potential density isoline of 27.0 kg/m^3 (see Fig 3.0), but below the mixed layer. The formation and transport of the Central Water is influenced by the currents in the shallow layer and finally forms a relative distinct body of water in both the horizontal and vertical. Mode Waters, on the other hand, are considered as the precursor or the prototype of the central waters (Alvarez et al., 2014; Cianca et al., 2009). In this study we will refer to Mode Waters in the description in defining or formation of the central waters but do not relate to their details.

3.1.1 Eastern North Atlantic Central Water (ENACW)

The main water mass in the upper layer of the region east of the Mid Atlantic Ridge (MAR) is the East North Atlantic Central Water (ENACW) (Harvey, 1982). This water mass is formed during winter and gets subducted in the seas west of Iberian Penisular. In addition, one component of the Subpolar Mode Water (SPMW) is carried by the south branch of North Atlantic Current (Figure 3a) and mixed in ESAW contributing to the properties of this water mass (McCartney and Talley, 1982) so that ENACW shows a typical linear T-S relationship (Pollard et al., 1996). ENACW advects in the general southern direction along the south branch of the North Atlantic Current (Arhan, 1990), passes northwest Africa, and then turns southwest into Canary basin. In the vertical scale, ENACW occupies

at the upper ~500m with a relative low salinity, while SAIW is often occupying the water column below ENACW, often with contribution of MOW from the east in the intermediate depth (Garcia-Ibanez et al., 2015; Pollard et al., 1996; Pollard and Pu, 1985; Prieto et al., 2015). This straticication can also be clearly seen in the salinity/depth plot of Figure 3c where the MOW is primarily characterized by high salinity (see also Figure 9c and discription of MOW).

In our analysis, we follow the analysis of Pollard et al. (1996) and choose latitude between 39 and 48 °N and between 15 and 25 °E of longitude (east of Mid-Atlantic-Ridge) as the formation area of ENACW (Figure 3a). Based on the work of (Pollard and Pu, 1985) we choose potential density, σ_θ = 26.50 kg/m^3 as higher boundary and σ_θ = 27.30 kg/m^3 as the lower boundary to define ENACW in our analysis.

In Figure 3b, we can see clearly the linear T-S distribution of this water masses, consistent with Pollard et al. (1996) and the definition of $ENACW_{12}$ in Garcia-Ibanez et al. (2015). In Garcia-Ibanez et al. (2015), there is another definition $ENACW_{16}$, but water samples show a discrete distribution warmer than 16 °C by GLODAPv2 data set in this region, so also samples with potential temperature below 16 °C are selected in this study. As shown in Figure 3c, ENACW dominates the upper 500m depth. The main character of ENACW is the large potential temperature and salinity ranges and low nutrients (especially low in silicate).

3.1.2 Western North Atlantic Central Water (WNACW)

Western North Atlantic Central Water (WNACW) is another SWT formed during winter through subduction (McCartney and Talley, 1982; Worthington, 1959). WNACW is formed at the south flank of the Gulf Stream (Klein and Hogg, 1996) and is in some literatures referred to as 18 ° water since a potential temperature of around 18 °C and salinity around 36.5 are standard features of this SWT (Talley and Raymer, 1982). In general, ocean water in the Northeast Atlantic has higher salinity than in the Northwest Atlantic due to the stronger winter convection (Pollard and Pu, 1985) and input of MOW (Pollard et al., 1996; Prieto et al., 2015). However, for the central waters, we find the opposite. WNACW has a significantly higher salinity than ENACW by 0.9 PSU units. This is due to a number of reasons, such as different latitudes of formation; WNACW is formed in lower latitude than ENACW so that surface water with higher salinity subducts during winter convection to form WNACW.

In this study, we follow McCartney and Talley (1982) and choose the region 24-37°N, 50-70°W as the formation area and pressures less than 1000 m. By defining the depth of this SWT water samples show a discrete T-S distribution with potential densities lower than 26.30 or larger than 26.60 kg/m^3. Besides the potential density constraint, we added the constraint that concentrations of phosphate have to be lower than 0.3 and silicate lower than 3 μmol kg^{-1}.

The properties of WNACW are shown in Figure 4. Besides the linear T-S relationship, a feature of all central waters, another feature of this water mass is, as the alternative name suggests, a potential temperature around18 °C. This is the warmest of the four STWs in the Atlantic Ocean since it has the lowest latitude of formation and is influenced by the high salinity Gulf Stream during formation. Low nutrients, including silicate, phosphate and nitrate are other features compared to other central waters that generally are low in nutrients compared to deeper water masses

3.1.3 Western South Atlantic Central Water (WSACW)

Western South Atlantic Central Water (WSACW) is located in the starting point that central water is transported to the north during the Meridional Overturning Circulation (Kuhlbrodt et al., 2007). For this reason, the importance of WSACW is clear. The WSACW is formed with little directly influence from other central water masses (Stramma and England, 1999), while the origin of other central water masses (e.g. ESACW or ENACW) can, to some extent at least, be traced back to WSACW (Peterson and Stramma, 1991). This water mass is a product of three mode waters mixed together: the Brazil current brings Salinity Maximum Water (SMW) and Subtropical Mode Water (STMW) from the north, while the Falkland Current brings Subarctic Mode Water (SAMW) from the south (Alvarez et al., 2014). Here we follow the work of Stramma and England (1999) and Alvarez et al. (2014) that choose the meeting region of these two currents (25-60°W, 30-45°S) as the formation region of WSACW. We choose potential density (σ_θ) between 26.0 and 27.0 kg/m^3 and salinity higher than 34.5 for defining WSACW. In addition to the physical properties we used the requirement of silicate concentrations lower than 10 µmol kg^{-1} and oxygen concentrations lower than 230 µmol kg^{-1} to define this SWT.

The temperature distribution in this region indicates another peak in the abundance (histogram) for potential densities higher than 27.0 kg m^{-3}, indicating that the boundary between WSACW and AAIW is at σ_θ = 27.0 kg m^{-3} in this region. The hydrochemical properties of WSACW are shown in Figure 5. Similar to other central waters, WSACW shows a linear T-S relationship with large T and S ranges and low concentration of nutrients, especially low silicate.

3.1.4 Eastern South Atlantic Central Water (ESACW)

The other formation area of SACW in the eastern South Atlantic Ocean is located in area southwest of South Africa. In this region the Agulhas Current brings water from the Indian Ocean (Deruijter, 1982; Lutjeharms and van Ballegooyen, 1988) that meets and mixes with the South Atlantic Current (Gordon et al., 1992; Stramma and Peterson, 1990) from the west. Water mass formed during this process spreads to the northwest and intrudes water from the Benguela Current and enters the subtropical gyre (Peterson and Stramma, 1991). Tracing back to the origin of ESACW, it can be considered as partly originating from WSACW, but since water from Indian Ocean is added by the Agulhas Current we can define WSACW as a new independent STW with characteristic properties.

We choose the meeting region of Agulhas Current and South Atlantic Current (30-40 °S, 0-20 °E) as the formation area of ESACW and display properties of this SWT. To investigate the properties of ESACW, we also follow Stramma and England (1999), and choose 200-700m as the core of this water mass. For the properties, potential density (σ_θ) between 26.00 and 27.20 kg m^{-3} and oxygen concentration between 200 and 240 µmol kg^{-1} are used to define ESACW.

Figure 6a clearly shows the linear T-S relationship for potential density (σ_θ) between 26.00 and 27.20 kg m^{-3}, which is consists with the general property of Central Waters (Alvarez et al., 2014; Emery and Meincke, 1986; Harvey, 1982). As shown in Figure 6b, ESACW exhibits a relative large potential temperature and salinity range and low nutrient concentrations (especially low in silicate) compared to the AAIW below. The properties in ESACW are similar to that of WSACW, although with higher nutrient concentrations due to input from the Agulhas current.

3.2 The Intermediate Layer

The intermediate water masses origins from the upper part of the ocean (i.e. the upper 500m of the water column) but subduct into intermediate depth (1000-1500m) during their formation process. Similarly to the water masses of the central layer, currents in this layer play a significant role to influence the distribution and transport of intermediate water masses. The potential density (σ_θ) of the intermediate water masses usually is between 27.00 and 27.70 kg m^{-3}.

In the Atlantic Ocean we find two main intermediate water masses: SAIW that originates from the north and AAIW that originates from the south, Figure 8. These two water masses are formed in the surface of sub-polar region, and then sink during their way towards the lower latitudes.

Besides AAIW and SAIW here we also define MOW as an intermediate water mass in the north Atlantic since the MOW occupies a similar density range as AAIW and SAIW, although the formation is different. Schematic of main currents in the intermediate layer is shown in Figure 7.

3.2.1 Antarctic Intermediate Water (AAIW)

AAIW is the main water mass in the intermediate depth of the South Atlantic Ocean. This water mass originates from the surface layer (upper 200m) north of the Antarctic Circumpolar Current (ACC) and east of Drake Passage (Alvarez et al., 2014; McCartney, 1982). After formation AAIW subducts and spreads northward along the continental slope of South America (Piola and Gordon, 1989). AAIW can be found through most of the Atlantic Ocean at the depth between 500 and 1200m, below the layer of central water and above the deep waters (Talley, 1996). Two characteristic features of AAIW is low salinity and high oxygen concentration (Stramma and England, 1999).

Based on the work by Stramma and England (1999), we choose the region between 55 and 40°S (east of the Drake Passage) as the formation area of AAIW and look at depths below 200 m so that not only AAIW samples in the formation area but also some samples during the subduction and spreading in

the primary stage are considered. As for the boundaries between AAIW and surrounding SWTs, including SACW in the north and NADW in the deep, there are several slightly different definitions. Piola and Georgi (1982) and Talley (1996) define AAIW to have potential densities between 27.00-27.10 and 27.40 kg/m^3. Here however we follow Stramma and England (1999) that define the boundary between AAIW and SACW at σ_θ = 27.00 kg m^{-3} and the boundary between AAIW and NADW at σ_1 = 32.15 kg m^{-3}.

Although the density difference between AAIW and AABW is significant, in the formation areas, there is a direct contact between AAIW and AABW near Drake Strait. Since AABW is easily separated from AAIW on higher silicate concentrations we used silicate concentrations lower than 20 µmol kg^{-1} as a criteria for AAIW. Furthermore we used these criteria in our selection of AAIW: potential density between 26.95 and 27.50 kg m^{-3} and pressure within 300m. More criteria are required to identify AAIW with neighboring SWTs, since the formation area of AAIW is bordered with WSACW in the north and AABW in the south. High oxygen (> 230 µmol kg^{-1}) is the important sign that distinguishes AAIW from Central Waters (WSACW and ESACW), while relative high potential temperature (>-0.5 °C) and low silicate (< 30 µmol kg^{-1}) are differentiated standards between AAIW and AABW. As shown in Figure 8, most of the AAIW samples have a potential density between σ_θ = 27.00-27.40 kg m^{-3}; the few exceptions still adhere to the boundary σ_1 < 32.15 kg m^{-3}. The characteristics of AAIW show low salinity, high oxygen and low silicate concentrations compared to SACW and NADW, and low silicate concentration.

3.2.2 Subarctic Intermediate Water (SAIW)

Subarctic Intermediate Water (SAIW) originates from the surface layer of the western boundary of the North Atlantic Subpolar Gyre, along the Labrador Current (Lazier and Wright, 1993; Pickart et al., 1997). This SWT subducts and spreads southeast in the region north of the NAC, advects across the MAR and finally interacts with MOW, that comes from the eastern Atlantic below ENACW (Arhan, 1990; Arhan and King, 1995). The formation of SAIW is mixture of two surface water types: Water with high temperature and salinity carried by the NAC and cold and fresh water from the Labrador Current (Garcia-Ibanez et al., 2015; Read, 2000). In Garcia-Ibanez et al. (2015), there are two definitions of SAIW, $SAIW_6$, which is biased to the warmer and saltier NAC, and $SAIW_4$, which is closer to the cooler and fresher Labrador Current. In this study we discuss the combination of these two end-members when considering the whole Atlantic Ocean scale.

For the spatial boundaries we follow Arhan (1990) and choose longitudes between 35 and 55°W, and latitudes between 50 and 60 °N, i.e. the region along the Labrador Current and north of the NAC as the formation area of SAIW (Figure 9a). Within this area we follow Read (2000), and choose potential densities higher than 27.65 kg m^{-3} and potential temperature higher than 4.5 °C to define SAIW. Similar to the definition of AAIW, we include samples in the depth range from the MLD to 500m as the core layer of SAIW; this pressure includes formation and subduction of SAIW.

In the T-S relationship (Figure 9b), the mixing of two main sources, the warmer and saltier NAC and the colder and fresher Labrador Current, is evident. In Figure 9c we can see that this SWT is characterized by relative low potential temperature, salinity and silicate concentration but is high in oxygen

3.2.3 Mediterranean Overflow Water (MOW)

The predecessor of the Mediterranean Overflow Water (MOW) is Mediterranean Waters flowing out through the Strait of Gibraltar whose main component is modified Levantine Intermediate Water. This is a SWT characterized by high salinity and temperature and intermediate potential density in the Northeast Atlantic Ocean (Carracedo et al., 2016). After passing the Strait of Gibraltar, the Mediterranean water mixes rapidly with the overlying ENACW leading to a sharp decrease of salinity and potential density (Baringer and Price, 1997). In Gulf of Cadiz, the outflow of MOW turns into two branches: One branch continues to the west, descending the continental slope, mixing with surrounding water masses in the intermediate depth and influence the water mass composition as far west as the MAR (Price et al., 1993). The other branch spreads northwards along the coast of Iberian peninsula and along the European coast and its influence can be observed as far north as the Norwegian Sea (Reid, 1978, 1979).

Here we follow Baringer and Price (1997) and consider MOW to be represented by the high salinity (salinity between 36.35 and 36.65) samples west of the Strait of Gibraltar as a SWT in the Northeast Atlantic (Figure 10) although the Mediterranean waters in the Strait are characterized by salinity higher than 38.4).

Almost the entire Northeast Atlantic, east of the MAR, intermediate layer is influenced by MOW. As the most characteristic property of MOW is the high salinity, we display a salinity section plot (Figure 10d) of A05 cruise from 2005 (74AB2005050), where the high salinity of MOW can be seen and how the high salinity core erodes westward towards the MAR. The high potential temperature and salinity compared to other water samples at same depth, and the characteristically low and nutrient concentrations are evident in Figure 10b. Due to the limited number of samples (less than 200) within our definition of MOW in GLODAPv2, we refrain from showing the histogram. The properties of MOW can be seen in Figure 10 and Table 3.

3.3 The Deep and Overflow Layer

To the deep and overflow water masses belongs those below the Intermediate Layer, approximately from 1500 to 4000m, with potential densities between 27.7 and 27.88 kg m^{-3}. Relative high salinity in the deep (compared to the intermediate and bottom waters) is another significant property. The source region of these waters is confined to the North Atlantic, the formation areas and main currents in this layer are shown in Figure 11. The southward flow of NADW in the North Atlantic, as well as northward flow of AABW in the South Atlantic are indispensable components of Atlantic Meridional

Overturning Circulation (AMOC) (Lynch-Stieglitz et al., 2007) (Broecker and Denton, 1989; Elliot et al., 2002).

The North Atlantic Deep Water (NADW) is the main water mass in this layer. NADW is mainly formed in the Labrador Sea and Irminger Basin in relative high latitude region in North Atlantic by mixing of Labrador Sea Water and the two variations of overflow waters; ISOW and DSOW. We make a distinction of upper and lower NADW, the upper portion origins from LSW and lower portion origins from ISOW and DSOW. From the formation area, NADW spreads to the south mainly with the Deep Western Boundary Current (DWBC) (Dengler et al., 2004), through the most Atlantic Ocean until ~50 °S where it meets Antarctic Circumpolar Current. During the south way along DWBC, NADW also spreads significantly in the zonal direction, so that we can find NADW in the whole Atlantic basin at these densities (Lozier, 2012).

Both Denmark Strait Overflow Water (DSOW) and Iceland-Scotland Overflow water (ISOW) originate from Arctic Ocean and the Nordic Seas. In North Atlantic, these two water masses sink and flow west and east of Iceland respectively, and finally, they meet and mix with each other in the Irminger Basin (Stramma et al., 2004; Tanhua et al., 2005b). As two main contributions to the formation of lower portion of NADW, they play a significant role in AMOC. Here we show our analysis based on GLODAPv2 database and discuss DSOW and ISOW separately.

3.3.1 Labrador Sea Water (LSW)

As an important water mass by its own virtue and for the formation of North Atlantic Deep Water (NADW), LSW is predominant in mid-depth (between 1000m and 2500m depth) in the Labrador Sea region (Elliot et al., 2002). LSW is characterized by relative low salinity (lower than 34.9) and high oxygen concentration (~290 µmol kg^{-1}) (Talley and Mccartney, 1982). Another important criterion of LSW is the potential density (σ_θ), that ranges from 27.68 to 27.88 kg m^{-3} (Clarke and Gascard, 1983; Gascard and Clarke, 1983; Kieke et al., 2006; Stramma et al., 2004). In the large spatial scale, LSW can be considered as one water mass (Dickson and Brown, 1994), however significant differences of different "vintages" of LSW exitst (Kieke et al., 2006; Stramma et al., 2004). LSW can broadly be divided into upper Labrador Sea Water (uLSW) and classic Labrador Sea Water (cLSW) with the boundary between them at potential density of 27.74 kg m^{-3} (Kieke et al., 2007; Kieke et al., 2006; Smethie and Fine, 2001).

The following results show our analysis based on GLODAPv2 in the Labrador Sea and Irminger Basin, west of Mid-Atlantic-Ridge. For the purpose of our analysis (the whole scale of the Atlantic Ocean) we consider LSW as one integral water mass. Although the Labrador Sea is located in North Atlantic between the Labrador Peninsula and Greenland, for this analysis we consider the formation region of LSW (Figure 12a). Within this geographical region we follow the definition from Clarke and Gascard

(1983) and Stramma and England (1999), defining LSW as samples with potential density (σ_θ) between 27.68 to 27.88 kg m^{-3} (Figure 12b) in the depth range of 500-2000m (Elliot et al., 2002).

Obvious characteristics of LSW are relative low salinity and high oxygen concentration is obvious. Figure 12c shows the histogram of all samples that we consider to represent LSW in this analysis. The relatively large spread in properties is indicative of the different "vintages" of LSW, in particular the bi-modal distribution of density, and partly for oxygen.

3.3.2 Denmark Strait Overflow Water (DSOW)

In North Atlantic, a number of water masses from the Arctic Ocean and the Nordic Seas flows through Denmark Strait west of Iceland. At the sill of the Denmark Strait and during the descent into the Irminger Sea these water masses undergo intense mixing. Here we use samples from the Irminger Sea with potential density higher than 27.88 kg m^{-3} (Tanhua et al., 2005b) for our definition of DSOW. In addition we require the silicate concentration to be lower than 11 µmol kg^{-1} to distinguish DSOW from NEABW, which has a high silicate concentration.

As shown in Figure 13b DSOW is mostly found close to the bottom between 2000 and 4000m, as expected for an overflow water. In addition to the high density and low temperature DSOW also has high oxygen concentration (~ 290-310 µmol kg^{-1}).

3.3.3 Iceland-Scotland Overflow Water (ISOW)

The Iceland Scotland Overflow Water, ISOW, flows from the Iceland Sea to the North Atlantic in the region east of Iceland, mainly through the Faroe-Bank Channel close to the bottom. ISOW flows and turn into two main branches when passing the Charlie-Gibbs Fracture Zone (CGFZ). The first one flows through the Mid-Atlantic-Ridge, into the Irminger basin, meets and mixes with DSOW there, and finally joins the lower portion of NADW. The other branch goes southward and mixes with Northeast Atlantic Bottom Water (NEABW) (Garcia-Ibanez et al., 2015). The pathway of ISOW closely follows the Mid-Atlantic-Ridge in the Iceland Basin where also NEABW could be found, characterized by high nutrient and low oxygen concentration. In order to safely distinguish ISOW from LSW in the region west of MAR, we define ISOW as samples with salinity higher than 34.95, potential density higher than 27.83 kg m^{-3}. Figure 14 displays our characterization of ISOW based on GLODAPv2 in the Iceland Basin, which is consistent from the result in the literature (Garcia-Ibanez et al., 2015).

3.3.4 Upper North Atlantic Deep Water (uNADW)

The uNADW is formed by mixing of mainly ISOW and LSW and we consider this to be a distinct water mass just south of the Labrador Sea as this region is identified as the formation area of upper and lower NADW (Dickson and Brown, 1994).

We select the region between latitude 40 and 50°N, west of the MAR as the formation area of NADW (Figure 15b) and use the criteria of potential density between 27.72 and 27.82 kg m^{-3} with depth range from 1200 to 2000m to define the upper NADW (Stramma et al., 2004).

As a product of mixing from LSW and ISOW, upper NADW inherits main properties from LSW but also contains some of characteristics from ISOW. Relative low salinity and high salinity is still significant features of uNADW. However, as shown in Figure 15d, relatively increased salinity and decreased oxygen concentration can be found due to the impact from ISOW. Furthermore, ISOW also brings slight increase of nutrients including silicate, phosphate and nitrate.

3.3.5 Lower North Atlantic Deep Water (lNADW)

We select water samples from the same geographic region as upper NADW to define the lower NADW. Below the uNADW in this region, ISOW and DSOW (with influence of LSW) mix with each other and form the lower portion of NADW (Stramma et al., 2004). We use water samples found at depths between 2000 and 3000 m with potential densities between 27.76 and 27.88 kg m^{-3} to define lower NADW.

From the data shown on Figure 16d, we can see lower NADW has properties more inclined to ISOW compared with DSOW. For instance, values of salinity and oxygen concentration are between ISOW and DSOW but obviously closer to ISOW. The nutrients, lower NADW have almost the same values to ISOW, further verified this inference. High potential temperature shows that the impact from LSW to lower NADW cannot be ignored.

3.4 The Bottom Layer

We define bottom waters as the densest water masses that occupy the lowest layers of the water column, typically below 4000 m depth and with potential densities higher than 27.88 kg m^{-3}. These water masses have an origin in the Southern Ocean (Figure 17) and are also characterized by their high silicate concentrations (higher than 100 μmol kg^{-1}), in addition to the high densities.

Antarctic Bottom Water (AABW) is the main water mass in the bottom layer, and is formed in the Weddell Sea region, south of Antarctic Circumpolar Current (ACC) through mixing of Circumpolar Deep Water (CDW) and Weddell Sea Bottom Water (WSBW) (van Heuven et al., 2011). After the formation, AABW spreads to the north across the equator and further northwards until ~40 °N, where we define this water mass as North East Atlantic Bottom Water (NEABW).

3.4.1 Antarctic Bottom Water (AABW)

Antarctic Bottom Water (AABW) is the main bottom water in the South Atlantic Ocean and is also an important bottom water mass in the North Atlantic. As one of the important components in Atlantic Meridional Overturning Circulation (AMOC), AABW spreads northward below 4000m depth, mainly

west of Mid-Atlantic-Ridge (MAR) and plays a significant role in the Thermohaline Circulation (Andrié et al., 2003; Rhein et al., 1998). The origin of AABW in Atlantic section can be traced back to the Weddell Sea as a product of mixing of Weddell Sea Bottom Water (WSBW) and Circumpolar Deep Water (CDW) (Alvarez et al., 2014; Foldvik and Gammelsrod, 1988).

The definition of AABW is all water samples formed south of the Antarctic Circumpolar Current (ACC), i.e. south of 63°S in the Weddell Sea, with neutral density (γ) larger than 28.27 kg m^{-3} (Orsi et al., 1999; Weiss et al., 1979). As an additional constraint we define AABW as water samples with silicate higher than 120 µmol kg^{-1} to distinguish AABW from other water masses in this region as high silicate is a trade mark characteristic of AABW. The main source region of AABW is the Weddell Sea.

In Figure 18, we can see clearly that there are two main original water masses (red points) in the selected formation area of AABW (blue points). This result is also consistent with Orsi et al. (1999) and van Heuven et al. (2011). The first water mass is the relative warm (θ>0 °C) remnants from CDW, which comes with the ACC from the north. The other one, which is the extremely cold Shelf Water (θ<-1.0°C) comes as Weddell Sea Bottom Water (WSBW) from the south. As shown in Figure 18 we find AABW from 1000m to 5500m depth. The characterisitc properties of AABW is the low temperature (θ<0 °C), salinity (<34.68) and high nutrient concentration, especially the high silicate concentrations. In Figure 17c we can see a relative complex distribution of potential temperature, probably due to the mixing between different water masses with quite different temperatures (warm CDW and cold shelf water) that forms AABW.

3.4.2 Northeast Atlantic Bottom Water (NEABW)

Northeast Atlantic Bottom Water (NEABW), also called lower Northeast Atlantic Deep Water (lNEADW in Garcia-Ibanez et al. (2015)), is mainly found below 4000m depth in the eastern basin of the North Atlantic. This water mass is an extension of AABW during the way to the north, since the characteristics of AABW changes significantly on the slow transport north we choose to define this as a new water mass north of the Equator, similar to the formation of NADW south of the Labrador Sea.

To define we choose the region east of the MAR and between the equator and 30 °N, i.e. before NEABW enters the Iberian Basin, as the formation area (Figure 19). We also use the criteria of water samples from a depth deeper than 4000m and potential temperature above 1.8 °C. In the T-S diagram of NEABW (Figure 19) we can see the linear T-S relationship similar to AABW in the Weddell Sea, but with significantly higher potential temperatures and salinities, roughly 1.95 °C and 34.887, respectively. Most NEABW samples have a potential density higher than 27.88 kg m^{-3} and NEABW is characterized by low potential temperature (θ), low salinity but high silicate concentration. This shows that NEABW originates from AABW, although most properties have been changed significantly from the South Atlantic.

3.4.3 Circumpolar Deep Water (CDW) / Warm Deep Water (WDW)

Circumpolar Deep Water (CDW) or, as it is also called, Warm Deep Water (WDW), is the lighter of the two SWTs that constitutes AABW. In our study we consider water mass that mixes with WSBW directly as CDW (WDW in van Heuven et al. (2011)) and the region between 55 and 65 °S as the formation area. The origin of CDW can be tracked to the southward flow of NADW. At about 50°S NADW is deflected upward by AABW before reaching the ACC area, this NADW mixes with other water masses in ACC and forms a new water mass called CDW. Then CDW flows further southward and passes the ACC.

To specify CDW we selected water samples with from depth between 200 and 1000m in the region east of 60°W between 55 and 65°S as the core of CDW. We also placed the additional constraints of having salinity lower than 34.64 and potential density higher than 27.80 kg m^{-3}. The properties of CDW are shown in Figure 20. Similar to other bottom SWTs, CDW is characterized by high nutrient concentrations (silicate, phosphate and nitrate) and low oxygen concentration. The potential temperature of CDW is between 0 and 1 °C while the potential density is larger than 27.8 kg m^{-3}, and the salinity higher than 34.63.

3.4.4 Weddell Sea Bottom Water (WSBW)

The Weddell Sea Bottom Water (WSBW) is the denser SWT that takes part in the formation of AABW. Similar to CDW, WSBW is also formed in the Weddell Sea region, relative warm water (σ_θ > 0 °C) flows southward and cools down to σ_θ lower than -1°C by mixing with extremely cold shelf water that is transported down along the continental slop. WSBW is thus formed in the Weddell Sea basin below the depth of 3000m, before it meets and mixes with CDW/WDW. Compared with CDW, its low potential temperature is a significant property of WSBW (van Heuven et al., 2011).

We follow van Heuven et al. (2011) and choose water samples in the latitudinal boundaries of 55 - 65 °S in the Weddell Sea with pressures larger than 3000 m as the formation core area. We additionally constrain our selection to samples with potential temperature lower than -0.7 °C and silicate higher than 105 µmol/kg. The properties of WSBW are shown in Figures 21a and b. In addition to the physical properties, such as low potential temperature and high potential density, WSBW has high nutrient concentrations, but dislike CDW, WSBW has high oxygen concentration.

4. Discussion

We have defined Atlantic Ocean Water Masses (WMs) in their formation area as source water types (SWTs) in a 7-dimensional hydrochemical space. The properties of SWTs are important since this is the fundamental basis to label and investigate water mass transport, distribution and mixing. Table 3 provides an overview of the properties, and the standard deviation, of the 16 Atlantic Ocean SWTs considered in this study. We used seven often measured hydrochemical and physical variables to

characterize 16 main SWTs in the Atlantic Ocean. To guide the water mass descriptions we divided the distribution of SWTs into four main vertical layers roughly separated by potential density in the shallow and concentration of silicate in the deep southern Hemisphere. The upper layer (σ_Θ<27.00 kg m^{-3}) occupies the most shallow layer (typically down to about 500 m depth) of the ocean below the mixed layer, that we do not consider in this analysis. The upper layer is occupied by central waters: ENACW, WNACW, WSACW and ESACW, mainly characterized by relative high potential temperature and salinity. The intermediate layer is situated between the upper layer and the deep layer at roughly 1000 and 2000m depth. Of the three SWTs in this layer, AAIW and SAIW are both characterized have relative low salinity and temperature, while the MOW has high salinity and temperature. In the deep and overflow layer between roughly 2000 and 4000m we find SWTs with an origin in the north Atlantic. The bottom layer is occupied by SWTs with a southern origin; these are very cold SWTs with high densities and silicate concentrations.

In Figure 22 we show an overview of the position of the SWTs in a Salinity-Temperature plot where we plotted the SWTs from the different layers in different colors. It is obvious that a range of additional variables other than temperature and salinity is helpful, if not necessary, to reliable distinguish different water masses from each other, and to calculate the mixing ratios of water masses in a water sample with a particular characteristic.

The here presented characteristics and (property value and the standard deviation) of Atlantic Ocean SWTs is intended to guide water mass analysis of hydrographic data.

Acknowledgements

This work is based on the comprehensive and detailed data from GLODAP data set throughout the past few decades. In particular, we are grateful to the efforts from all the scientists and crews on cruises, who generated funding and dedicated time on committing the collection of data. We also would like to thank the working groups of GLODAP for their support and information of the collation, quality control and publishing of data. Their contributions and selfless sharing are prerequisites for the completion of this work. Thanks to the China Scholarship Council (CSC) for providing funding support to Mian Liu's PhD study in GEOMAR Helmholtz Centre for Ocean Research Kiel.

References

Alvarez, M., Brea, S., Mercier, H., Alvarez-Salgado, X.A., 2014. Mineralization of biogenic materials in the water masses of the South Atlantic Ocean. I: Assessment and results of an optimum multiparameter analysis. Prog Oceanogr 123, 1-23.

Andrié, C., Gouriou, Y., Bourlès, B., Ternon, J.F., Braga, E.S., Morin, P., Oudot, C., 2003. Variability of AABW properties in the equatorial channel at 35°W. Geophysical Research Letters 30, n/a-n/a.

Arhan, M., 1990. The North Atlantic current and subarctic intermediate water. J Mar Res 48, 109-144.

Arhan, M., King, B., 1995. Lateral Mixing of the Mediterranean Water in the Eastern North-Atlantic. J Mar Res 53, 865-895.

Baringer, M.O., Price, J.F., 1997. Mixing and spreading of the Mediterranean outflow. Journal of Physical Oceanography 27, 1654-1677.

Broecker, W.S., Denton, G.H., 1989. The Role of Ocean-Atmosphere Reorganizations in Glacial Cycles. Geochimica Et Cosmochimica Acta 53, 2465-2501.

Carracedo, L., Pardo, P.C., Flecha, S., Pérez, F.F., 2016. On the Mediterranean Water Composition. Journal of Physical Oceanography 46, 1339-1358.

Castro, C.G., Perez, F.F., Holley, S.E., Rios, A.F., 1998. Chemical characterisation and modelling of water masses in the Northeast Atlantic. Prog Oceanogr 41, 249-279.

Cianca, A., Santana, R., Marrero, J., Rueda, M., Llinás, O., 2009. Modal composition of the central water in the North Atlantic subtropical gyre. Ocean Science Discussions 6, 2487-2506.

Clarke, R.A., Gascard, J.-C., 1983. The Formation of Labrador Sea Water. Part I: Large-Scale Processes. Journal of Physical Oceanography 13, 1764-1778.

Defant, A., 1929. Dynamische Ozeanographie. Springer.

Dengler, M., Schott, F.A., Eden, C., Brandt, P., Fischer, J., Zantopp, R.J., 2004. Break-up of the Atlantic deep western boundary current into eddies at 8° S. Nature 432, 1018.

Deruijter, W., 1982. Asymptotic Analysis of the Agulhas and Brazil Current Systems. Journal of Physical Oceanography 12, 361-373.

Dickson, R.R., Brown, J., 1994. The Production of North-Atlantic Deep-Water - Sources, Rates, and Pathways. J Geophys Res-Oceans 99, 12319-12341.

Elliot, M., Labeyrie, L., Duplessy, J.C., 2002. Changes in North Atlantic deep-water formation associated with the Dansgaard-Oeschger temperature oscillations (60-10 ka). Quaternary Science Reviews 21, 1153-1165.

Emery, W.J., Meincke, J., 1986. Global Water Masses - Summary and Review. Oceanologica Acta 9, 383-391.

Foldvik, A., Gammelsrod, T., 1988. Notes on Southern-Ocean Hydrography, Sea-Ice and Bottom Water Formation. Palaeogeography Palaeoclimatology Palaeoecology 67, 3-17.

Garcia-Ibanez, M.I., Pardo, P.C., Carracedo, L.I., Mercier, H., Lherminier, P., Rios, A.F., Perez, F.F., 2015. Structure, transports and transformations of the water masses in the Atlantic Subpolar Gyre. Prog Oceanogr 135, 18-36.

Gascard, J.-C., Clarke, R.A., 1983. The Formation of Labrador Sea Water. Part II. Mesoscale and Smaller-Scale Processes. Journal of Physical Oceanography 13, 1779-1797.

Gordon, A.L., Weiss, R.F., Smethie, W.M., Warner, M.J., 1992. Thermocline and Intermediate Water Communication between the South-Atlantic and Indian Oceans. J Geophys Res-Oceans 97, 7223-7240.

Haine, T.W.N., Hall, T.M., 2002. A generalized transport theory: Water-mass composition and age. Journal of Physical Oceanography 32, 1932-1946.

Harvey, J., 1982. Theta-S Relationships and Water Masses in the Eastern North-Atlantic. Deep-Sea Research Part a-Oceanographic Research Papers 29, 1021-1033.

Helland-Hansen, B.r., 1916. Nogen hydrografiske metoder. Scand. Naturforsker Mote. Kristiana. Oslo.

Jullion, L., Jacquet, S., Tanhua, T., 2017. Untangling biogeochemical processes from the impact of ocean circulation: First insight on the Mediterranean dissolved barium dynamics. Global Biogeochemical Cycles 31, 1256-1270.

Key, R.M., Tanhua, T., Olsen, A., Hoppema, M., Jutterström, S., Schirnick, C., van Heuven, S., Kozyr, A., Lin, X., Velo, A., Wallace, D.W.R., Mintrop, L., 2010. The CARINA data synthesis project: introduction and overview. Earth Syst. Sci. Data 2, 105-121.

Kieke, D., Rhein, M., Stramma, L., Smethie, W.M., Bullister, J.L., LeBel, D.A., 2007. Changes in the pool of Labrador Sea Water in the subpolar North Atlantic. Geophysical Research Letters 34.

Kieke, D., Rhein, M., Stramma, L., Smethie, W.M., LeBel, D.A., Zenk, W., 2006. Changes in the CFC inventories and formation rates of Upper Labrador Sea Water, 1997-2001. Journal of Physical Oceanography 36, 64-86.

Klein, B., Hogg, N., 1996. On the variability of 18 Degree Water formation as observed from moored instruments at 55 degrees W. Deep-Sea Research Part I-Oceanographic Research Papers 43, 1777-&.

Kuhlbrodt, T., Griesel, A., Montoya, M., Levermann, A., Hofmann, M., Rahmstorf, S., 2007. On the driving processes of the Atlantic meridional overturning circulation. Reviews of Geophysics 45.

Lauvset, S.K., Key, R.M., Olsen, A., van Heuven, S., Velo, A., Lin, X., Schirnick, C., Kozyr, A., Tanhua, T., Hoppema, M., Jutterström, S., Steinfeldt, R., Jeansson, E., Ishii, M., Perez, F.F., Suzuki, T., Watelet, S., 2016. A new global interior ocean mapped climatology: the 1° × 1° GLODAP version 2. Earth Syst. Sci. Data 8, 325-340.

Lazier, J.R.N., Wright, D.G., 1993. Annual Velocity Variations in the Labrador Current. Journal of Physical Oceanography 23, 659-678.

Lozier, M.S., 2012. Overturning in the North Atlantic. Ann Rev Mar Sci 4, 291-315.

Lutjeharms, J.R., van Ballegooyen, R.C., 1988. Anomalous upstream retroflection in the agulhas current. Science 240, 1770.

Lynch-Stieglitz, J., Adkins, J.F., Curry, W.B., Dokken, T., Hall, I.R., Herguera, J.C., Hirschi, J.J., Ivanova, E.V., Kissel, C., Marchal, O., Marchitto, T.M., McCave, I.N., McManus, J.F., Mulitza, S., Ninnemann, U.,

Peeters, F., Yu, E.F., Zahn, R., 2007. Atlantic meridional overturning circulation during the Last Glacial Maximum. Science 316, 66-69.

McCartney, M.S., 1982. The subtropical recirculation of Mode Waters. J Mar Res 40, 427-464.

McCartney, M.S., Talley, L.D., 1982. The subpolar mode water of the North Atlantic Ocean. Journal of Physical Oceanography 12, 1169-1188.

Montgomery, R.B., 1958. Water characteristics of Atlantic Ocean and of world ocean. Deep Sea Research (1953) 5, 134-148.

Orsi, A.H., Johnson, G.C., Bullister, J.L., 1999. Circulation, mixing, and production of Antarctic Bottom Water. Prog Oceanogr 43, 55-109.

Peterson, R.G., Stramma, L., 1991. Upper-Level Circulation in the South-Atlantic Ocean. Prog Oceanogr 26, 1-73.

Pickart, R.S., Spall, M.A., Lazier, J.R.N., 1997. Mid-depth ventilation in the western boundary current system of the sub-polar gyre. Deep-Sea Research Part I-Oceanographic Research Papers 44, 1025-+.

Piola, A.R., Georgi, D.T., 1982. Circumpolar properties of Antarctic intermediate water and Subantarctic Mode Water. Deep Sea Research Part A. Oceanographic Research Papers 29, 687-711.

Piola, A.R., Gordon, A.L., 1989. Intermediate Waters in the Southwest South-Atlantic. Deep-Sea Research Part a-Oceanographic Research Papers 36, 1-16.

Pollard, R.T., Griffiths, M.J., Cunningham, S.A., Read, J.F., Perez, F.F., Rios, A.F., 1996. Vivaldi 1991-A study of the formation, circulation and ventilation of Eastern North Atlantic Central Water. Prog Oceanogr 37, 167-192.

Pollard, R.T., Pu, S., 1985. Structure and Circulation of the Upper Atlantic Ocean Northeast of the Azores. Prog Oceanogr 14, 443-462.

Price, J.F., Baringer, M.O., Lueck, R.G., Johnson, G.C., Ambar, I., Parrilla, G., Cantos, A., Kennelly, M.A., Sanford, T.B., 1993. Mediterranean outflow mixing and dynamics. Science 259, 1277-1282.

Prieto, E., Gonzalez-Pola, C., Lavin, A., Holliday, N.P., 2015. Interannual variability of the northwestern Iberia deep ocean: Response to large-scale North Atlantic forcing. J Geophys Res-Oceans 120, 832-847.

Read, J., 2000. CONVEX-91: water masses and circulation of the Northeast Atlantic subpolar gyre. Prog Oceanogr 48, 461-510.

Reid, J.L., 1978. On the middepth circulation and salinity field in the North Atlantic Ocean. Journal of Geophysical Research: Oceans 83, 5063-5067.

Reid, J.L., 1979. On the contribution of the Mediterranean Sea outflow to the Norwegian-Greenland Sea. Deep Sea Research Part A. Oceanographic Research Papers 26, 1199-1223.

Rhein, M., Stramma, L., Krahmann, G., 1998. The spreading of Antarctic bottom water in the tropical Atlantic. Deep-Sea Research Part I-Oceanographic Research Papers 45, 507-527.

Schaffer, A.J., JACOBSEN, A.W., 1927. Mikulicz's syndrome: a report of ten cases. American Journal of Diseases of Children 34, 327-346.

Smethie, W.M., Fine, R.A., 2001. Rates of North Atlantic Deep Water formation calculated from chlorofluorocarbon inventories. Deep-Sea Research Part I-Oceanographic Research Papers 48, 189-215.

Sprintall, J., Tomczak, M., 1993. On the formation of Central Water and thermocline ventilation in the southern hemisphere. Deep Sea Research Part I: Oceanographic Research Papers 40, 827-848.

Stramma, L., England, M.H., 1999. On the water masses and mean circulation of the South Atlantic Ocean. J Geophys Res-Oceans 104, 20863-20883.

Stramma, L., Kieke, D., Rhein, M., Schott, F., Yashayaev, I., Koltermann, K.P., 2004. Deep water changes at the western boundary of the subpolar North Atlantic during 1996 to 2001. Deep Sea Research Part I: Oceanographic Research Papers 51, 1033-1056.

Stramma, L., Peterson, R.G., 1990. The South-Atlantic Current. Journal of Physical Oceanography 20, 846-859.

Talley, L., 1996. Antarctic intermediate water in the South Atlantic, The South Atlantic. Springer, pp. 219-238.

Talley, L., Raymer, M., 1982. Eighteen degree water variability. J. Mar. Res 40, 757-775.

Talley, L.D., Mccartney, M.S., 1982. Distribution and Circulation of Labrador Sea-Water. Journal of Physical Oceanography 12, 1189-1205.

Tanhua, T., Olsson, K.A., Jeansson, E., 2005. Formation of Denmark Strait overflow water and its hydro-chemical composition. Journal of Marine Systems 57, 264-288.

Tomczak, M., 1981. A multi-parameter extension of temperature/salinity diagram techniques for the analysis of non-isopycnal mixing. Prog Oceanogr 10, 147-171.

Tomczak, M., 1999. Some historical, theoretical and applied aspects of quantitative water mass analysis. J Mar Res 57, 275-303.

Tomczak, M., Godfrey, J.S., 2013. Regional oceanography: an introduction. Elsevier.

Tomczak, M., Large, D.G.B., 1989. Optimum Multiparameter Analysis of Mixing in the Thermocline of the Eastern Indian-Ocean. J Geophys Res-Oceans 94, 16141-16149.

van Heuven, S.M.A.C., Hoppema, M., Huhn, O., Slagter, H.A., de Baar, H.J.W., 2011. Direct observation of increasing CO2 in the Weddell Gyre along the Prime Meridian during 1973–2008. Deep Sea Research Part II: Topical Studies in Oceanography 58, 2613-2635.

Weiss, R.F., Ostlund, H.G., Craig, H., 1979. Geochemical Studies of the Weddell Sea. Deep-Sea Research Part a-Oceanographic Research Papers 26, 1093-1120.

Worthington, L., 1959. The 18 water in the Sargasso Sea. Deep Sea Research (1953) 5, 297-305.

Wüst, G., Defant, A., 1936. Atlas zur Schichtung und Zirkulation des Atlantischen Ozeans: Schnitte und Karten von Temperatur, Salzgehalt und Dichte. W. de Gruyter.

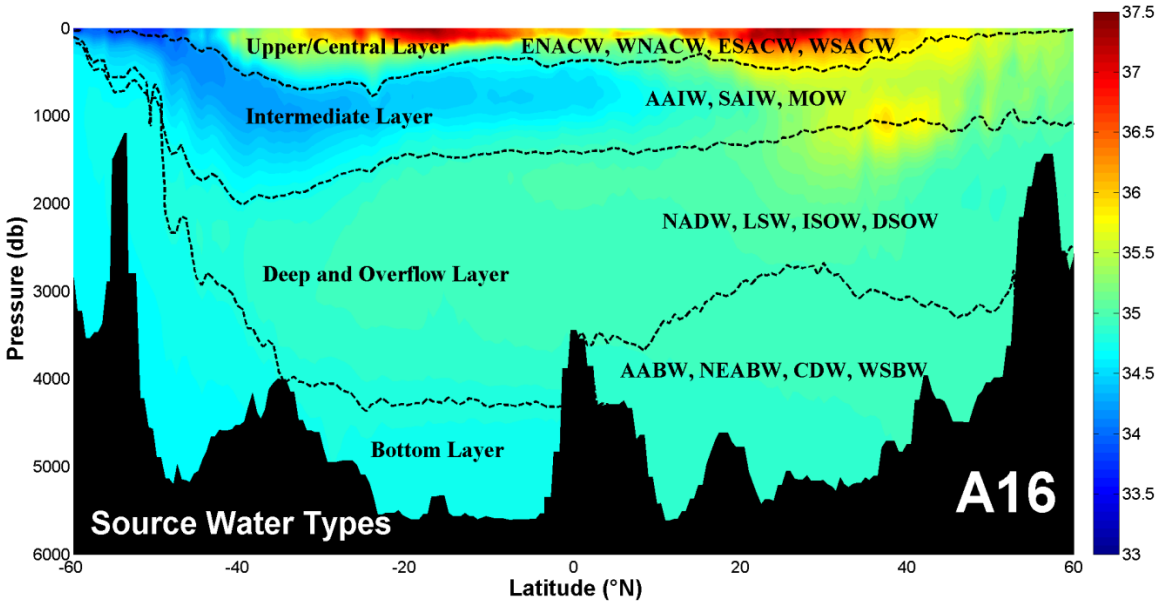

Figure 1: *Salinity section from the A16 GO-SHIP cruises in 2013*

(Expocode 33RO20130803 in North Atlantic & 33RO20131223 in South Atlantic)

The dashed lines show the four vertical layers divided by potential density except for the boundary between the deep and bottom layers in the south hemisphere which is based on the concentration of silicate.

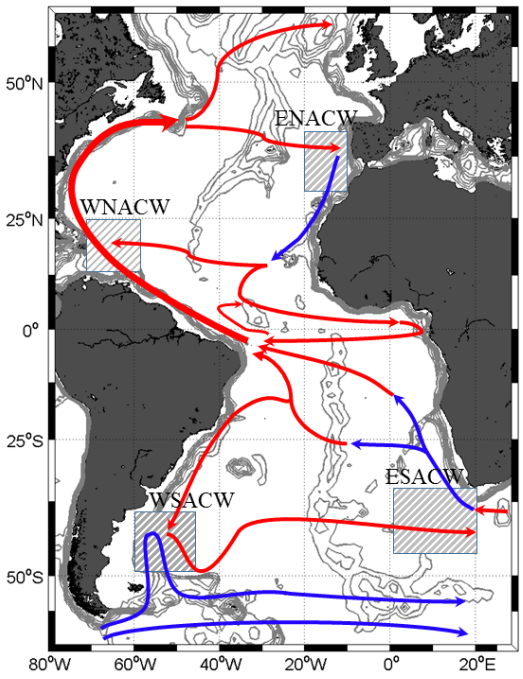

Figure 2*: The water mass formation areas and the schematic of main currents (Warm currents in red and cold currents in blue) in the Upper Layer.*

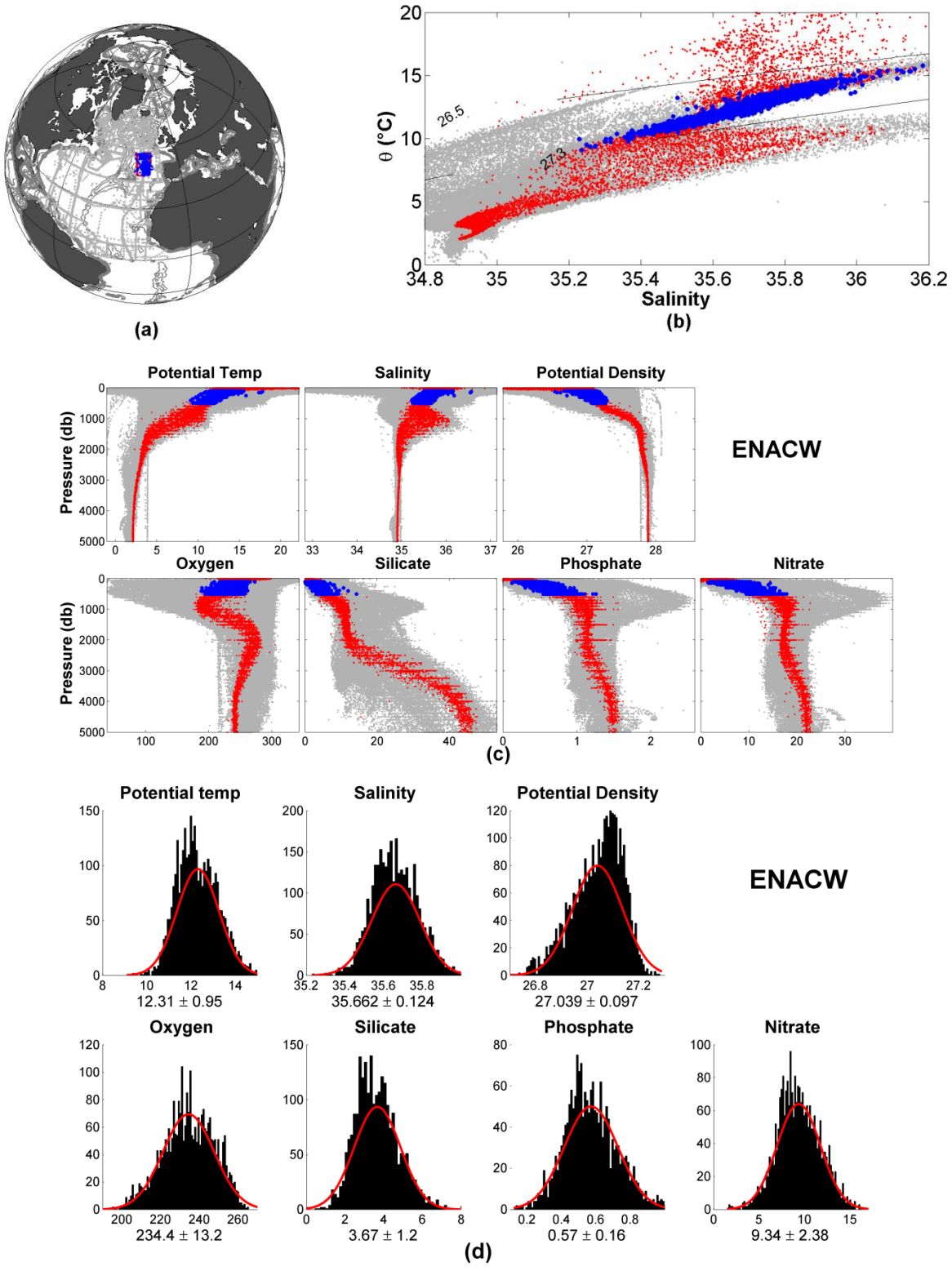

Figure 3: *Overview of Eastern North Atlantic Central Water (ENACW): Panel a) shows the formation area used to define the water mass, panel b) show a T-S diagram and panel c) the distribution of key properties vs. pressure. In panel d) we show bar plots of the data distribution of samples used to define the water mass. Potential Temperature in (°C), Potential Density in kg/m^3, Oxygen and nutrients in µmol/kg^3. The red Gaussian fit shows mean and σ based on selected data.*

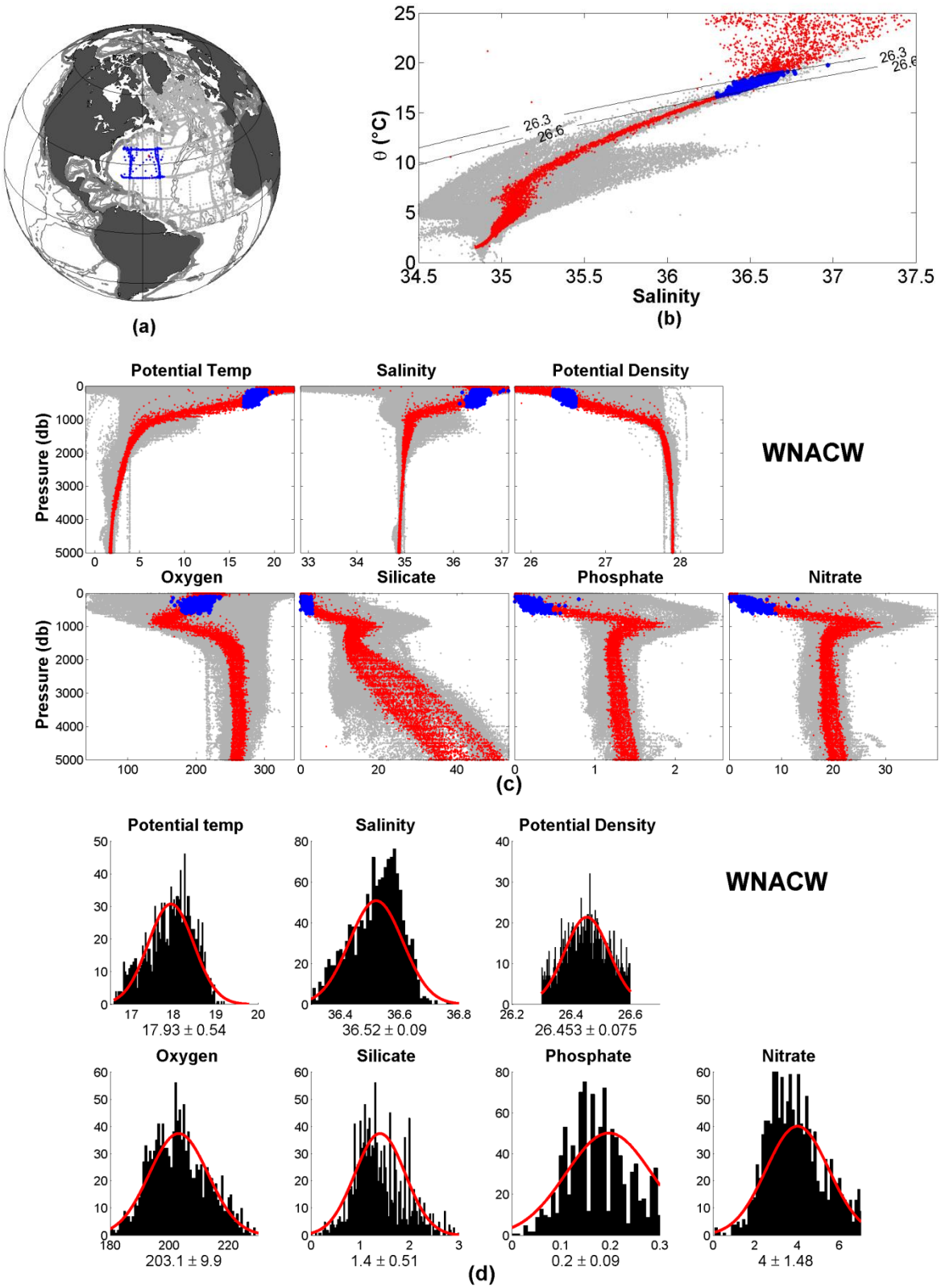

Figure 4: *Overview of Western North Atlantic Central Water (WNACW): Panel a) shows the formation area used to define the water mass, panel b) show a T-S diagram and panel c) the distribution of key properties vs. pressure. In panel d) we show bar plots of the data distribution of samples used to define the water mass. Potential Temperature in (°C), Potential Density in kg/m^3, Oxygen and nutrients in µmol/kg^3. The red Gaussian fit shows mean and σ based on selected data.*

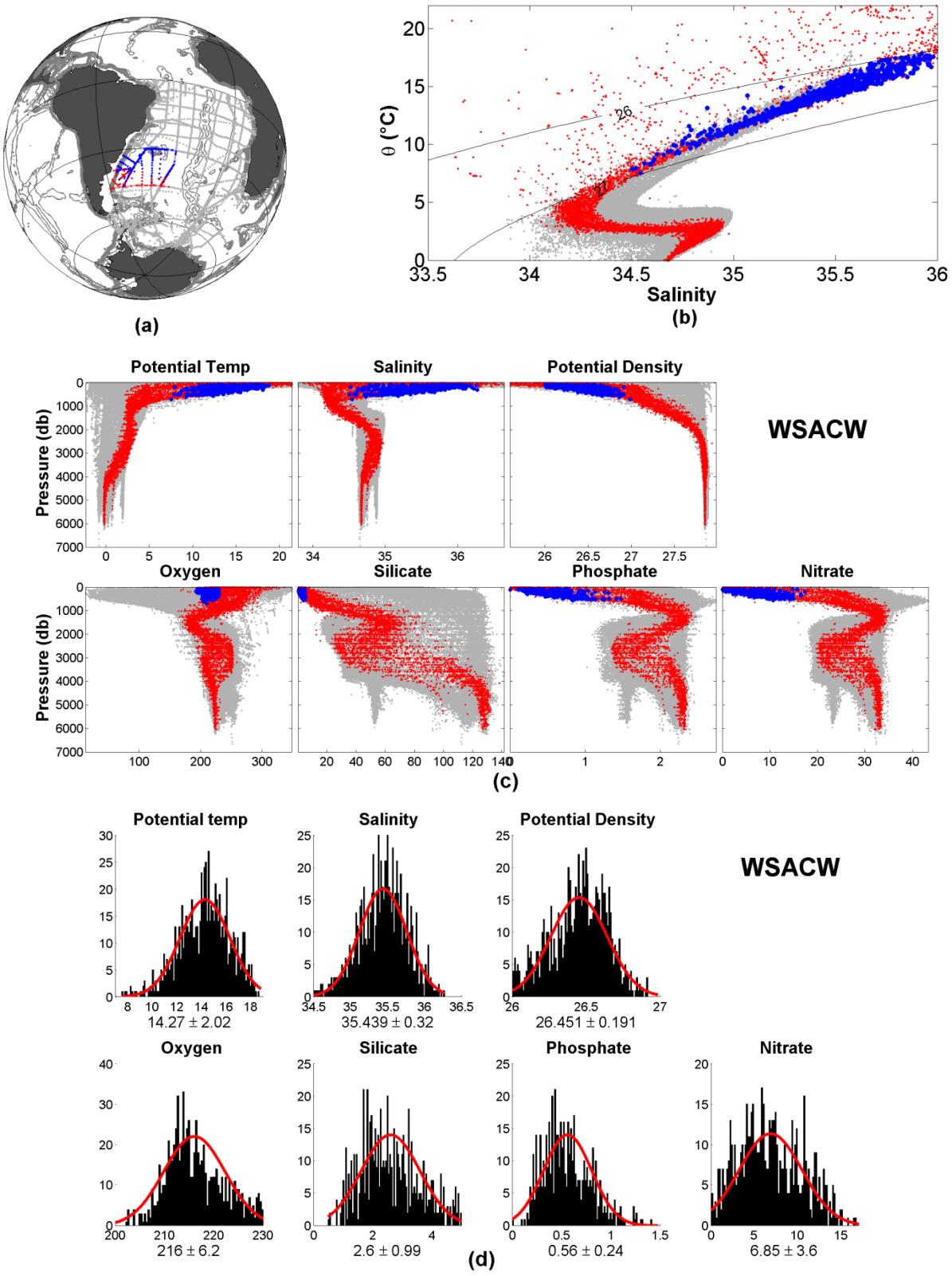

Figure 5: *Overview of Western South Atlantic Central Water (WSACW): Panel a) shows the formation area used to define the water mass, panel b) show a T-S diagram and panel c) the distribution of key properties vs. pressure. In panel d) we show bar plots of the data distribution of samples used to define the water mass. Potential Temperature in (°C), Potential Density in kg/m^3, Oxygen and nutrients in µmol/kg^3. The red Gaussian fit shows mean and σ based on selected data.*

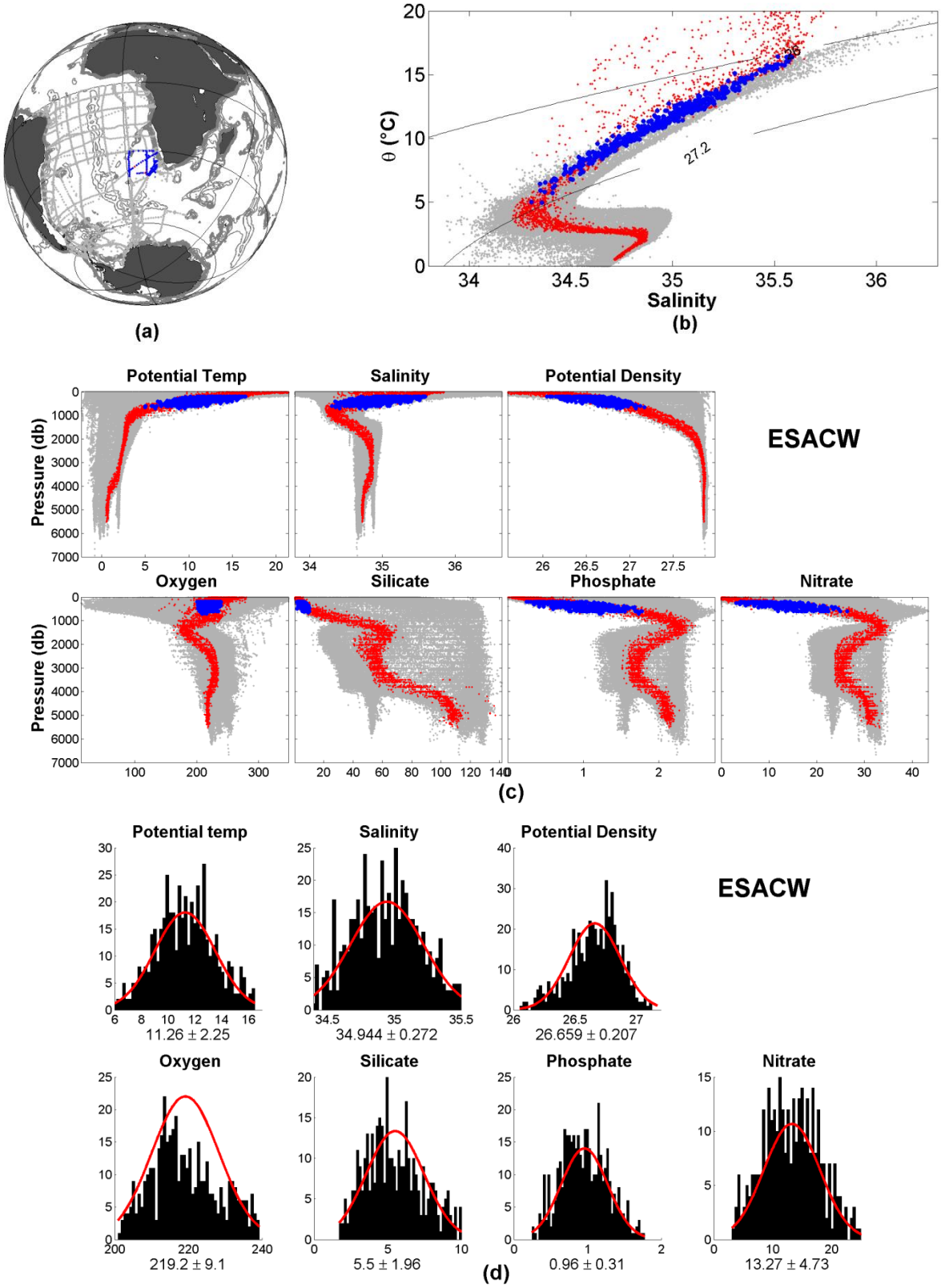

Figure 6: *Overview of Eastern South Atlantic Central Water (ESACW): Panel a) shows the formation area used to define the water mass, panel b) show a T-S diagram and panel c) the distribution of key properties vs. pressure. In panel d) we show bar plots of the data distribution of samples used to define the water mass. Potential Temperature in (°C), Potential Density in kg/m^3, Oxygen and nutrients in µmol/kg^3. The red Gaussian fit shows mean and σ based on selected data.*

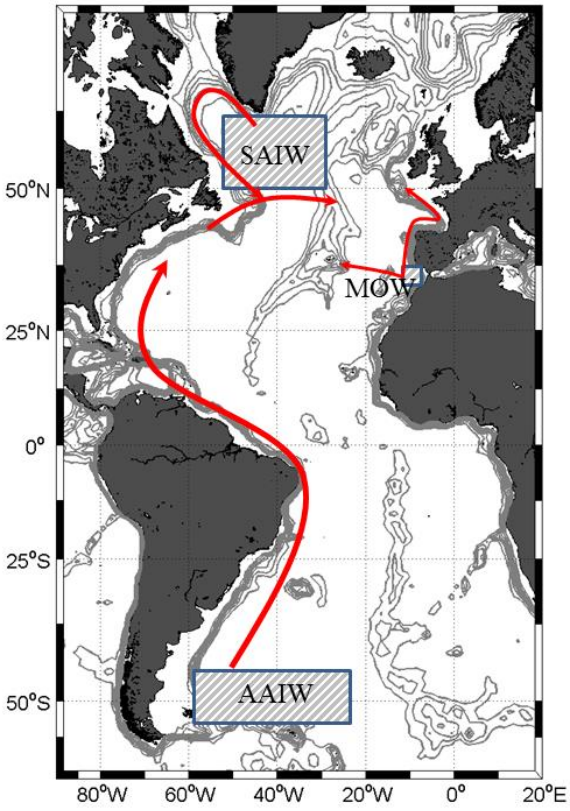

***Figure 7**: The water mass formation areas and the schematic of main currents in the Intermediate Layer*

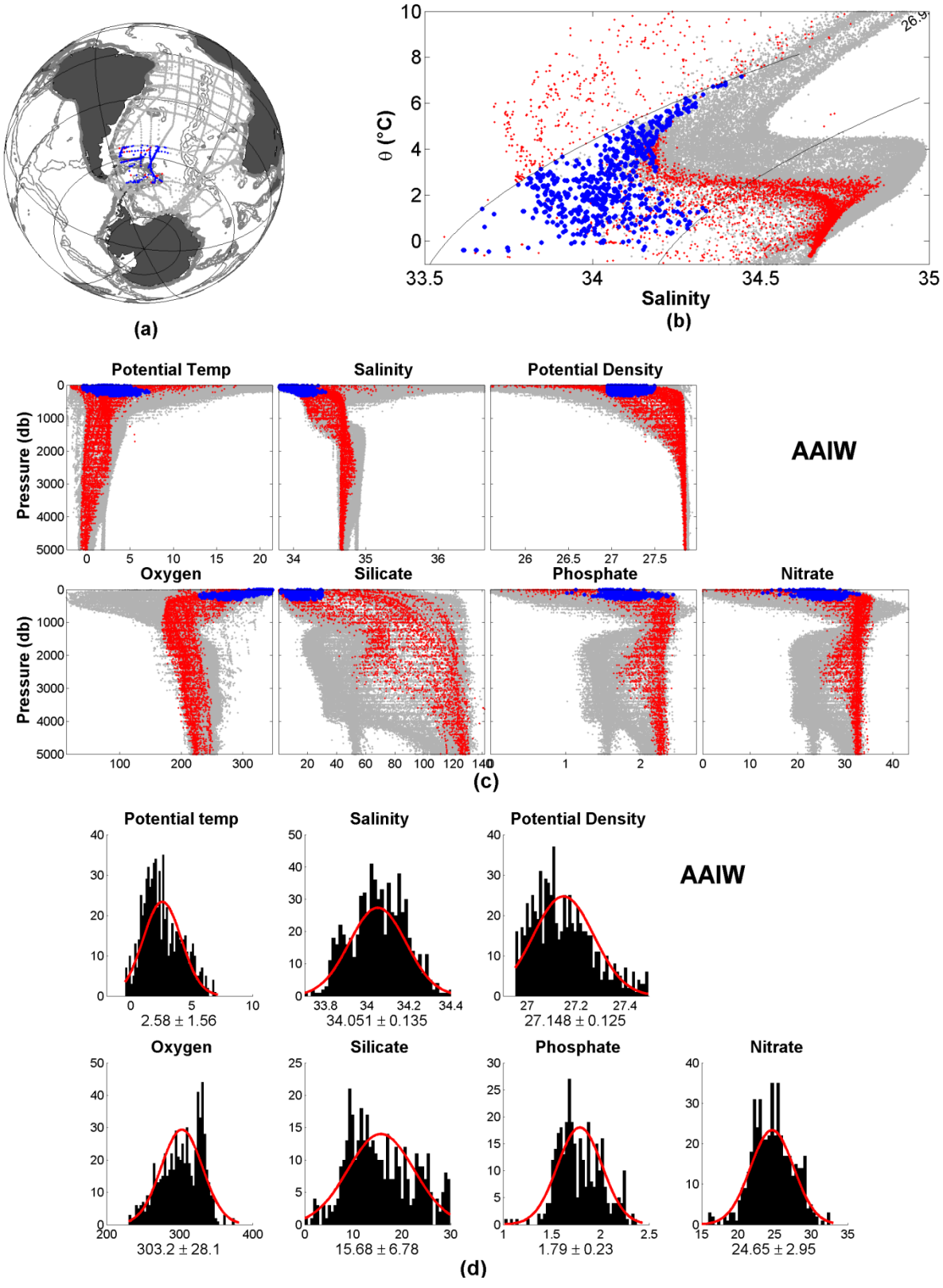

Figure 8: *Overview of Antarctic Intermediate Water (AAIW):*
Panel a) shows the formation area used to define the water mass, panel b) show a T-S diagram and panel c) the distribution of key properties vs. pressure. In panel d) we show bar plots of the data distribution of samples used to define the water mass. Potential Temperature in (°C), Potential Density in kg/m^3, Oxygen and nutrients in µmol/kg^3. The red Gaussian fit shows mean and σ based on selected data.

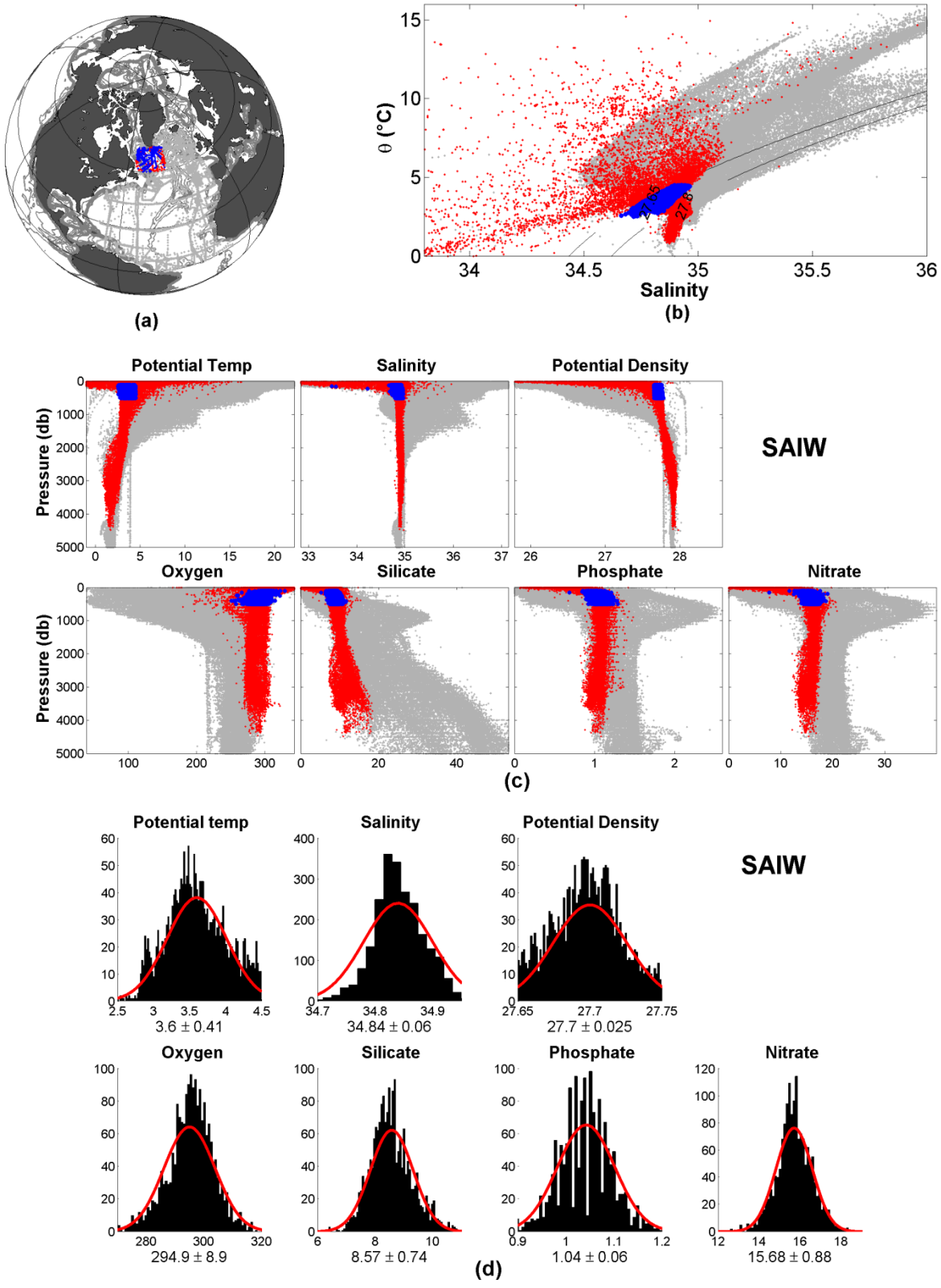

Figure 9: *Overview of Subarctic Intermediate Water (SAIW):*
Panel a) shows the formation area used to define the water mass, panel b) show a T-S diagram and panel c) the distribution of key properties vs. pressure. In panel d) we show bar plots of the data distribution of samples used to define the water mass. Potential Temperature in (°C), Potential Density in kg/m^3, Oxygen and nutrients in µmol/kg^3. The red Gaussian fit shows mean and σ based on selected data.

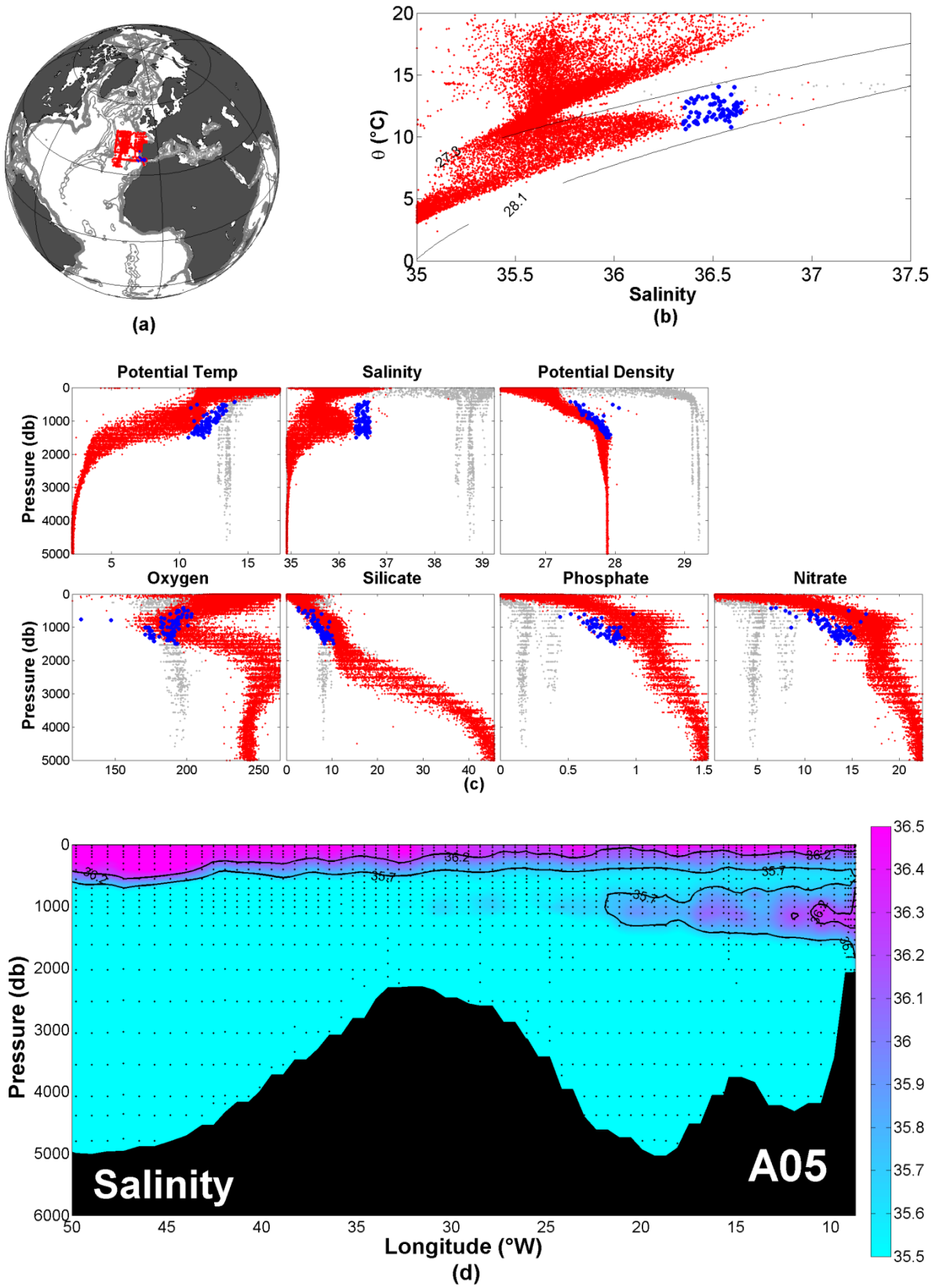

Figure 10: *Overview of Mediterranean Overflow Water (MOW):*
Panel a) shows the formation area used to define the water mass, panel b) show a T-S diagram and panel c) the distribution of key properties vs. pressure. In panel d) we show the salinity along A05 cruise.

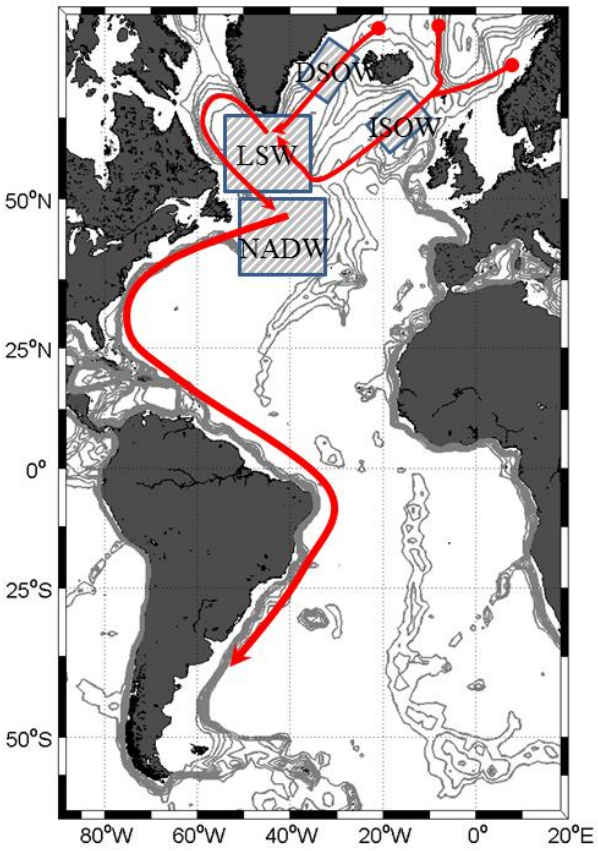

Figure 11: *The water mass formation areas and the schematic of main currents in the Deep and Overflow Layer.*

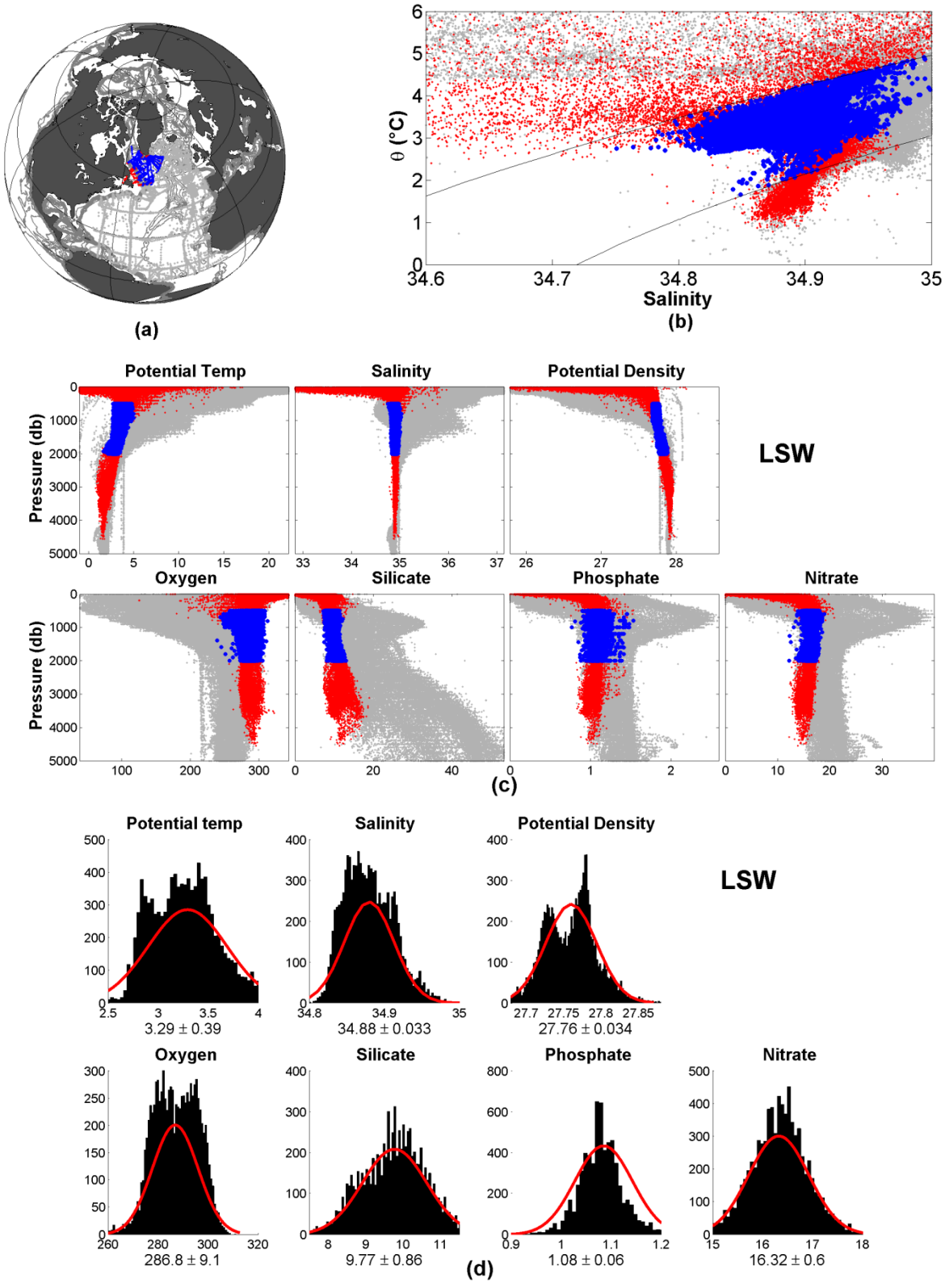

Figure 12: *Overview of Labrador Sea Water (LSW):*
Panel a) shows the formation area used to define the water mass, panel b) show a T-S diagram and panel c) the distribution of key properties vs. pressure. In panel d) we show bar plots of the data distribution of samples used to define the water mass. Potential Temperature in (°C), Potential Density in kg/m^3, Oxygen and nutrients in µmol/kg^3. The red Gaussian fit shows mean and σ based on selected data.

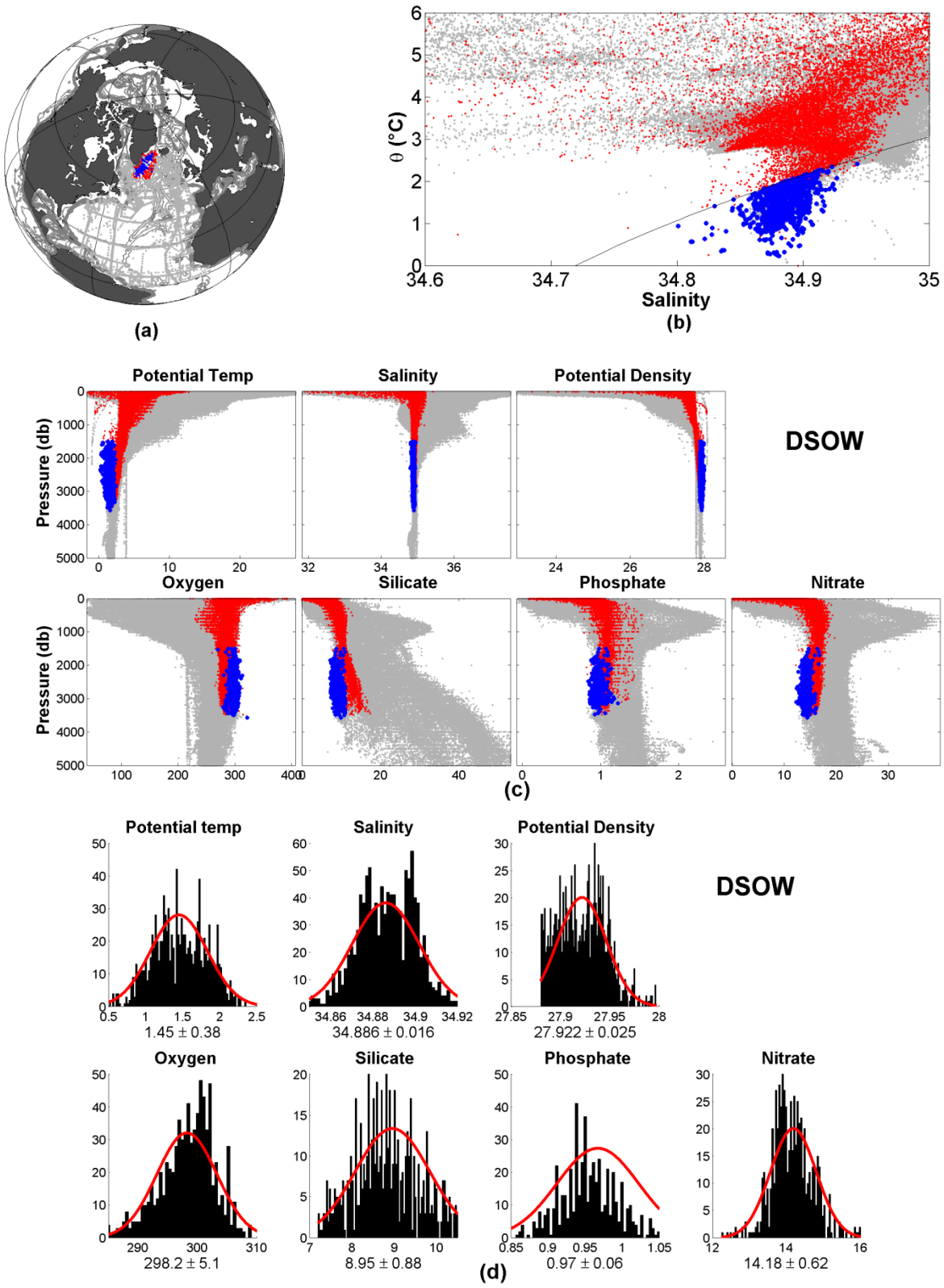

Figure 13: *Overview of Denmark Strait Overflow Water (DSOW):*
Panel a) shows the formation area used to define the water mass, panel b) show a T-S diagram and panel c) the distribution of key properties vs. pressure. In panel d) we show bar plots of the data distribution of samples used to define the water mass. Potential Temperature in (°C), Potential Density in kg/m^3, Oxygen and nutrients in µmol/kg^3. The red Gaussian fit shows mean and σ based on selected data.

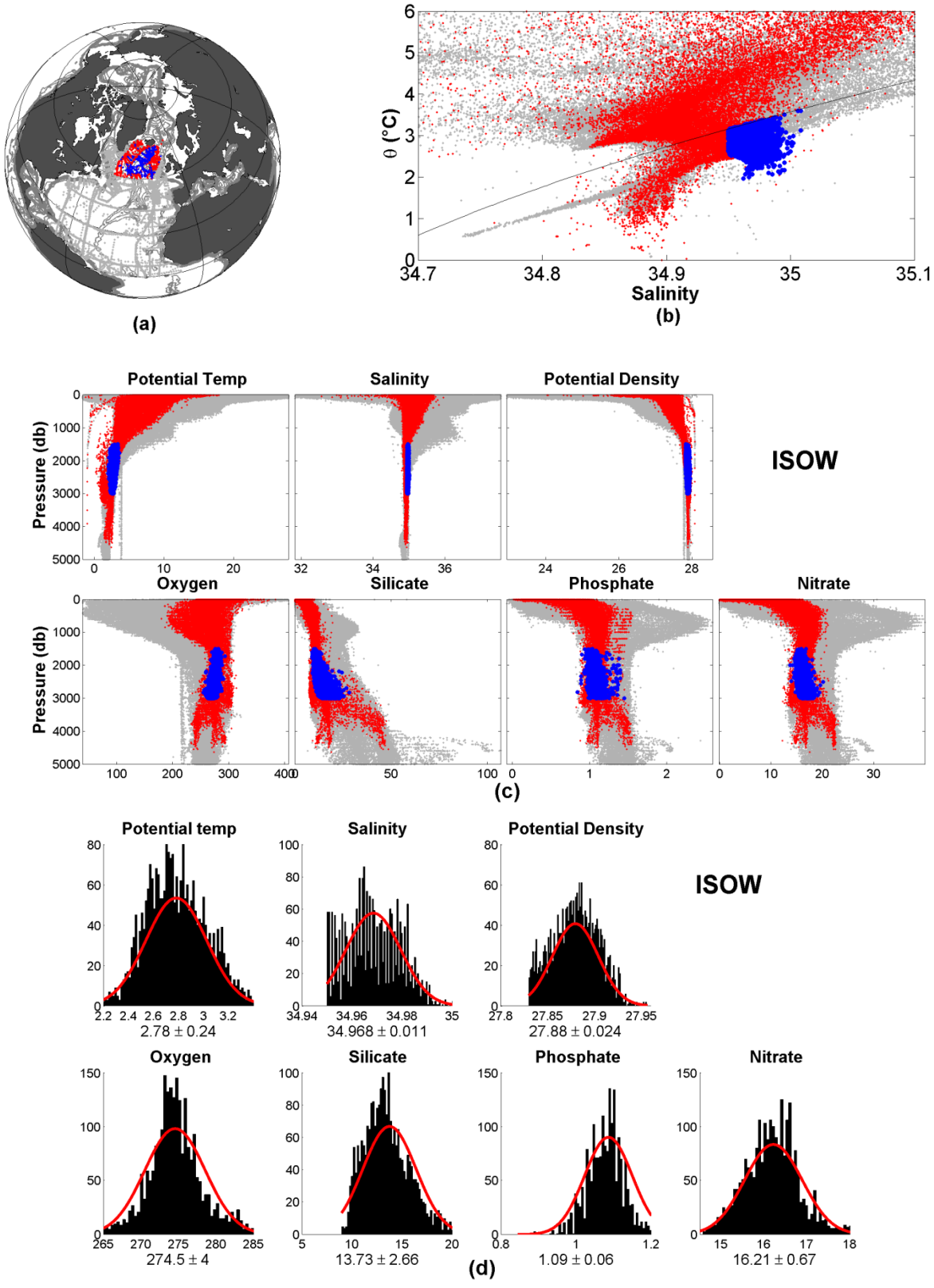

Figure 14: *Overview of Iceland-Scotland Overflow Water (ISOW):*
Panel a) shows the formation area used to define the water mass, panel b) show a T-S diagram and panel c) the distribution of key properties vs. pressure. In panel d) we show bar plots of the data distribution of samples used to define the water mass. Potential Temperature in (°C), Potential Density in kg/m^3, Oxygen and nutrients in µmol/kg^3. The red Gaussian fit shows mean and σ based on selected data.

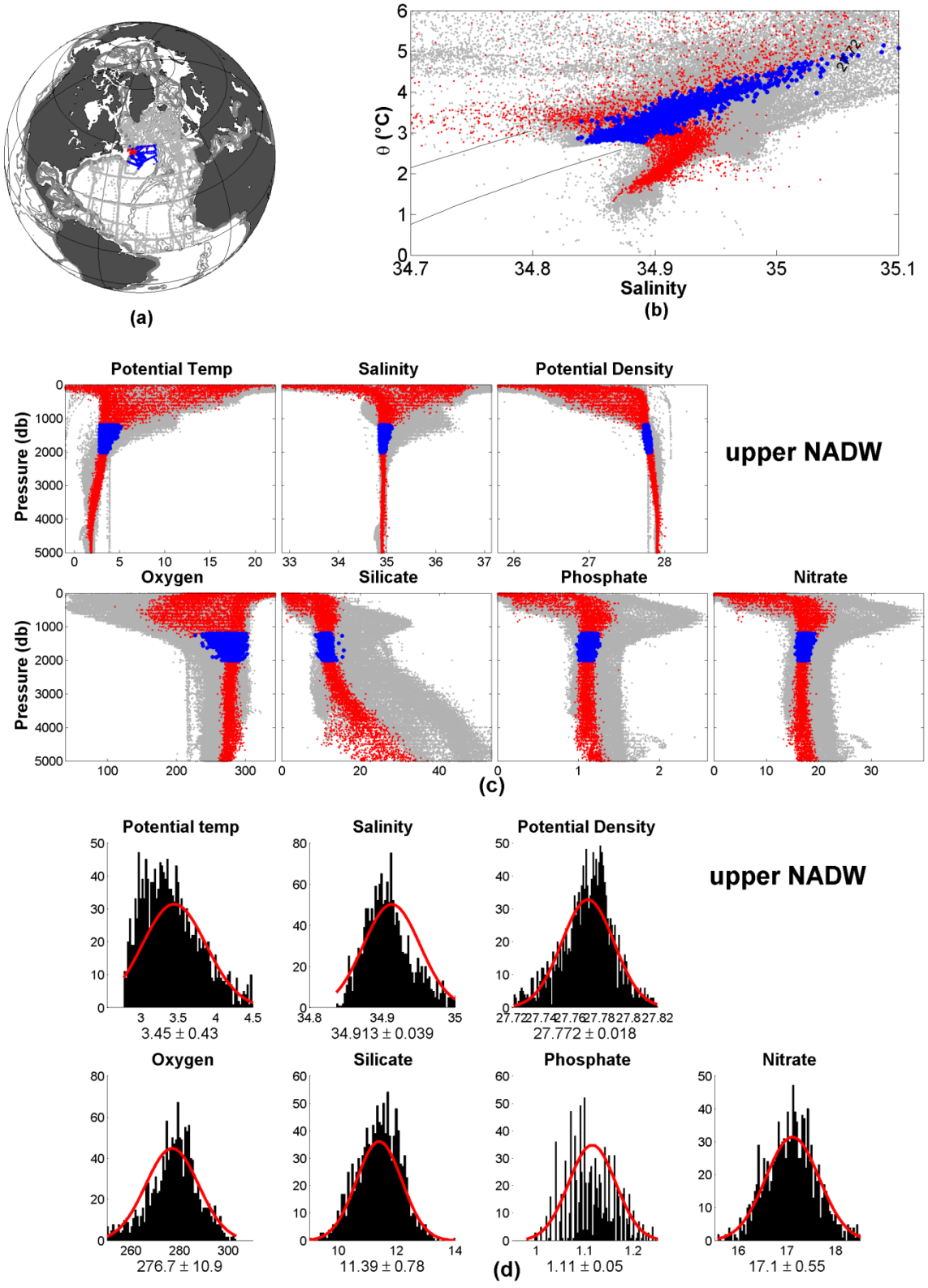

Figure 15: *Overview of upper North Atlantic Deep Water (uNADW):*
Panel a) shows the formation area used to define the water mass, panel b) show a T-S diagram and panel c) the distribution of key properties vs. pressure. In panel d) we show bar plots of the data distribution of samples used to define the water mass. Potential Temperature in (°C), Potential Density in kg/m^3, Oxygen and nutrients in µmol/kg^3. The red Gaussian fit shows mean and σ based on selected data.

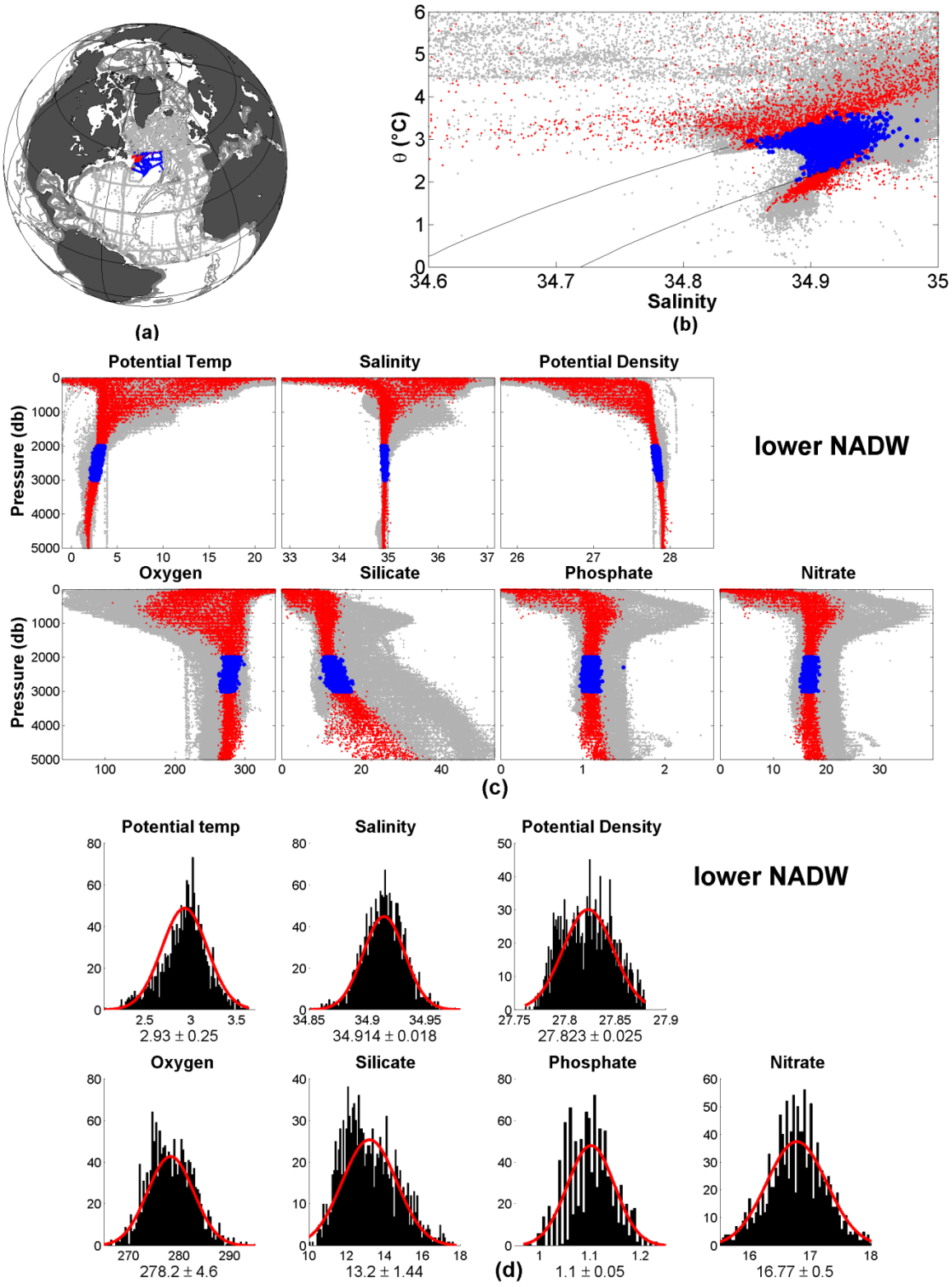

Figure 16: *Overview of lower North Atlantic Deep Water (lNADW):*
Panel a) shows the formation area used to define the water mass, panel b) show a T-S diagram and panel c) the distribution of key properties vs. pressure. In panel d) we show bar plots of the data distribution of samples used to define the water mass. Potential Temperature in (°C), Potential Density in kg/m^3, Oxygen and nutrients in µmol/kg^3. The red Gaussian fit shows mean and σ based on selected data.

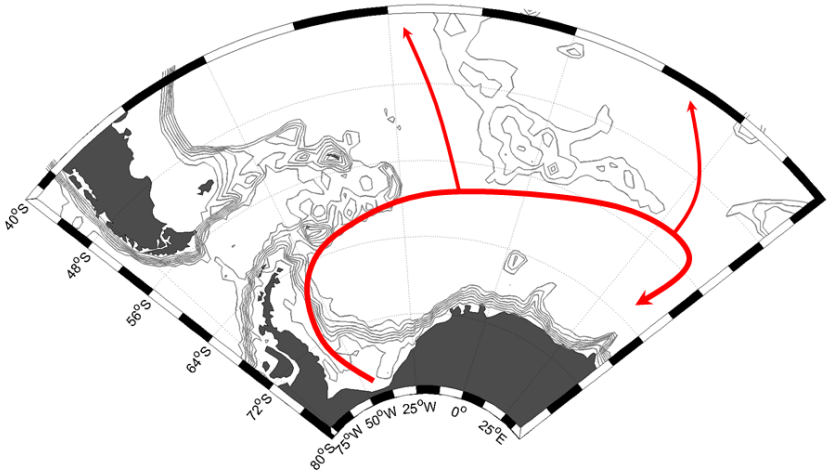

Figure 17: *The water mass formation areas and the schematic of main currents in the Bottom Layer*

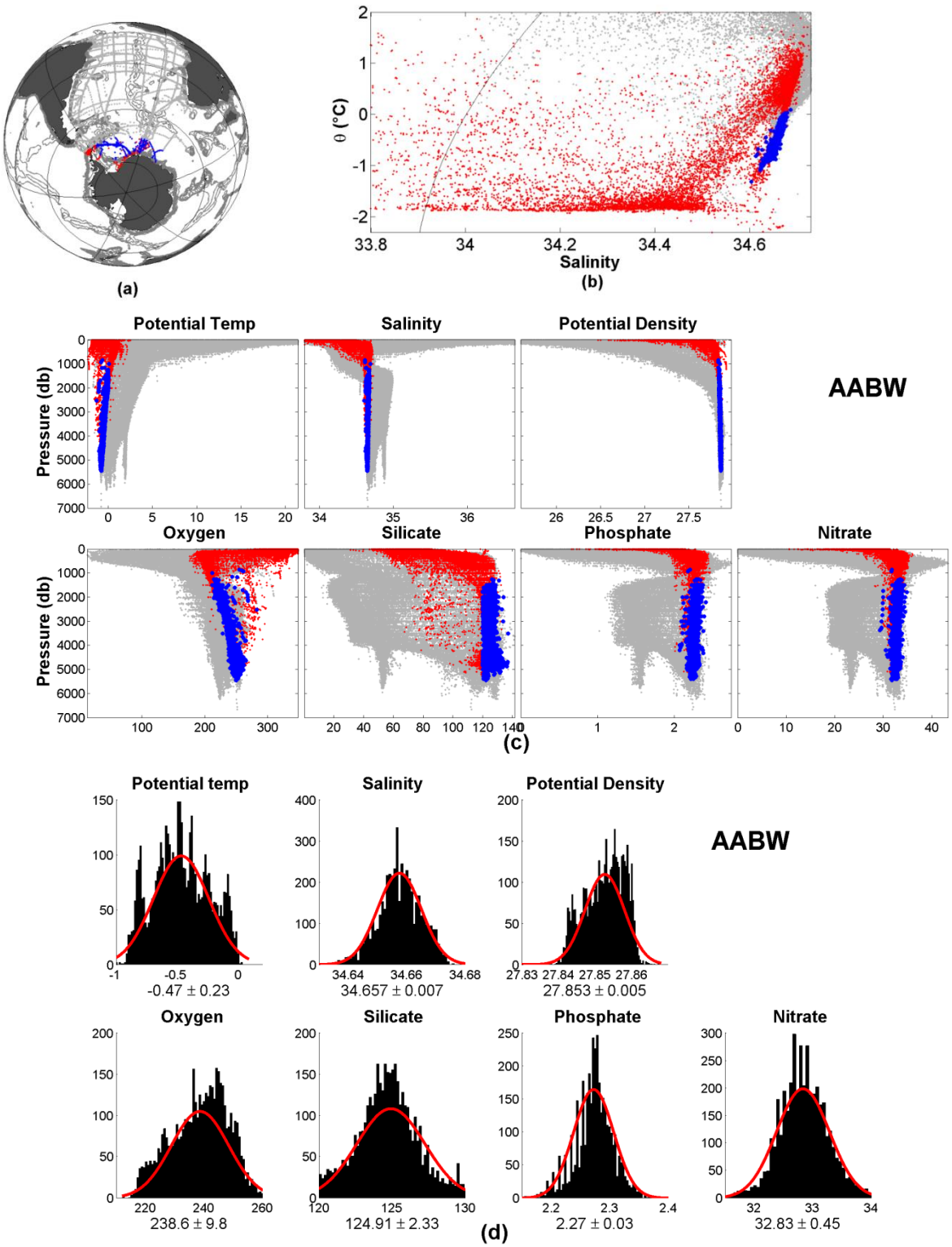

Figure 18: *Overview of Antarctic Bottom Water (AABW):*
Panel a) shows the formation area used to define the water mass, panel b) show a T-S diagram and panel c) the distribution of key properties vs. pressure. In panel d) we show bar plots of the data distribution of samples used to define the water mass. Potential Temperature in (°C), Potential Density in kg/m^3, Oxygen and nutrients in µmol/kg^3. The red Gaussian fit shows mean and σ based on selected data.

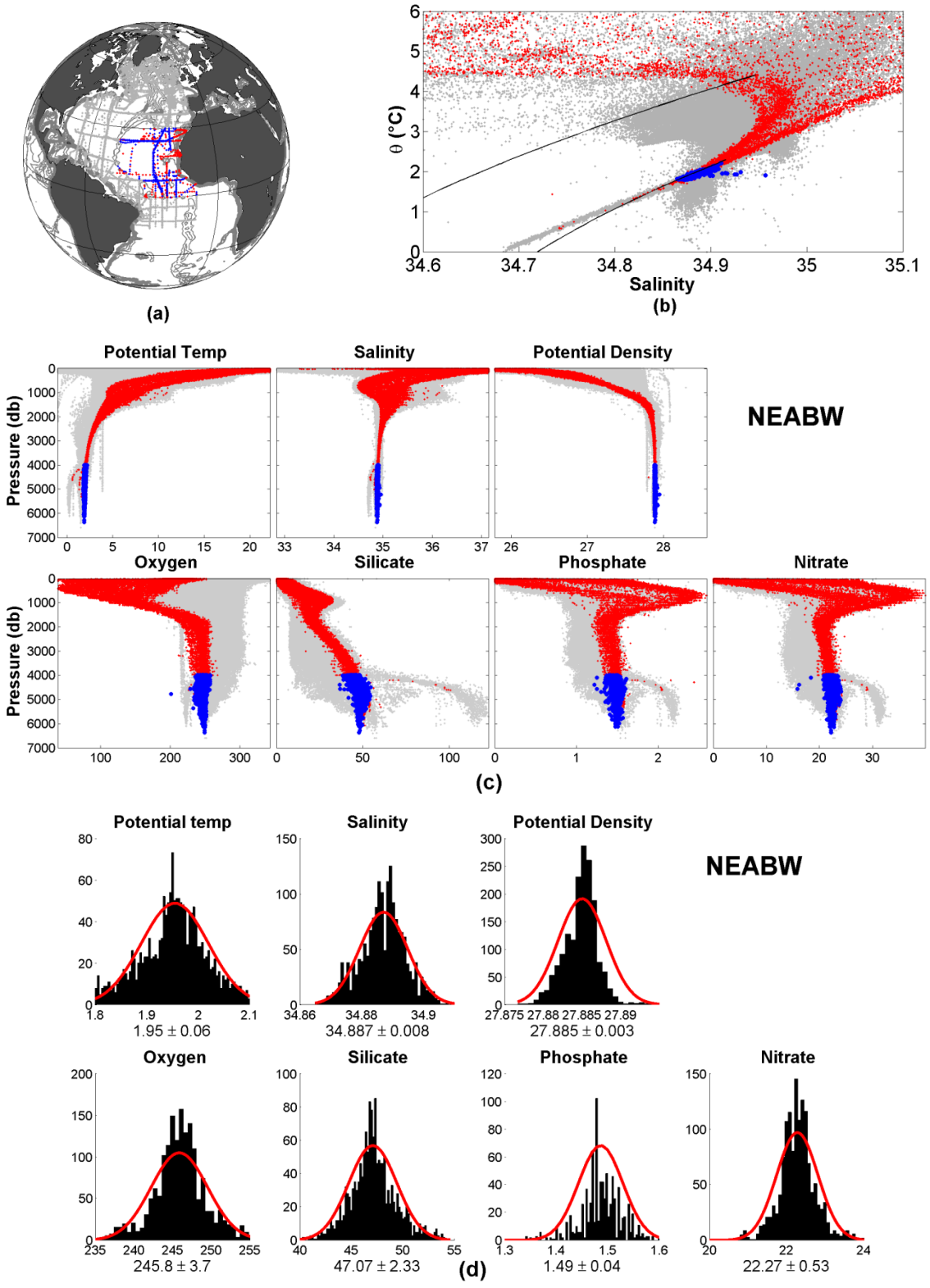

Figure 19: *Overview of Northeast Atlantic Bottom Water (NEABW): Panel a) shows the formation area used to define the water mass, panel b) show a T-S diagram and panel c) the distribution of key properties vs. pressure. In panel d) we show bar plots of the data distribution of samples used to define the water mass. Potential Temperature in (°C), Potential Density in kg/m^3, Oxygen and nutrients in µmol/kg^3. The red Gaussian fit shows mean and σ based on selected data.*

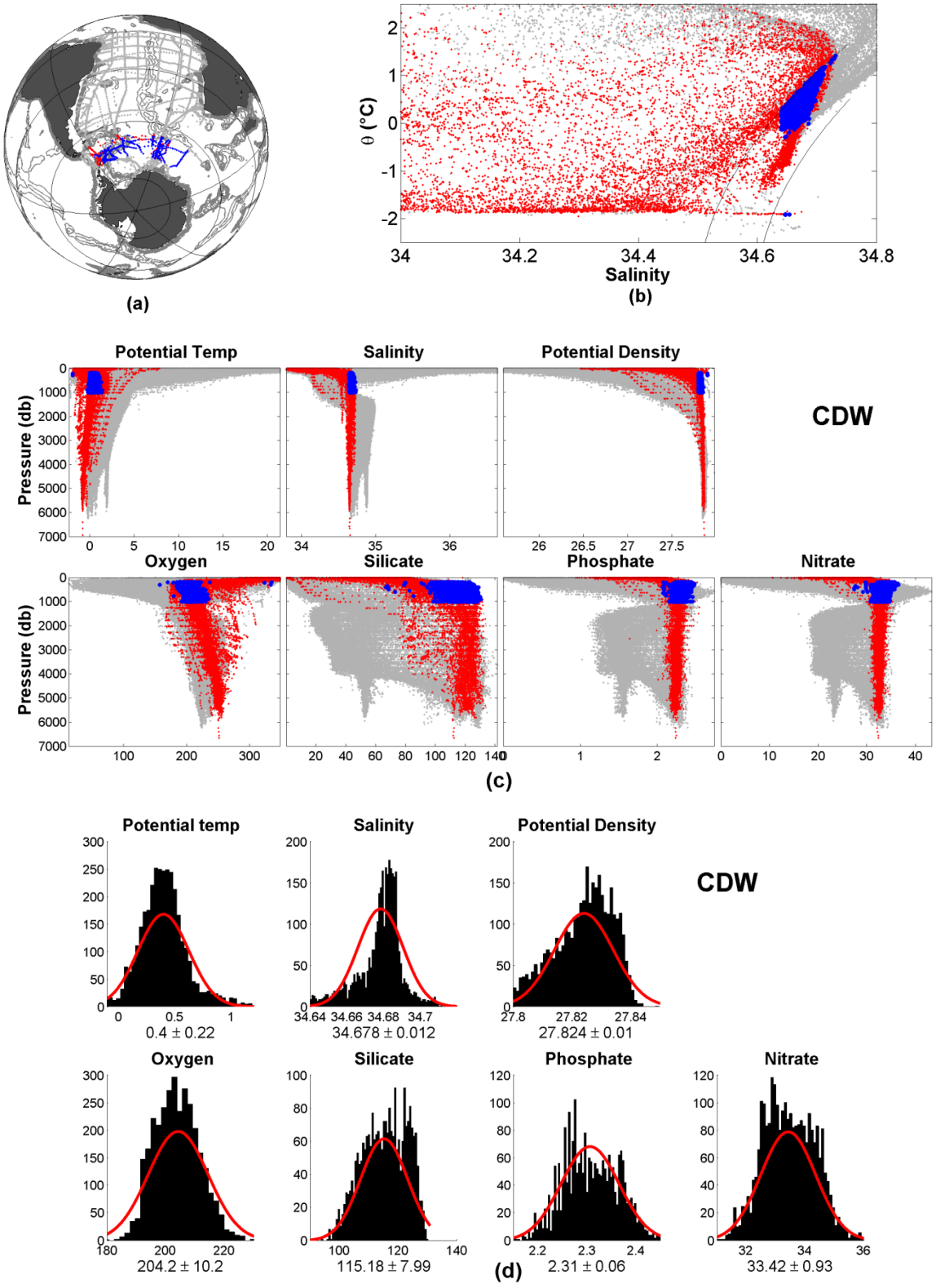

Figure 20: *Overview of Circumpolar Deep Water (CDW):*
Panel a) shows the formation area used to define the water mass, panel b) show a T-S diagram and panel c) the distribution of key properties vs. pressure. In panel d) we show bar plots of the data distribution of samples used to define the water mass. Potential Temperature in (°C), Potential Density in kg/m^3, Oxygen and nutrients in µmol/kg^3. The red Gaussian fit shows mean and σ based on selected data.

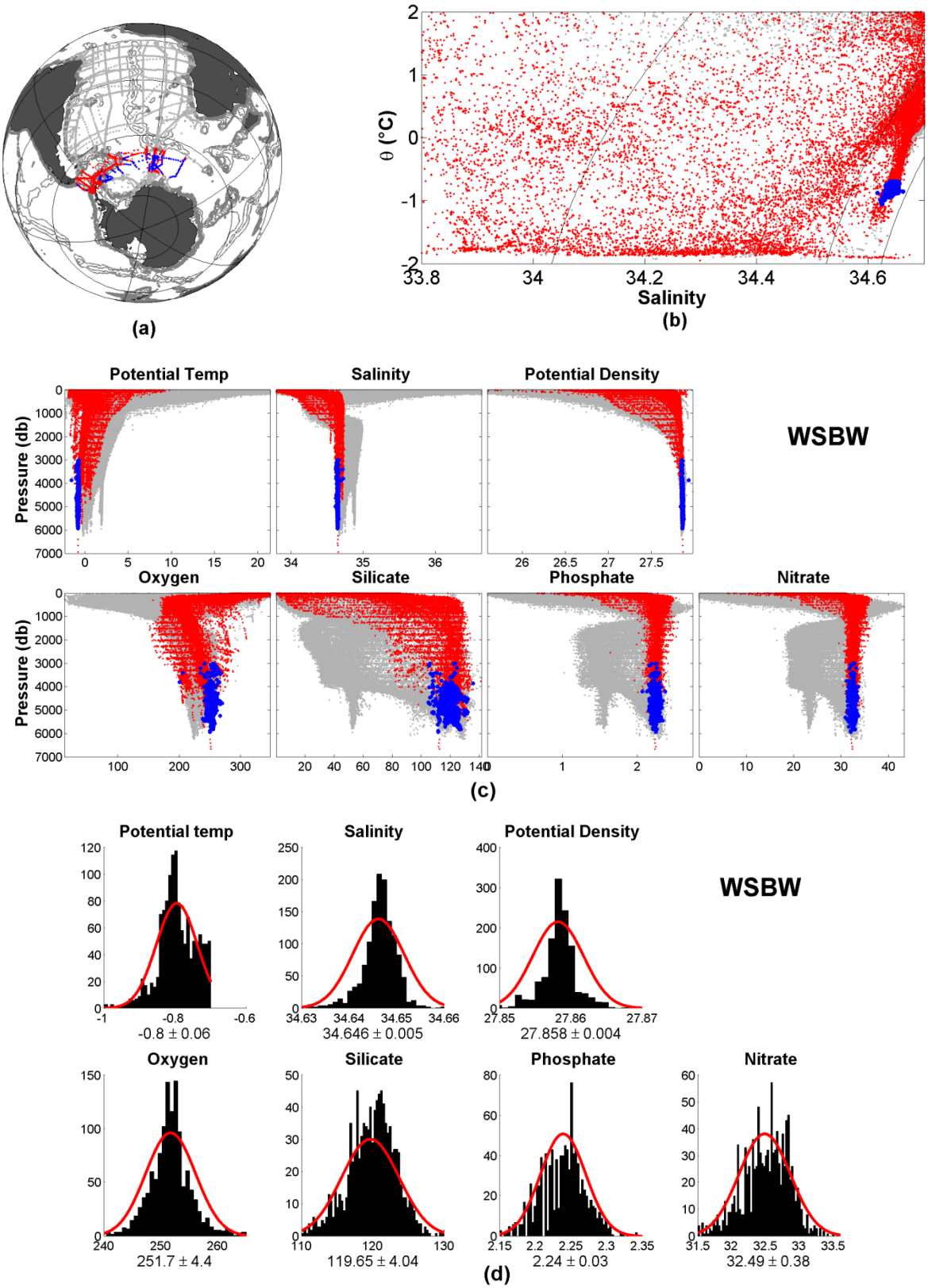

Figure 21: *Overview of Weddell Sea Bottom Water (WSBW):*
Panel a) shows the formation area used to define the water mass, panel b) show a T-S diagram and panel c) the distribution of key properties vs. pressure. In panel d) we show bar plots of the data distribution of samples used to define the water mass. Potential Temperature in (°C), Potential Density in kg/m^3, Oxygen and nutrients in µmol/kg^3. The red Gaussian fit shows mean and σ based on selected data.

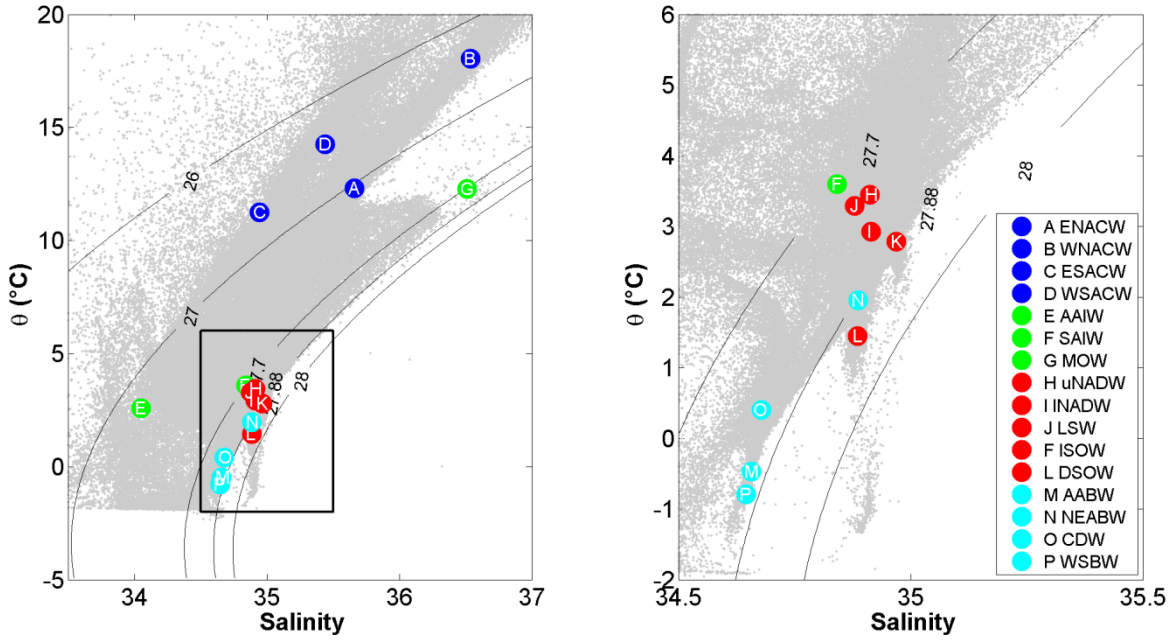

***Figure 22**: Potential temperature / Salinity distribution of the 16 main SWTs in the Atlantic Ocean discussed in this study. Colored dots with letters A-P show the mean value of each SWT and gray dots show all the data from GLODAPv2.*

Table 1: *Table of all the water masses and the four main layers as defined in this study.*

The variables defined are used to select water samples that defines water masses in the formation regions.

Layer	SWT	Longitude	Latitude	Pressure dbar	Potential Temperature °C	Salinity	Potential Density kg m^{-3}	Oxygen µmol kg^{-1}	Silicate µmol kg^{-1}
Upper Layer	ENACW	15°W—25°W	39°N—48°N	100 — 500	---	---	26.50—27.30	---	---
	WNACW	50°W—70°W	24°N—37°N	100 —1000	---	---	26.30—26.60	---	< 3
	WSACW	25°W—60°W	30°S—45°S	100 —1000	---	> 34.5	26.00—27.00	< 230	< 5
	ESACW	0—15°E	30°S—40°S	200 — 700	---	---	26.00—27.20	200--240	< 10
Intermediate Layer	AAIW	25°W—55°W	45°S—60°S	> 300	> -0.5	---	26.95—27.50	> 230	< 30
	SAIW	35°W—55°W	50°N—60°N	100 — 500	> 4.5	< 34.6	> 27.65	---	---
	MOW	6°W—24°W	33°N—48°N	> 300	---	36.35—36.65	---	---	---
Deep and Overflow Layer	uNADW	32°W—50°W	40°N—50°N	1200—2000	---	---	27.72—27.82	---	---
	lNADW	32°W—50°W	40°N—50°N	2000—3000	---	---	27.76—27.88	---	---
	LSW	24°W—60°W	48°N—66°N	500 —2000	---	---	27.68—27.88	---	---
	ISOW	0—45°W	50°N—66°N	1500—3000	---	> 34.95	> 27.83	---	---
	DSOW	19°W—46°W	55°N—66°N	>1500	---	---	> 27.88	---	< 11
Bottom Layer	AABW	---	> 63°S	---	---	---	>28.27	---	> 120
	CDW	< 60°W	55°S—65°S	200—1000	0—1	> 34.64	> 27.80	---	---
	WSBW	---	55°S—65°S	3000---6000	< -0.7	---	---	---	> 105
	NEABW	10°W—45°W	0—30°N	> 4000	> 1.8	---	---	---	---

Table 2: *The full name of the water masses discussed in this study, and the abbreviation.*

Full name of Water Mass	Abbreviation
East North Atlantic Central Water	ENACW
West North Atlantic Central Water	WNACW
West South Atlantic Central Water	WSACW
East South Atlantic Central Water	ESACW
Antarctic Intermediate Water	AAIW
Subarctic Intermediate Water	SAIW
Mediterranean Overflow Water	MOW
Upper North Atlantic Deep Water	uNADW
Lower North Atlantic Deep Water	lNADW
Labrador Sea Water	LSW
Iceland-Scotland Overflow Water	ISOW
Denmark Strait Overflow Water	DSOW
Antarctic Bottom Water	AABW
Circumpolar Deep Water	CDW
Weddell See Bottom Water	WSBW
Northeast Atlantic Bottom Water	NEABW

Table 3: *Table of the mean value, and the standard deviation, of all variables for all the water masses discussed in this study.*

Layer	SWTs	Potential Temperature (°C)	Salinity	Potential Density (kg m^{-3})	Oxygen (µmol kg^{-1})	Silicate (µmol kg^{-1})	Phosphate (µmol kg^{-1})	Nitrate (µmol kg^{-1})
Upper Layer	ENACW	12.31±0.95	35.662±0.124	27.039±0.097	234.4±13.2	3.67±1.20	0.57±0.16	9.34±2.38
	WNACW	18.03±0.47	36.536±0.079	26.441±0.069	204.3±9.3	1.32±0.46	0.17±0.06	3.68±1.16
	ESACW	11.26±2.25	34.944±0.272	26.659±0.207	219.2±9.1	5.50±1.96	0.96±0.31	13.27±4.73
	WSACW	14.27±2.02	35.439±0.320	26.451±0.191	216.0±6.2	2.60±0.99	0.56±0.24	6.85±3.60
Intermediate Layer	AAIW	2.58±0.56	34.051±0.135	27.148±0.125	303.2±28.1	15.68±6.78	1.79±0.23	24.65±2.95
	SAIW	3.60±0.41	34.841±0.043	27.700±0.025	294.9±8.9	8.57±0.74	1.04±0.06	15.69±0.86
	MOW	12.28±0.77	36.510±0.081	27.704±0.150	186.3±10.7	7.22±1.75	0.74±0.11	12.61±1.96
Deep and Overflow Layer	Upper NADW	3.45±0.43	34.913±0.039	27.772±0.018	276.7±10.9	11.39±0.78	1.11±0.05	17.10±0.55
	Lower NADW	2.93±0.25	34.914±0.018	27.823±0.025	278.2±4.6	13.21±1.44	1.10±0.05	16.77±0.50
	LSW	3.29±0.39	34.880±0.033	27.760±0.034	286.8±9.1	9.77±0.86	1.08±0.06	16.32±0.60
	ISOW	2.78±0.24	34.968±0.011	27.880±0.024	274.5±4.0	13.73±2.66	1.09±0.06	16.21±0.67
	DSOW	1.45±0.38	34.886±0.016	27.922±0.025	298.2±5.1	8.95±0.88	0.97±0.06	14.18±0.62
Bottom Layer	AABW	-0.47±0.23	34.657±0.007	27.853±0.005	238.6±9.8	124.91±2.33	2.27±0.03	32.83±0.45
	CDW	0.40±0.22	34.678±0.012	27.824±0.010	204.2±10.2	115.18±7.99	2.31±0.06	33.42±0.93
	WSBW	-0.80±0.06	34.646±0.005	27.858±0.004	251.7±4.4	119.65±4.04	2.24±0.03	32.49±0.38
	NEABW	1.95±0.06	34.887±0.008	27.885±0.003	245.8±3.7	47.07±2.33	1.49±0.04	22.27±0.53

Chapter III: Distribution of Water Masses in the Atlantic Ocean based on GLODAPv2 dataset

Mian Liu

Toste Tanhua

GEOMAR Helmholtz Centre for Ocean Research Kiel,

Marine Biogeochemistry, Chemical Oceanography

Düsternbrooker Weg 20, 24105 Kiel, Germany

Correspondence to: T. Tanhua (ttanhua@geomar.de)

Abstract: The distribution of the main water masses in the Atlantic Ocean are investigated with the Optimal Multi-Parameter (OMP) method. The properties of the main water masses in the Atlantic Ocean are described in a companion article; here these definitions are used to map out the general distribution of those water masses. Six key properties, including conservative (potential temperature and salinity) and non-conservative (oxygen, silicate, phosphate and nitrate), are incorporated into the OMP analysis to determine the contribution of the water masses in the Atlantic Ocean based on the GLODAP v2 observational data. To facilitate the analysis the Atlantic Ocean is divided into four vertical layers based on potential density. Due to the high seasonal variability in the mixed layer, this layer is excluded from the analysis. Central waters are the main water masses in the upper/central layer, generally featuring high potential temperature and salinity and low nutrient concentrations and are easily distinguished from the intermediate water masses. In the intermediate layer, the Antarctic Intermediate Water (AAIW) from the south can be detected to ~30 °N, whereas the Subarctic Intermediate Water (SAIW), having similarly low salinity to the AAIW flows from the north. Mediterranean Overflow Water (MOW) flows from the Strait of Gibraltar as a high salinity water. NADW dominates the deep and overflow layer both in the North and South Atlantic. In the bottom layer, AABW is the only natural water mass with high silicate signature spreading from the Antarctic to the North Atlantic. Due to the change of water mass properties, in this work we renamed to North East Antarctic Bottom Water NEABW north of the equator. Similarly, the distributions of Labrador Sea Water (LSW), Iceland Scotland Overflow Water (ISOW), and Denmark Strait Overflow Water (DSOW) forms upper and lower portion of NADW, respectively roughly south of the Grand Banks between ~50 and 66 °N. In the far south the distributions of Circumpolar Deep Water (CDW) and Weddell Sea Bottom Water (WSBW) are of significance to understand the formation of the AABW.

Key words: Water Masses, Optimal-Multi-Parameter Analysis, Atlantic Ocean

1. Introduction

The distribution of properties in the ocean tends to be distributed along bodies of water with similar history, or water masses (Mackas et al., 1987). The properties of water masses further more tend to change along the flow path of a water mass, partly due to biological or chemical changes, i.e. non-conservative behavior of properties, and due to mixing with surrounding water masses (Hinrichsen and Tomczak, 1993; Klein and Tomczak, 1994). Knowledge of the distribution and variation of water masses is of fundamental importance in oceanography, particularly for biogeochemical and biological applications where the transformation of properties over time can be successfully viewed in the water mass frame-work. For instance, the process of deep water formation from near surface waters enable the effects of air-sea gas exchange to penetrate the deep waters. In the North Atlantic deep water formation transports anthropogenic carbon and oxygen from the surface to the deep ocean (e.g. Garcia-Ibanez et al., 2015). Furthermore, the interactions of water masses influence the distribution of biologically important elements, such as oxygen, carbon and nutrients (e.g. Karstensen et al., 2008). All of these studies show that the study of water masses plays not only an important role in physical oceanography, but also irreplaceable role in biogeochemistry.

With an increasing number of publications focusing on water mass characterization on a global (e.g. Stramma and England, 1999) and regional scale (e.g. Carracedo et al., 2016; Talley, 1996), differences in research goals and areas has resulted in different definitions and names of water masses by researchers. For example, in a study focusing on T-S distribution, shallow water masses are named as Mode Water due to their linear, T-S relationship (McCartney and Talley, 1982). But other works referred the same water masses as Central Water, since the authors focused more on the distribution and transport of mass and chemical constituents (Garcia-Ibanez et al., 2015). Here we follow the approach by Garcia-Ibanez et al. (2015) and utilize the definitions of water masses that we present in a companion paper to map out the general distribution of water masses in the Atlantic Ocean.

In the Atlantic Ocean, warm upper/central waters are generally transported northward into the high latitude North Atlantic, where the dense and cold deep water is formed, and subsequently sinks and spreads southward across the equator into the South Atlantic (Fyfe et al., 2007).

Consistent with the work in our companion paper (Liu and Tanhua, 2019), we divide the water column into four vertical layers based on potential density (σ_θ). Water masses in the upper/central layer (σ_θ < 27 kg/m^3) origin from seawater that subduct into the thermocline during winter time. Four water masses are located in this layer: the East North Atlantic Central Water (ENACW), West North Atlantic Central Water (WNACW), East South Atlantic Central Water (ESACW) and West South Atlantic Central Water (WSACW). In the intermediate layer (σ_θ = 27 – 27.7 kg/m^3), three water masses are identified. In the South Atlantic, Antarctic Intermediate Water (AAIW) originates from the surface (upper 200m) in the region north of Antarctic Circumpolar Current (ACC) and east of Drake

Passage (Alvarez et al., 2014; Talley, 1996). In the North Atlantic, Subarctic Intermediate Water (SAIW) originates from surface in the western boundary of Subpolar Gyre and spreads southward along the Labrador Current (Pickart et al., 1997). In the east, Mediterranean Overflow Water (MOW) flows through the Strait of Gibraltar with a feature of high salinity. North Atlantic Deep Water (NADW) is the dominant water mass in the deep and overflow layer (σ_θ = 27.7 – 27.88 kg/m^3). This water mass is formed in the high latitude North Atlantic, with relatively high potential density due to the low potential temperature and high salinity. We further divide the NADW into upper and lower portions by different potential density and origins. Labrador Sea Water (LSW) is the origin of upper version of NADW (uNADW) whereas Iceland-Scotland Overflow Water (ISOW) and Denmark Strait Overflow Water (DSOW) are origins of lower NADW. Antarctic Bottom Water (AABW) is the main water mass in the bottom layer (σ_θ > 27.88 kg/m^3). This water mass is a mixed product between Weddell Sea Bottom Water (WSBW) and Circumpolar Deep Water (CDW) (van Heuven et al., 2011; Weiss et al., 1979). In regions north of the equator we define AABW as a new water mass, the Northeast Atlantic Bottom Water (NEABW).

2. Data and Methods

There are some key features of the distribution of properties that are well known, but never the less are helpful in understanding the distribution of water masses in the Atlantic Ocean. We use a meridional section across the Atlantic Ocean to illustrate this, the WOCE/GO-SHIP A16 section as occupied by cruise 33RO20130803 (North Atlantic) & 33RO20131223 (South Atlantic), Figure 1. In the upper layer, high temperatures, salinities and low nutrients, especially nitrate can be seen on the section plots. The above characteristics are consistent with the properties of central water masses. The intermediate layer is characterized by low salinity and high nitrate and silicate in the South Atlantic. According to this feature, the location of AAIW can be initially determined. And relative high salinity distributes around 40 °N is the signal of MOW. High oxygen in the north helps to label SAIW. Relative higher salinity and oxygen but lower nutrients (silicate and nitrate) are important signals of water masses in deep and overflow layer (upper and lower NADW) to distinguish from intermediate and bottom waters. High silicate is one significant property to identify AABW in bottom layer. Also this layer has the lowest potential temperature. In the north hemisphere, there is a sudden reduction of silicate compared with south of equator. This is the reason that a new water mass, NEABW, is defined in this region.

2.1. The GLODAPv2 dataset

Marine surveys from different countries are actively organized and coordinated since late 1950s, after the establishment of the Scientific Committee for Marine Research (SCOR) in 1957 and the Intergovernmental Oceanographic Commission (IOC) in 1960. And meanwhile, academic exchanges between world countries and organizations became frequent and popular. WOCE (the World Ocean Circulation Experiment), JGOFS (Joint Global Ocean Flux Study) and OACES (Ocean Atmosphere

Carbon Exchange Study) are the three most typical representatives after entering 1990s. However, these programs are initiated by different countries and with their respective aims and goals. Hence, coordination and collaboration between the countries are necessary and beneficial. GLODAP (Global Ocean Data Analysis Project) is a data product that came into being in this context. In addition to create a global dataset based on above programs, the goals of GLODAP include also to describe distribution and biogeochemical properties in the global ocean and to make data publicly available (Key et al., 2004). The GLODAP dataset shows a good start for global data sharing however the shortcomings also cannot be ignored. From the spatial scale, few data in high latitude region, north of 60 °N or in the Arctic region, are collected in this dataset, and meanwhile, data from Mediterranean Sea are also not included. In the term of time, GLODAPv1.1 contains data only until 1999. The updated and expanded dataset GLODAPv2 successfully made up for the above disadvantages (Lauvset et al., 2016). In addition to the integration of two other datasets, CARINA (CARbon dioxide IN the Atlantic Ocean, Key et al., 2010) and PACIFICA (PACIFic ocean Interior Carbon, Ishii et al., 2011), GLODAPv2 also includes an 168 additional independent cruises those never been collected by any datasets. Thus GLODAPv2 is a dataset that includes relatively complete data and with an almost global coverage, and also include a mapped product.

2.2. OMP Analysis

For the water mass analysis we used in total 6 key properties, including two conservative (potential temperature and salinity) and four non-conservative (oxygen, silicate, phosphate and nitrate) properties to define the Source Water Types (SWTs) as origins of water masses, see the companion study (Liu and Tanhua 2019 for details). Based on the above observational data, it is obviously not enough to make accurate estimation of the distribution of the water masses only by displaying key properties. In order to determine the distribution of water masses exactly, we have to resort to more accurate mathematical calculations. Since the first publication of global distributions of water masses (Sverdrup, 1942), early studies on water masses are mainly based on potential temperature and salinity. Emery and Meincke made on summary and review on this kind of analysis in 1986 (Emery and Meincke, 1986). The limitation of this method is that distribution of more (more than three) water masses cannot be calculated at the same time with only these two parameters. So during the same time as the development of this theory, physical and chemical oceanographers also tried to add more parameters to the calculation and the Optimum Multi-parameter (OMP) analysis is one of the typical products.

Base on above results, Tomczak (1981) extended the analysis into more than three water masses by adding more parameters/water properties (such as phosphate and silicate) and solving the equations of linear mixing without assumptions. In Tomczak and Large (1989a), this method was successfully applied to the analysis of mixing in the thermocline in Eastern Indian Ocean. As a summary and practical use of the above results, the Optimal Multivariable Parameter (OMP) analysis was developed and successfully applied in the analysis of water masses in specific regions (e.g. Karstensen and

Tomczak, 1997, 1998a). Parameters (6 key water properties in our study) from the water samples are extracted and compared with SWTs of each water masses to identify their composition structure and percentage in detail.

Before we start the calculation of OMP analysis, some basic definitions of SWTs need to be reiterated again. SWTs are the origin water masses in their formation area and carry their own properties (Poole and Tomczak, 1999). During transport and mixing on the pathway, the total amount of water properties remains constant. In a mixed product of two water masses, contribution from each SWT can be calculated by using a linear set of mixing equations, if we know one water property (such as salinity) in this mixed product and both SWTs. But only one property/parameter becomes insufficient if there are three or more water masses mix together. As a result, we can calculate the percentages of each water mass in a final mixed product with more water masses, with the essential prerequisite that the number of water masses not larger than the number of variables plus one.

The theory and formulas in the OMP analysis are described in detail in Tomczak and Large (1989a) and the website http://omp.geomar.de/. Here we make a brief introduction to the OMP calculation that relates directly to our research, for more details see the references above. OMP calculation is based on a simple model of linear mixing, assuming that all key properties of water masses are affected by the same mixing process, and then to determine the distribution and of water masses through the following linear equations.

Gx - d = R;

Where **G** is a parameter matrix of defined source water types (6 key properties in this study), **x** is a vector containing the relative contributions of the water types to the sample (i.e. solution vector of the source water type fractions), **d** is a data vector of water samples (observational data from GLODAPv2 in this study) and **R** is a vector of residual. The solution is to find out the minimum the residual (**R**) with linear fit of parameters (key properties) for each data point with a non-negative values.

Prerequisites (or restrictions) for using classic OMP is that source water types are defined closely enough to the observational water samples with short transport times, so that the mixing can be assumed not influenced by biogeochemical processes (i.e. consider all the parameters as quasi-conservative). Obviously, this prerequisite does not apply to our investigation for the entire Atlantic scale, so we use the extended OMP analysis instead. The way of considering biogeochemical processes is to convert non-conservative parameters (phosphate and nitrate) into conservative parameters by introducing the "preformed" nutrients PO and NO, where PO and NO show the concentrations of Phosphate and Nitrate in sea water by considering the consumption of dissolved Oxygen from respiration (in other words, the alteration due to respiration is eliminated) (Broecker, 1974; Karstensen and Tomczak, 1998b).

2.3. OMP runs in this study

As mentioned in the companion paper (Liu and Tanhua, 2019) Source Water Types (SWTs) are the origin form of each water mass in the formation area and we grasp the properties of main SWTs in the Atlantic Ocean. In this study, we show the distributions of water masses in Atlantic Ocean after formations based on OMP analysis. The key properties of SWTs are used in OMP analysis as the basis to determining the distributions of water masses.

In order to map all the distribution of water masses in the Atlantic we analyzed all the GLODAPv2 data in the Atlantic Ocean with OMP method by using 6 key properties from each water sample (potential temperature, salinity, oxygen, silicate, phosphate and nitrate). However some of these variables co-vary to some extent, in particular phosphate and nitrate, so that we have to control that in each OMP run we should have less than 6 water masses. Some regional factors should also be considered, as some water masses mix and new SWTs are formed during their mixing process. For example, LSW, ISOW and DSOW mix in the North Atlantic after leaving their formation area, as a result, SWTs of upper and lower NADW are formed. Here we specify some 'mixing regions' for these water masses. Between 40 and 60 °N, we define such a 'mixing region', since all the five water masses including already formed LSW, ISOW and DSOW and newly formed upper and lower NADW simultaneously exist. So in this region, key properties from all these five SWTs are used simultaneously in OMP runs. In south of 40 °N, only upper and lower NADW are used while north of 60 °N, only LSW, ISOW and DSOW are used. A similar situation exists in the South Atlantic where we consider south of 50 °S as another 'mixing region', since a new SWT of AABW is formed here due to the mixing of CDW and WSBW. So in this region, key properties from all the three SWTs are used in the OMP runs while in north of 50 °S, only AABW is used.

Consolidate the above reasons, and also consider the distribution of all the water masses, all the data in the Atlantic Ocean are divided into four, almost vertical, layers by potential density, since all the water masses distribute within their core layer and only mix with neighboring water masses at the boundary of each layer. In horizontal direction, Atlantic Ocean is manually divided into several horizontal sections in order to remove water masses that are not likely to appear in the area to avoid excessive (more than 6) water masses in each OMP run. The central layer is divided into two sections by 35 °N to distinguish SAIW and AAIW, which has similar properties. In the intermediate and deep layer, Atlantic Ocean is divided into three sections. The region north of 60 °N contains the LSW, ISOW and DSOW. From 40 to 60 °N is defined as mixing region. LSW, ISOW, DSOW mix with each other and finally form upper and lower NADW. As a result, all the five SWTs should be contained in one OMP runs in this section. And the third part, from 50 °S to 40 °N, only upper and lower NADW are considered. In high latitude region in South Atlantic, mixing region of CDW and WSBW is defined as south of 50 °S. In this mixing region, CDW, WSBW mix and AABW is formed, but no horizontal layer division in this area because the difference of density is not obvious. From north of 50°S only

AABW are used in OMP runs until equator. In addition, for relative special long transport water masses those across the equator, AAIW upper and lower NADW, we do not subject to restrictions of equator.

This way we end up with a set of 13 different OMPs that are used for estimating the fraction of water masses in each water sample. The density and the latitude of the water sample is used to determine which IMP should be applied, Table 1. Note that all water masses are present in more than one OMP so that reasonable smooth (i.e. realistic) transitions between the different OMPs can be realized. However, it is unavoidable that there will occasionally be step-like features across the vertical and horizontal boundaries defined in Table 1.

3. Result: Distribution of water masses based on GLODAPv2

In this section, the horizontal and vertical distributions of the main water masses are displayed in different density layers. On the maps of horizontal view, water mass fractions are plotted at each station with the interpolated format at their core densities. In order to avoid large interpolation errors, a station is considered as without data and plotted as grey rather than colored dots if there is no data within ±0.1 kg/m^3 from core density.

To exemplify the vertical distribution of the water masses we are also display sections from representative cruises. For this we use 5 selected WOCE/GO-SHIP cruises that together provide a reasonable representation of the Atlantic Ocean, as shown in Figure 2. These are the A16 cruise (Expocodes: 33RO20130803 & 33RO20131223) that is a meridional overview of all the main water masses in the Atlantic Ocean, and that was also used for the distribution of the properties in Figure 1. The A05 (Expocode: 74AB20050501) and A10 (Expocode: 33RO20110906) sections displays the zonal distribution of the water masses in the North (A05) and South (A10) Atlantic separately. The A25 (Expocode: 06MM20060523) section is located at a relative higher latitude region compared to the A05 section and better represent the deep and overflow waters in particular. From this cruise, we focus on the investigation of LSW, ISOW and DSOW, with the purpose to show origin of upper and lower NADW. The SR04 (Expocode: 06AQ20101128) on the other hand is a section in the Antarctic region near Weddell Sea with certain significance for the origin and formation of AABW. For each figure with horizontal distribution we also display a map with a cartoon of the main currents in that density layer and with the main formation region of each water mass indicated as striped boxes.

In this section horizontal and vertical distribution of all water masses discussed and defined in the companion paper (Liu and Tanhua, 2019) are displayed on maps and sections respectively. We start with the Upper Layer and work our way down the water column. In the Upper Layer (σ_θ < 27 kg/m^3 and mostly with depths above ~500-1000m), central waters are the dominate water masses in this layer, where we define four SWTs, ENACW, WNACW, ESACW and WSACW (see table 3 in the

companion paper, Liu and Tanhua, 2019 for definitions). Below the Upper Layer resides the Intermediate Layer (σ_θ between 27 and 27.7 kg/m^3 and mostly with depths between ~1000 and 2000m). In this layer, we have the following SWTs; SAIW from the north AAIW from the south and MOW from the east. The Deep Layer resides from ~2000 to 4000m and σ_θ between 27.7 and 27.88 kg/m^3. The upper and lower NADW are two main SWTs in mid and low latitude region in this layer. Their origin, LSW, ISOW and DSOW will also be investigated in relative high latitude region. Both bottom waters are located in the Bottom Layer below 4000m with σ_θ>27.88 kg/m^3. AABW and NEABW are two main water masses in this layer and have similar properties, especially high silicate. Traced back to the source, NEABW is a branch from AABW after passing the equator. After spanning most Atlantic there is a sharp reduction of silicate concentration this is the reason why we define a new SWT of NEABW.

3.1. The Upper Layer: ENACW, WNCAW, ESACW and WSCAW

The horizontal distributions of four main water masses in the Upper Layer are shown on the maps in Figure 3. In general, eastern central waters, both for the northern and southern variation, have relative higher potential density and are located at deeper depth (i.e. higher density) compared with western central waters. In spatially distribution, the East North Atlantic Central Water (ENACW) is mainly located in the north east part of North Atlantic, near the formation area. The ENACW is formed during winter subduction in the seas west of Iberian Peninsula and drifts to the south along the south branch of the North Atlantic Current (McCartney and Talley, 1982) and mainly locates in north east part of North Atlantic, near the formation area (Garcia-Ibanez et al., 2015; Talley and Raymer, 1982). The WNACW, which is formed at the south flank of the Gulf Stream (Klein and Hogg, 1996), spreads along the North Atlantic Current and distributes in east-west band between ~ 10 °N and 40 °N.

East South Atlantic Central Water (ESACW) distributes all over most South Atlantic and with lower percentages (~30 -- 40%) can also be found in the tropical and subtropical north Atlantic below (at higher densities) than the West North Atlantic Central Water (WNACW). WNACW is located in north tropical and subtropical North Atlantic, where this water mass is formed. West South Atlantic Central Water (WSACW) dominates the upper layer of South Atlantic, resides over ESACW and can also be seen above ENACW in the North Atlantic. In the South Atlantic, our results are similar to those of (Kirchner et al., 2009) that found that the WSACW and ESACW spread all over the South Atlantic, eastward along South Atlantic Current, and then northwest along the Benguela Current and South Equator Current, and finally southward along Brazilian Current. In general, both WSACW and ESACW dominate the central/upper layer in South Atlantic and across the equator until ~10 °N.

The WSACW is formed in the region near the South America coast between 30 and 45 °S, where surface South Atlantic Current brings central water to the east (Kuhlbrodt et al., 2007). Formation of ESACW takes place in the eastern South Atlantic Ocean close to the area southwest of South Africa

(Deruijter, 1982; Lutjeharms and van Ballegooyen, 1988) and spreads to the north along the Benguela Current (Peterson and Stramma, 1991).

From the A16 and A05 sections the meridional and zonal distribution of WNACW and ENACW, the both dominating central water masses in North Atlantic, can be seen. The vertical distribution shows that the WNACW is located at lower densities compared to the ENACW. In the zonal A05 section the difference between east and west of the Mid-Atlantic-Ridge (MAR) is obvious; west of the MAR WNACW dominates the upper layer. Both thickness and percentage are significantly larger than east, while the situation in east of MAR is the opposite, due to their distance from respective formation areas. ENACW is located at the upper ~500m—1000m below WNACW and over SAIW and MOW.

The vertical distribution of WSACW and ESACW based on A16 and A10 sections has similarities to the north central waters where the western variety is located at lower densities compared to the eastern variety. The distribution of WSACW and ESACW can be clearly seen by Figure 4 including their transports to the north that can be clearly seen by the A16 section. In contrast to the north Atlantic the difference between east and west of the MAR, as seen in the A10 section, is not clear compared with the A05 section for the North Atlantic.

3.2. The Intermediate Layer: AAIW, SAIW and MOW

In the intermediate layer (σ_θ between 27 and 27.7 kg/m^3) three water masses can be considered as dominating. Two of them, the Subarctic Intermediate Water (SAIW) and the Mediterranean Overflow Water (MOW), show Northwest-Southeast distinction in their distribution in the North Atlantic although with similar densities. The SAIW is located in north of 40 °N with higher percentages in the western part while the MOW is mainly distributed in the region east of the Mid-Atlantic-Ridge, which is consistent with results from (Read, 2000). The third water mass, the AAIW, has s southern origin and is found at lighter densities, Figure 5

In the South Atlantic, AAIW is the only water mass that origins from the south hemisphere in the Intermediate Layer and has the lowest potential density (main core with potential density ~27.2 kg/m^3) of these three water masses. The AAIW originates from the surface layer (upper 200m) north of the Antarctic Circumpolar Current (ACC) and east of Drake Passage (Alvarez et al., 2014; McCartney, 1982). Most AAIW is formed in the region south of 40 °S where it sinks and spreads to the north at pressures between ~1000 and 2000db at potential densities between 27.0 and 27.7 kg/m^3 (Talley, 1996).

On the map, the spread of AAIW covers most of the Atlantic Ocean until ~40 °N and the percentage shows a decrease trend to the north (Kirchner et al., 2009). The AAIW shows a general distribution within the intermediate layer based on potential density (σ_θ) between 27.0 and 27.7 kg/m^3, Figure 7. At ~40 °S, upper NADW injects into the space between AAIW and AABW (Figure 12) and all the

three water masses mix with each other in this area. From the observations on the meridional A16 section, the AAIW spreads northward after the leaving the formation area, across the equator and further north until ~40 °N, where it meets MOW and SAIW. The upper boundary between AAIW and central waters (ENACW and ESACW) are mostly along the potential density line σ_θ = 27.7 kg/m^3. Based on A10 section the zonal distribution of AAIW is consistent with the results A16 section and is the dominating intermediate water mass in the South Atlantic.

The SAIW, as one of the main intermediate water mass in North Atlantic, originates from the surface layer of the western boundary of the North Atlantic Subpolar Gyre, sinks and spreads along the Labrador Current, crossing the MAR in the region north of 40 °N (Lazier and Wright, 1993; Pickart et al., 1997).

From the A16 section, only some light trace of SAIW in the north can be found since this cruise in 2013 was distance away from the formation area of SAIW in northwest Atlantic. On the zonal A05 section SAIW is a dominating intermediate water mass above the LSW, Figure 6, particularly in the western basin since SAIW originates in the west.

MOW is another main intermediate water mass that is present in the North Atlantic. This water mass overflows from Strait of Gibraltar at ~40 °N and spreads in two branches to the north and the west (Price et al., 1993). The MOW originates from the east in the Gulf of Cadiz where Mediterranean Water exits the Strait of Gibraltar as a deep current and then turns into two branches after leaving the formation area near. One branch spreads to the north into the West European Basin until ~50°N, the other branch spreads to the west until, and past, the Mid-Atlantic-Ridge.

From the A16 section the MOW can be found between ~20 and 50 °N, surrounded by ENACW from the top, SAIW from the north, AAIW from the south and upper NADW from bottom. The observations from the A05 section shows that the MOW flows from the east and spreads westwards until passing the MAR. East of the MAR the trace of MOW is clear, particularly in the region close the Strait of Gibraltar.

3.3. The Deep and Overflow Layer: upper and lower NADW, LSW, ISOW and DSOW

As one of the main components of the thermohaline circulation in Atlantic Ocean, formation and distribution of North Atlantic Deep Water (NADW) is the focus of several studies. NADW is the only main water mass that dominates the deep and overflow layer with potential density (σ_θ) between 27.70 and 27.88 kg/m^3 and can be divided into two portions (upper and lower) due to different properties and origins (Smethie and Fine, 2001). In this section, both portions, together with their origins, are analyzed as independent water masses separately.

In the deep and overflow layer three water masses dominate the region north of 40 °N, Figure 7: Labrador Sea Water (LSW), Iceland-Scotland Overflow Water (ISOW) and Denmark Strait Overflow Water (DSOW). They are considered as the origin of North Atlantic Deep Water (NADW). In the region south from 40 °N the upper and lower NADW, considered as products from the original three overflow water masses, can be found all over the Atlantic Ocean in the deep and overflow layer.

The Labrador Sea Water (LSW) is formed in the region of Labrador Sea by deep convection during winter (Clarke and Gascard, 1983), and is typically found at mid-depth with σ_θ = ~27.77 kg/m^3. This water mass was noted by (Wüst and Defant, 1936) due to its salinity minimum and later defined and named by Smith et al. (1937). Since then, with the deepening of research on this water mass, the character was discovered as a contribution to the driving mechanism of northward heat transport in the Atlantic Meridional Overturning Circulation (AMOC) (Rhein et al., 2011). In the specific study on this water mass, LSW is divided into two units, 'upper' and 'classic', based on the differences in temperature and salinity (Kieke et al., 2007; Kieke et al., 2006). In the large scale as throughout the whole Atlantic Ocean, LSW is still treated as a unified water mass and considered as the main origin of upper NADW (Elliot et al., 2002; Talley and Mccartney, 1982). In the general scale, LSW distributes in the western part of the North Atlantic in Labrador Sea and Irminger Sea region and the distribution is influenced by the Gulf Stream, the Labrador Current and the North Atlantic Current (Elliot et al., 2002; Talley and Mccartney, 1982).

Seen from the aerial view of the analysis results to the whole GLODAPv2 dataset, Figure 8, LSW mainly distributes in the Northwest Atlantic north 40 °N near the Labrador Sea and Irminger Basin with core at σ_θ = ~27.77 kg/m^3. In terms of vertical distribution, A25 cruise (Expocode: 06MM20060523) shows that LSW dominates the depth between 500 and 2000m, and meanwhile, the fraction decreases with the spatial change to the east (direction to Iberian Peninsula) thus far away from the formation area (Greenland). This distribution is basically consistent with historical literatures. After southward transport with Labrador Current, LSW spreads eastward with Gulf Stream and North Atlantic Current until it meets MOW. In general, LSW is the dominate mid-depth water mass in the region north of 40 °N in Northwest Atlantic.

The Iceland–Scotland Overflow Water (ISOW) and Denmark Strait Overflow Water (DSOW), as original water masses that contribute to the formation of the lower NADW (Read, 2000), are located in the west and east part of North Atlantic (north of 40 °N) respectively with the main core near σ_θ = 27.88 kg/m3. Both ISOW and DSOW are formed by water masses from the Arctic Ocean and the Nordic Seas those reach the North Atlantic Ocean (Lacan and Jeandel, 2004; Tanhua et al., 2005b). As an indispensable link of the thermohaline circulation, the southward outflow of ISOW and DSOW to the Atlantic Ocean plays an important role, as well as LSW, in the deep-water component of the AMOC and has certain a certain impact on the European and even the global climate.

In general, ISOW is formed in the regions of Greenland, Iceland and Norwegian Seas, outflows southward in the west of Iceland, across the Faeroe Bank Channel into the eastern part of North Atlantic Ocean (Kissel et al., 1997; Swift, 1984). From a more specific perspective, ISOW has two branches. One branch passes near the Charlie-Gibbs Fracture Zone (CGFZ) and flow into Irminger basin at densities above the DSOW. The other branch goes southward into the West European Basin and meets the Northeast Atlantic Bottom Water (NEABW) (Garcia-Ibanez et al., 2015).

Consistent with literatures, the top view distribution from map shows ISOW mainly distributes in the Northeast Atlantic north 40 °N between Iceland and Iberian Peninsula with core at σ_θ = ~27.88 kg/m^3. In terms of vertical distribution, the A25 section shows that ISOW outflows at east of Iceland across Iceland-Faroe Ridge with core at depth between ~2000 and 3000m. In west of Iceland, ISOW can also be found in the Denmark Strait, where core of DSOW is located, with low fraction.

DSOW is the water mass that overflows through the Denmark Strait in west of Iceland and into Irminger Basin and Labrador Sea with σ_θ = ~27.88 kg/m^3 (Tanhua et al., 2005b). This overflow water mass is considered as the coldest and densest component of the sea water in the Northwest Atlantic Ocean and constitute a significant part of the southward flowing NADW (Swift, 1980). Compositions of DSOW can be traced to many surrounding water masses. Besides Arctic Intermediate Water (AIW), Re-circulating Atlantic Water (RAW), Polar Surface Water (PSW) and Arctic Atlantic Water (AAW) are all considered to be parts of the source (Clarke et al., 1990; Smethie Jr, 1993; Swift, 1980; Tanhua et al., 2005b). Rudels et al. (2002) noted the contribution from East Greenland Current (EGC) to the DSOW, EGC that brings Arctic Water in deep layer through the Fram Strait into the Greenland Sea is known as the main mechanism of forming DSOW and this provided us a theoretical basis for determining the distribution of DSOW.

According to the OMP calculations, and also referring to the above literature, the following conclusions about DSOW can be drawn. In the horizontal direction, map distribution shows DSOW mainly distributes along the drainage area of EGC with σ_θ = ~27.88 kg/m^3. DSOW starts from the Greenland Sea, southward flows into the Irminger Sea along EGC and then westward into Labrador Sea. The vertical distribution based on the A25 section shows that DSOW overflows through the Greenland-Scotland Ridge close proximity to the continental slope with core at depth between ~2500 and 3000m. Compared with ISOW, pathway of DSOW is relative narrow and limited within the eastern bottom in the Irminger Basin.

Main cores of ISOW and DSOW can be seen in both sides of Iceland separately below LSW. ISOW distributes all over the region between Greenland and Iberian Peninsula. After passing the Iceland, ISOW and DSOW convergence into one share and spread further southward. All the three water masses, LSW ISOW and DSOW, origin from the North Atlantic region, spread southward and finally become the dominate water masses in deep and overflow layer. Considering the change of properties

during the pathway, especially the final product of mixing compared with original ISOW and DSOW, also in order to comply with the needs of large-scale distribution in Atlantic Ocean and without paying too much attention to these details, two new water masses, upper and lower NADW based on SWTs in the companion paper (Liu and Tanhua, 2019), are adopted in the main Atlantic region south of 40 °N, whereas LSW ISOW and DSOW are not used in the OMP analysis and replaced upper and lower NADW.

After passing 40 °N, upper and lower NADW, considered as independent water masses, continue to spread until ~50 °S and dominate the most Atlantic Ocean in this layer. During the process to the south, NADW is transported along Deep West Boundary Current (DWBC) and also eastward with eddies (Lozier, 2012).

The OMP analysis shows that the upper and lower NADW are the main water masses in Deep and Overflow Layer, Figure 9. As the productions and considered as independent water masses, upper NADW distributes at a relative shallow pressure, while lower NADW with higher pressure close to their original water masses. After molding, upper and lower NADW are formed and spread southward with DWBC along the continental slope also spreads eastward and cover mostly all over the Atlantic Ocean in this layer due to eddies during the pathway (Lozier, 2012).

In horizontal scale, the map view shows that upper NADW covers the most area of deep and overflow layer, while lower NADW is found with higher fractions in the west region near the Deep Western Boundary Current (DWBC), especially in South Atlantic. In the vertical scale based on observation from meridional (A16) and zonal (A05 and A10) cruises, relative thicker lower NADW than upper NADW are discovered. Upper NADW, due to lower potential density, lies over lower NADW during the whole way to the south with their boundary at ~2000m depth. The boundary between upper NADW and intermediate water masses, AAIW and SAIW, are almost along our definition line (σ_θ = 27.7 kg/m^3). AABW is the only bottom water mass that contacts with upper NADW. In the region south of 40 °S, upper NADW is deflected up after it meets AABW and high mixing happens in this region due to ACC. Lower NADW is seen south to ~ 40 °S where it meets AABW.

3.4. The Bottom Layer: AABW and NEABW

AABW and NEABW dominate the bottom layer (σ_θ > 27.88 kg/m^3). In fact, both water masses have the same origin but distinguished by defining a new SWT as NEABW due to the sharp reduction of silicate, which is an important signal to label bottom water masses, after passing the equator. From aerial view of the maps, Figure 10, AABW and NEABW cover the most bottom area of South and North Atlantic respectively.

The AABW is formed in the Weddell Sea region south of the Antarctic Circumpolar Current (ACC). After leaving the formation area, AABW sinks to the bottom due to the high density during the way

north. After passing the ACC, AABW meets NADW and they have some water exchange from 50 °S until AABW reaches the equator (van Heuven et al., 2011). Due to dramatical change of properties after passing the equator, especially the sudden decrease of silicate, AABW is redefined as a new SWT, NEABW, in the north of equator. In the north of equator, water mass of NEABW origins from the newly defined SWT of NEWBW and as actually a continuation of AABW, becomes the dominate bottom water. Similar with AABW, NEABW also mainly mixed with lower NADW between equator and 40 °N. In north of 40 °N, NEABW spreads further north until ~50 °N, where it meets lower NADW origins from ISOW (Garcia-Ibanez et al., 2015).

In the A16 section in Figure 11, AABW sinks to the bottom between ~50 – 60 °S and spreads north to equator in the bottom layer below 4000m (σ_θ > 27.88 kg/m^3). After passing the ACC at ~ 40 °S, AABW meets upper NADW that is, in general, deflected upwards. During this process, part of AABW penetrate into the Deep and Overflow Layer (σ_θ between 27.7 and 27.88 kg/m3), so ~20 – 50 % of AABW can be seen in this layer in both the meridional (A16) and the zonal (A10) section. In the further north region, between 40 °S and the equator, AABW contacts mainly with lower NADW instead of upper NADW. The fraction of AABW also increases with pressure. North of equator, NEABW is the only bottom water mass and distributes in the bottom in both sides of the MAR with the main core located below ~4000m with σ_θ >27.88 kg/m^3. Observations from the A16 and A05 sections show NEABW in contact with lower NADW from the above and the fraction of NEABW increases with depth.

3.5. The Southern Water masses: WSBW, CDW, and AABW

In this section the formation of AABW in the Weddell Sea Region is investigated and displayed, Figure 12. Similarly to the situation of NADW, AABW originates from two initial water masses, CDW and WSBW in the Antarctic region. An additional section, SR04 is analyzed to display the detail about formation of AABW. The SR04 section in the Weddell Sea region is formed by two parts representing the formation of AABW in both the meridional and zonal directions.

In the zonal section across the Weddell Sea, AABW can be seen as the product from two original water masses, CDW and WSBW. The core of CDW distributes in the upper 1000m and WSBW origins at the surface and subducts along the continental slope into the bottom below 4000m. This result is consistent with (van Heuven et al., 2011). Both original water masses meet each other at depth between ~2000 and 4000m, where AABW is formed with main core locates at ~3000m.

The meridional section of SR04 cruise shows the northward outflow of AABW into the Atlantic Ocean. AABW is located between 2000 and 4000m, as a product from CDW and WSBW. After leaving Weddell Sea region, AABW is considered as an independent water mass from north of 60 °S and spreads further northward as the only bottom water mass until the equator. In relative low latitude

region (north of 60 °S), AAIW can also be found in shallow layer, since here is the boundary between formation area of AAIW and AABW.

4. Conclusion and Discussion

In this study, the distributions of water masses in Atlantic Ocean are investigated based on the GLODAPv2 dataset and the definition of water masses presented by (Liu and Tanhua, 2019). We have shown maps and sections of water mass distribution through the Atlantic Ocean basin. Water masses are mostly distributed within the density layer where they are formed, and mixing of water masses away from their formation areas are evident..

The central water masses, ENACW WNACW ESACW and WSACW, occupy the upper/central layer of the Atlantic Ocean by following the dividing line σ_θ < 27 kg/m3 and high salinity is also one significant property to identity them. Below the Upper layer, SAIW and MOW are the two main water masses in the intermediate layer in North Atlantic. SAIW comes from the northwest, sinks during the way to the southeast. In the eastern part, MOW overflows from the Mediterranean Sea, across the Strait of Gibraltar and spreads to the north and west. The most significant property of MOW is high salinity at around 1000m depth. In the South Atlantic, AAIW is the dominate water mass in intermediate layer. After the formation in the shallow layer, AAIW sinks into intermediate depth (around 1000m) and spreads to the north until ~ 40 °N and this water mass can easily be found with low salinity.

NADW is the main water mass in the Deep and Overflow Layer. In order to show more clearly the distribution of water masses in this layer, more detail are investigated to display upper and lower NADW, as well as their origin, LSW, ISOW and DSOW, separately.

For the bottom waters, AABW and NEABW, have similar properties, especially high silicate content, since NEABW, traced back to the source, is a branch from AABW after passing the equator. After spanning most Atlantic there is a sharp reduction of silicate concentration, the new defined SWT, NEABW becomes the dominate water mass in the bottom.

Acknowledgements

This work is based on the comprehensive and detailed data from GLODAP data set throughout the past few decades and we would like to thank the efforts from all the scientists and crews on cruises and the working groups of GLODAP for their contributions and selfless sharing. In particular, we are grateful to the theoretical and technical support from J. Karstensen and M. Tomczak for the OMP analysis. Thanks to the China Scholarship Council (CSC) for providing funding support to Mian Liu's PhD study in GEOMAR Helmholtz Centre for Ocean Research Kiel.

References

Alvarez, M., Brea, S., Mercier, H., Alvarez-Salgado, X.A., 2014. Mineralization of biogenic materials in the water masses of the South Atlantic Ocean. I: Assessment and results of an optimum multiparameter analysis. Prog Oceanogr 123, 1-23.

Broecker, W.S., 1974. No a Conservative Water-Mass Tracer. Earth Planet Sc Lett 23, 100-107.

Carracedo, L., Pardo, P.C., Flecha, S., Pérez, F.F., 2016. On the Mediterranean Water Composition. Journal of Physical Oceanography 46, 1339-1358.

Clarke, R.A., Gascard, J.-C., 1983. The Formation of Labrador Sea Water. Part I: Large-Scale Processes. Journal of Physical Oceanography 13, 1764-1778.

Clarke, R.A., Swift, J.H., Reid, J.L., Koltermann, K.P., 1990. The formation of Greenland Sea Deep Water: double diffusion or deep convection? Deep Sea Research Part A. Oceanographic Research Papers 37, 1385-1424.

Deruijter, W., 1982. Asymptotic Analysis of the Agulhas and Brazil Current Systems. Journal of Physical Oceanography 12, 361-373.

Elliot, M., Labeyrie, L., Duplessy, J.C., 2002. Changes in North Atlantic deep-water formation associated with the Dansgaard-Oeschger temperature oscillations (60-10 ka). Quaternary Science Reviews 21, 1153-1165.

Emery, W.J., Meincke, J., 1986. Global Water Masses - Summary and Review. Oceanologica Acta 9, 383-391.

Fyfe, J.C., Saenko, O.A., Zickfeld, K., Eby, M., Weaver, A.J., 2007. The role of poleward-intensifying winds on Southern Ocean warming. Journal of Climate 20, 5391-5400.

Garcia-Ibanez, M.I., Pardo, P.C., Carracedo, L.I., Mercier, H., Lherminier, P., Rios, A.F., Perez, F.F., 2015. Structure, transports and transformations of the water masses in the Atlantic Subpolar Gyre. Prog Oceanogr 135, 18-36.

Hinrichsen, H.H., Tomczak, M., 1993. Optimum multiparameter analysis of the water mass structure in the western North Atlantic Ocean. Journal of Geophysical Research: Oceans 98, 10155-10169.

Ishii, M., Suzuki, T., Key, R., 2011. Pacific Ocean Interior Carbon Data Synthesis, PACIFICA, in Progress. PICES Press 19, 20.

Karstensen, J., Stramma, L., Visbeck, M., 2008. Oxygen minimum zones in the eastern tropical Atlantic and Pacific oceans. Prog Oceanogr 77, 331-350.

Karstensen, J., Tomczak, M., 1997. Ventilation processes and water mass ages in the thermocline of the southeast Indian Ocean. Geophysical Research Letters 24, 2777-2780.

Karstensen, J., Tomczak, M., 1998a. Age determination of mixed water masses using CFC and oxygen data. Journal of Geophysical Research: Oceans 103, 18599-18609.

Karstensen, J., Tomczak, M., 1998b. Age determination of mixed water masses using CFC and oxygen data. J Geophys Res-Oceans 103, 18599-18609.

Key, R.M., Kozyr, A., Sabine, C.L., Lee, K., Wanninkhof, R., Bullister, J.L., Feely, R.A., Millero, F.J., Mordy, C., Peng, T.H., 2004. A global ocean carbon climatology: Results from Global Data Analysis Project (GLODAP). Global biogeochemical cycles 18.

Key, R.M., Tanhua, T., Olsen, A., Hoppema, M., Jutterström, S., Schirnick, C., van Heuven, S., Kozyr, A., Lin, X., Velo, A., Wallace, D.W.R., Mintrop, L., 2010. The CARINA data synthesis project: introduction and overview. Earth Syst. Sci. Data 2, 105-121.

Kieke, D., Rhein, M., Stramma, L., Smethie, W.M., Bullister, J.L., LeBel, D.A., 2007. Changes in the pool of Labrador Sea Water in the subpolar North Atlantic. Geophysical Research Letters 34.

Kieke, D., Rhein, M., Stramma, L., Smethie, W.M., LeBel, D.A., Zenk, W., 2006. Changes in the CFC inventories and formation rates of Upper Labrador Sea Water, 1997-2001. Journal of Physical Oceanography 36, 64-86.

Kirchner, K., Rhein, M., Huttl-Kabus, S., Boning, C.W., 2009. On the spreading of South Atlantic Water into the Northern Hemisphere. J Geophys Res-Oceans 114.

Kissel, C., Laj, C., Lehman, B., Labyrie, L., Bout-Roumazeilles, V., 1997. Changes in the strength of the Iceland-Scotland Overflow Water in the last 200,000 years: Evidence from magnetic anisotropy analysis of core SU90-33. Earth Planet Sc Lett 152, 25-36.

Klein, B., Hogg, N., 1996. On the variability of 18 Degree Water formation as observed from moored instruments at 55 degrees W. Deep-Sea Research Part I-Oceanographic Research Papers 43, 1777-&.

Klein, B., Tomczak, M., 1994. Identification of diapycnal mixing through optimum multiparameter analysis: 2. Evidence for unidirectional diapycnal mixing in the front between North and South Atlantic Central Water. Journal of Geophysical Research: Oceans 99, 25275-25280.

Kuhlbrodt, T., Griesel, A., Montoya, M., Levermann, A., Hofmann, M., Rahmstorf, S., 2007. On the driving processes of the Atlantic meridional overturning circulation. Reviews of Geophysics 45.

Lacan, F., Jeandel, C., 2004. Neodymium isotopic composition and rare earth element concentrations in the deep and intermediate Nordic Seas: Constraints on the Iceland Scotland Overflow Water signature. Geochemistry Geophysics Geosystems 5.

Lauvset, S.K., Key, R.M., Olsen, A., van Heuven, S., Velo, A., Lin, X., Schirnick, C., Kozyr, A., Tanhua, T., Hoppema, M., Jutterström, S., Steinfeldt, R., Jeansson, E., Ishii, M., Perez, F.F., Suzuki, T., Watelet, S., 2016. A new global interior ocean mapped climatology: the 1° × 1° GLODAP version 2. Earth Syst. Sci. Data 8, 325-340.

Lazier, J.R.N., Wright, D.G., 1993. Annual Velocity Variations in the Labrador Current. Journal of Physical Oceanography 23, 659-678.

Lozier, M.S., 2012. Overturning in the North Atlantic. Ann Rev Mar Sci 4, 291-315.

Lutjeharms, J.R., van Ballegooyen, R.C., 1988. Anomalous upstream retroflection in the agulhas current. Science 240, 1770.

Mackas, D.L., Denman, K.L., Bennett, A.F., 1987. Least squares multiple tracer analysis of water mass composition. Journal of Geophysical Research: Oceans 92, 2907-2918.

McCartney, M.S., 1982. The subtropical recirculation of Mode Waters. J Mar Res 40, 427-464.

McCartney, M.S., Talley, L.D., 1982. The subpolar mode water of the North Atlantic Ocean. Journal of Physical Oceanography 12, 1169-1188.

Peterson, R.G., Stramma, L., 1991. Upper-Level Circulation in the South-Atlantic Ocean. Prog Oceanogr 26, 1-73.

Pickart, R.S., Spall, M.A., Lazier, J.R.N., 1997. Mid-depth ventilation in the western boundary current system of the sub-polar gyre. Deep-Sea Research Part I-Oceanographic Research Papers 44, 1025-+.

Poole, R., Tomczak, M., 1999. Optimum multiparameter analysis of the water mass structure in the Atlantic Ocean thermocline. Deep-Sea Research Part I-Oceanographic Research Papers 46, 1895-1921.

Price, J.F., Baringer, M.O., Lueck, R.G., Johnson, G.C., Ambar, I., Parrilla, G., Cantos, A., Kennelly, M.A., Sanford, T.B., 1993. Mediterranean outflow mixing and dynamics. Science 259, 1277-1282.

Read, J., 2000. CONVEX-91: water masses and circulation of the Northeast Atlantic subpolar gyre. Prog Oceanogr 48, 461-510.

Rhein, M., Kieke, D., Huttl-Kabus, S., Roessler, A., Mertens, C., Meissner, R., Klein, B., Boning, C.W., Yashayaev, I., 2011. Deep water formation, the subpolar gyre, and the meridional overturning circulation in the subpolar North Atlantic. Deep-Sea Research Part Ii-Topical Studies in Oceanography 58, 1819-1832.

Rudels, B., Fahrbach, E., Meincke, J., Budéus, G., Eriksson, P., 2002. The East Greenland Current and its contribution to the Denmark Strait overflow. ICES Journal of Marine Science 59, 1133-1154.

Smethie Jr, W.M., 1993. Tracing the thermohaline circulation in the western North Atlantic using chlorofluorocarbons. Prog Oceanogr 31, 51-99.

Smethie, W.M., Fine, R.A., 2001. Rates of North Atlantic Deep Water formation calculated from chlorofluorocarbon inventories. Deep-Sea Research Part I-Oceanographic Research Papers 48, 189-215.

Smith, E.H., Soule, F.M., Mosby, O., 1937. The Marion and General Greene Expeditions to Davis Strait and Labrador Sea, Under Direction of the United States Coast Guard: 1928-1931-1933-1934-1935: Scientific Results, Part 2: Physical Oceanography. US Government Printing Office.

Stramma, L., England, M.H., 1999. On the water masses and mean circulation of the South Atlantic Ocean. J Geophys Res-Oceans 104, 20863-20883.

Sverdrup, 1942. The Oceans: Their Physics, Chemistry and General Biology.

Swift, J.H., 1984. The Circulation of the Denmark Strait and Iceland Scotland Overflow Waters in the North-Atlantic. Deep-Sea Research Part a-Oceanographic Research Papers 31, 1339-1355.

Swift, S.M., 1980. Activity patterns of pipistrelle bats (Pipistrellus pipistrellus) in north‐east Scotland. Journal of Zoology 190, 285-295.

Talley, L., 1996. Antarctic intermediate water in the South Atlantic, The South Atlantic. Springer, pp. 219-238.

Talley, L., Raymer, M., 1982. Eighteen degree water variability. J. Mar. Res 40, 757-775.

Talley, L.D., Mccartney, M.S., 1982. Distribution and Circulation of Labrador Sea-Water. Journal of Physical Oceanography 12, 1189-1205.

Tanhua, T., Olsson, K.A., Jeansson, E., 2005. Formation of Denmark Strait overflow water and its hydro-chemical composition. Journal of Marine Systems 57, 264-288.

Tomczak, M., 1981. A multi-parameter extension of temperature/salinity diagram techniques for the analysis of non-isopycnal mixing. Prog Oceanogr 10, 147-171.

Tomczak, M., Large, D.G., 1989. Optimum multiparameter analysis of mixing in the thermocline of the eastern Indian Ocean. Journal of Geophysical Research: Oceans 94, 16141-16149.

van Heuven, S.M.A.C., Hoppema, M., Huhn, O., Slagter, H.A., de Baar, H.J.W., 2011. Direct observation of increasing CO2 in the Weddell Gyre along the Prime Meridian during 1973–2008. Deep Sea Research Part II: Topical Studies in Oceanography 58, 2613-2635.

Weiss, R.F., Ostlund, H.G., Craig, H., 1979. Geochemical Studies of the Weddell Sea. Deep-Sea Research Part a-Oceanographic Research Papers 26, 1093-1120.

Wüst, G., Defant, A., 1936. Atlas zur Schichtung und Zirkulation des Atlantischen Ozeans: Schnitte und Karten von Temperatur, Salzgehalt und Dichte. W. de Gruyter.

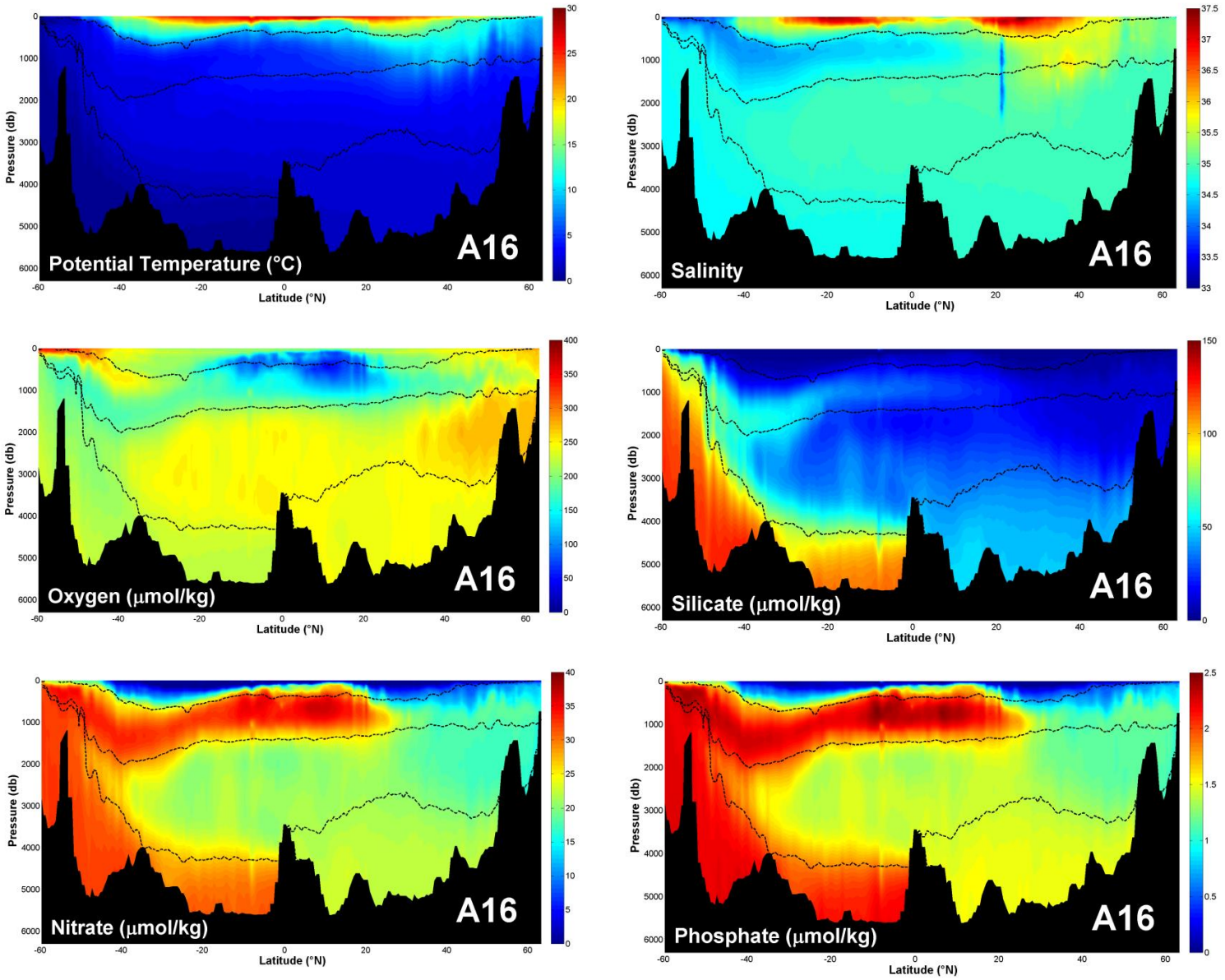

Fig 1 Key properties required by OMP analysis based on A16 cruises in 2013
Expocode: 33RO20130803 in North Atlantic & 33RO20131223 in South Atlantic

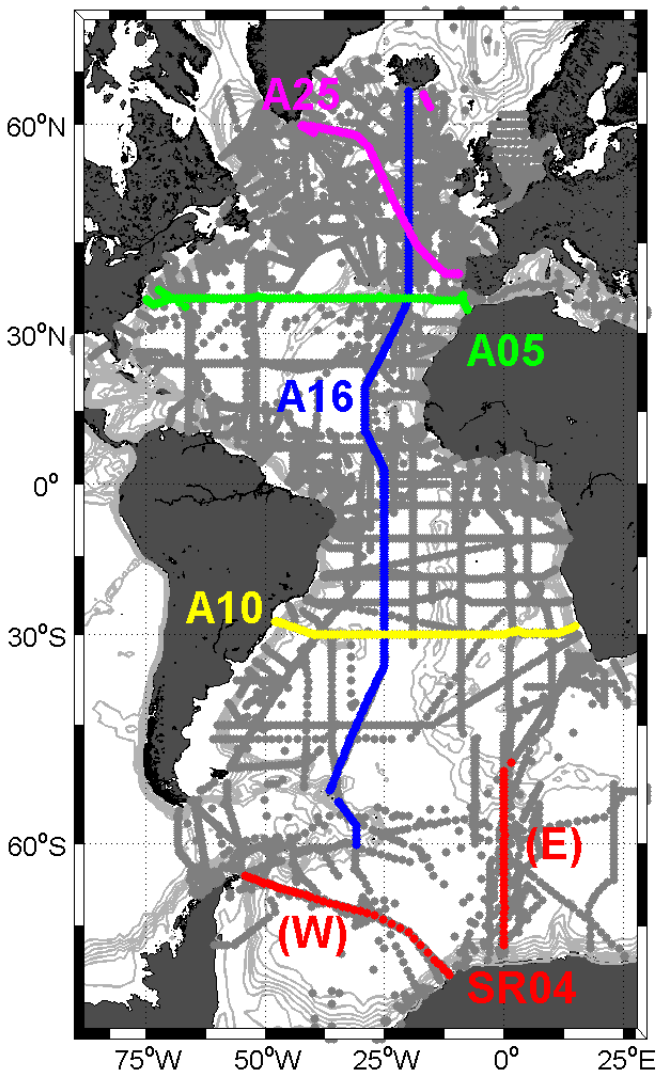

Fig 2 Maps of Cruises
Color lines show representative cruises analyzed in this paper while gray dots show all the GLODAPv2 stations

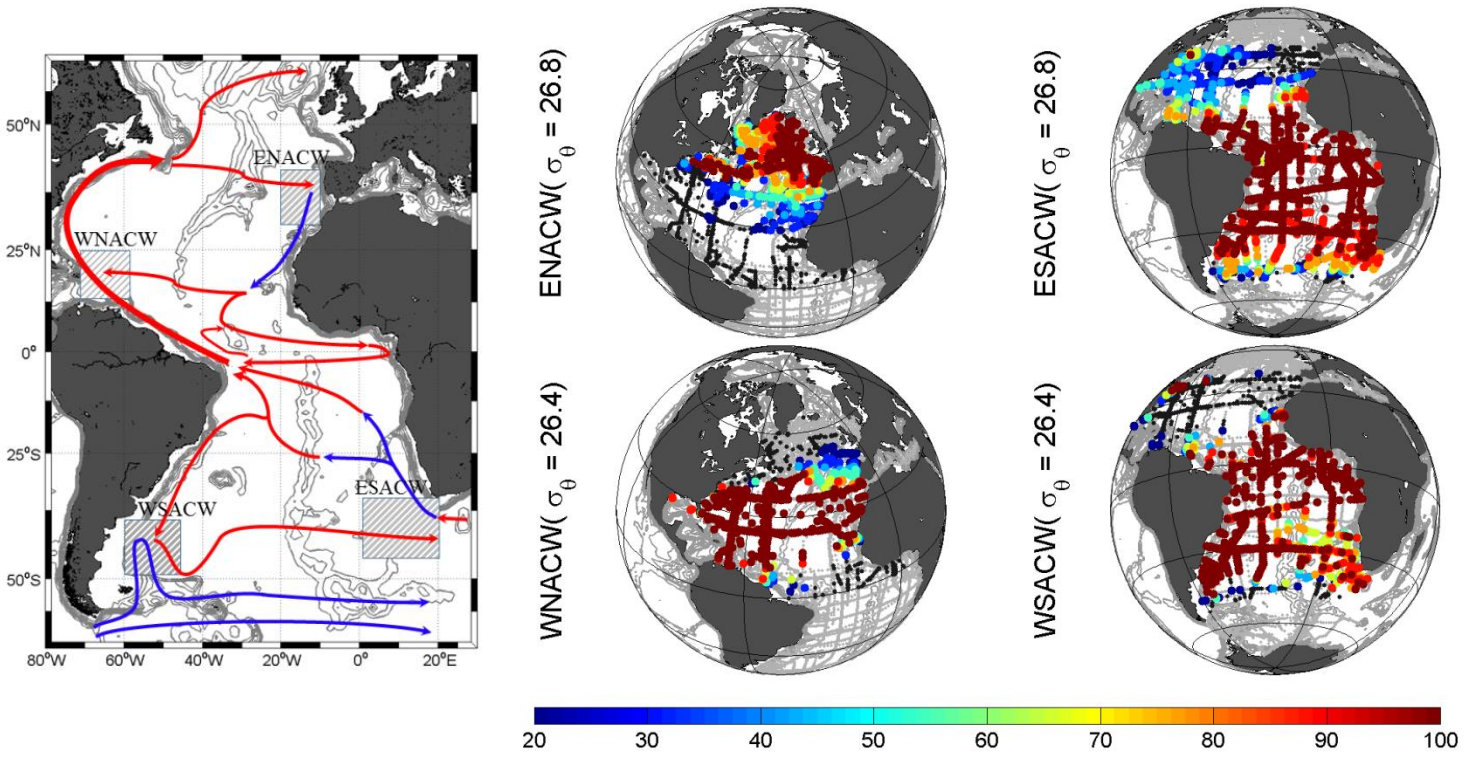

Fig. 3 Currents (left) and Water Masses (right) in the Upper Layer
Left: The arrows show the warm (red) and cold (blue) currents and rectangular shadow areas show the formation areas of water masses in the Upper Layer.
Right: Color dots show fractions (from 20% to 100%) of water masses in each station around core potential density (kg/m^3). Stations with fractions less than 20% are marked by black dots while gray dots show the GLODAPv2 stations without specified water mass.

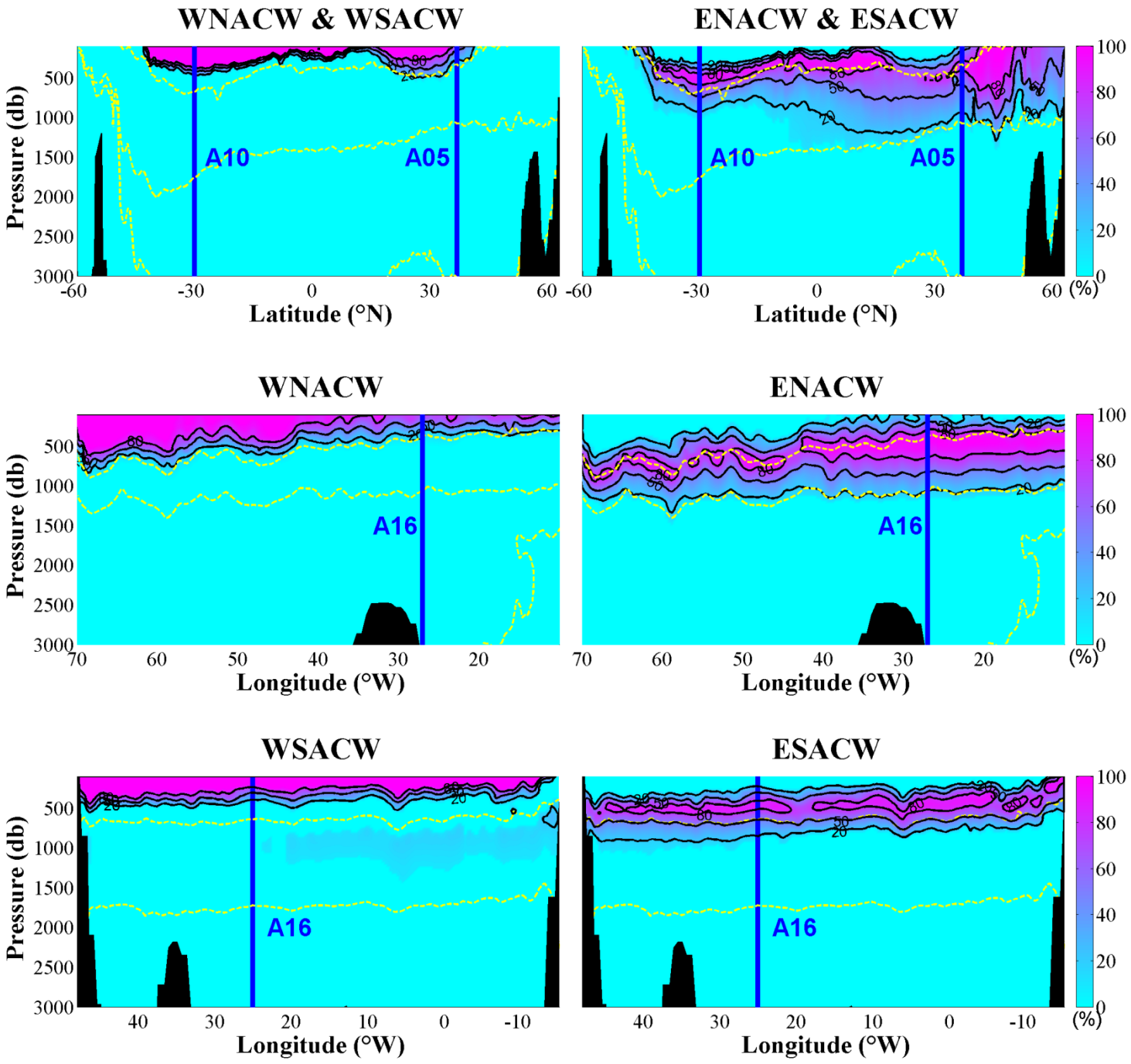

Fig. 4 Distribution of Central Water Masses based on A16 (upper), A05 (middle), A10 (lower) cruises within 3000m Contour lines show fractions of 20% 50% and 80%, blue lines show cross section of other cruises, yellow dashed lines show the boundaries of vertical water columns layers (potential density at 27, 27.7 and 27.88 kg/m^3)

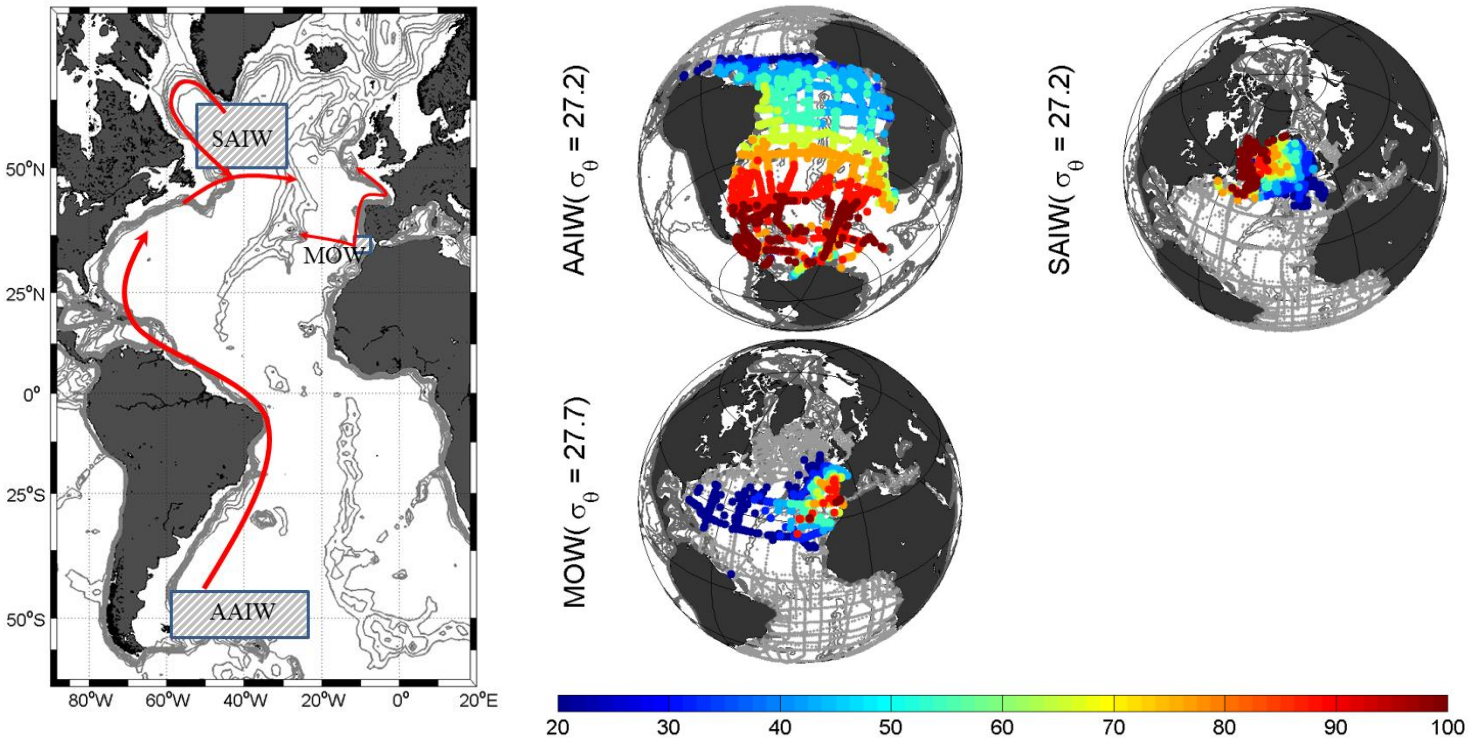

Fig.5 Currents (left) and Water Masses (right) in the Intermediate Layer
Left: The arrows show the currents and rectangular shadow areas show the formation areas of water masses in the Intermediate Layer.
Right: Color dots show fractions (from 20% to 100%) of water masses in each station around core potential density (kg/m^3). Stations with fractions less than 20% are marked by black dots while gray dots show the GLODAPv2 stations without specified water mass.

.

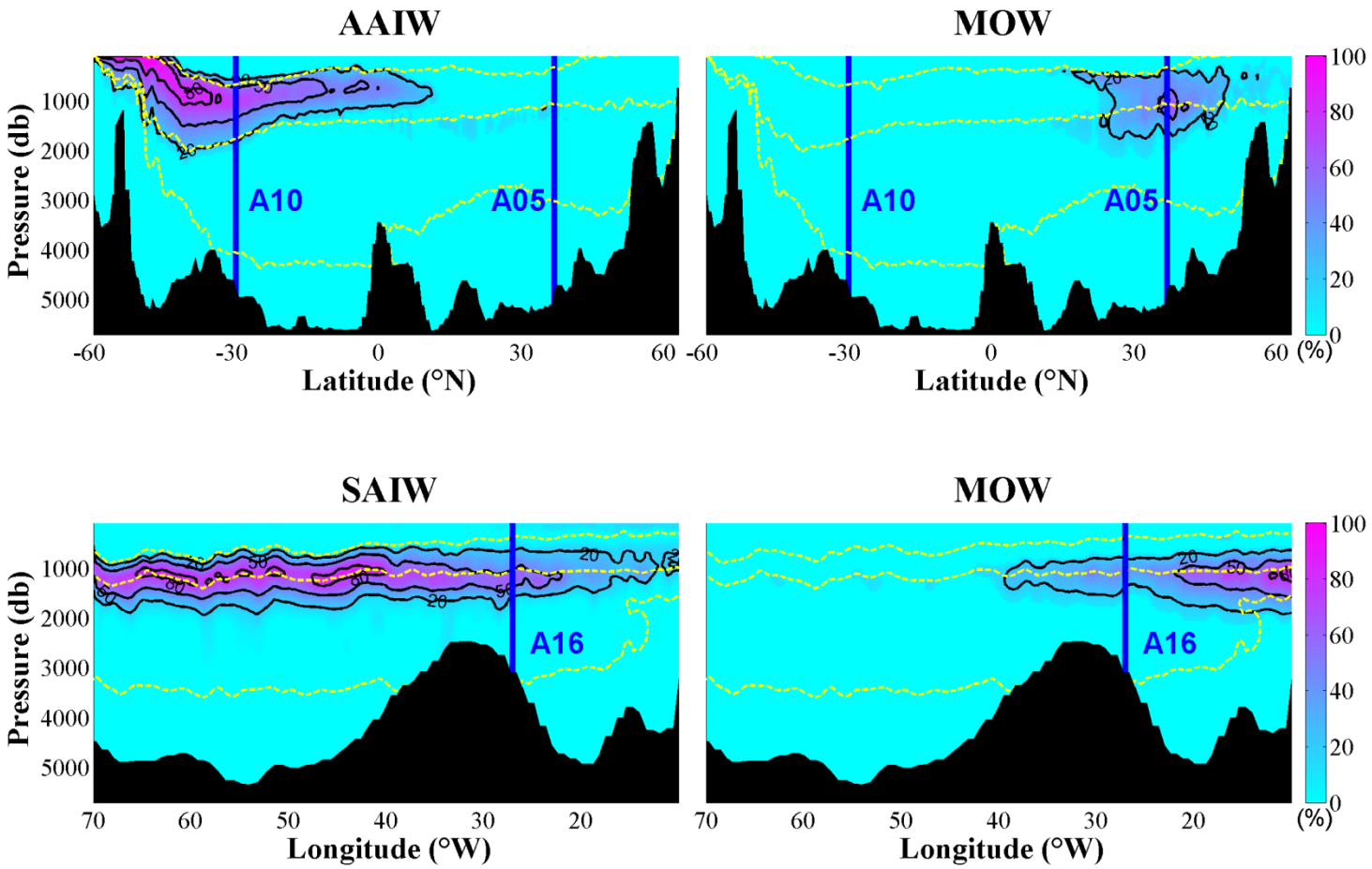

Fig. 6 Distribution of Water Masses in the Intermediate Layer based on A16 (upper) and A05 (lower) cruises Contour lines show fractions of 20% 50% and 80%, blue lines show cross section of other cruises, yellow dashed lines show the boundaries of vertical water columns layers (potential density at 27, 27.7 and 27.88 kg/m^3)

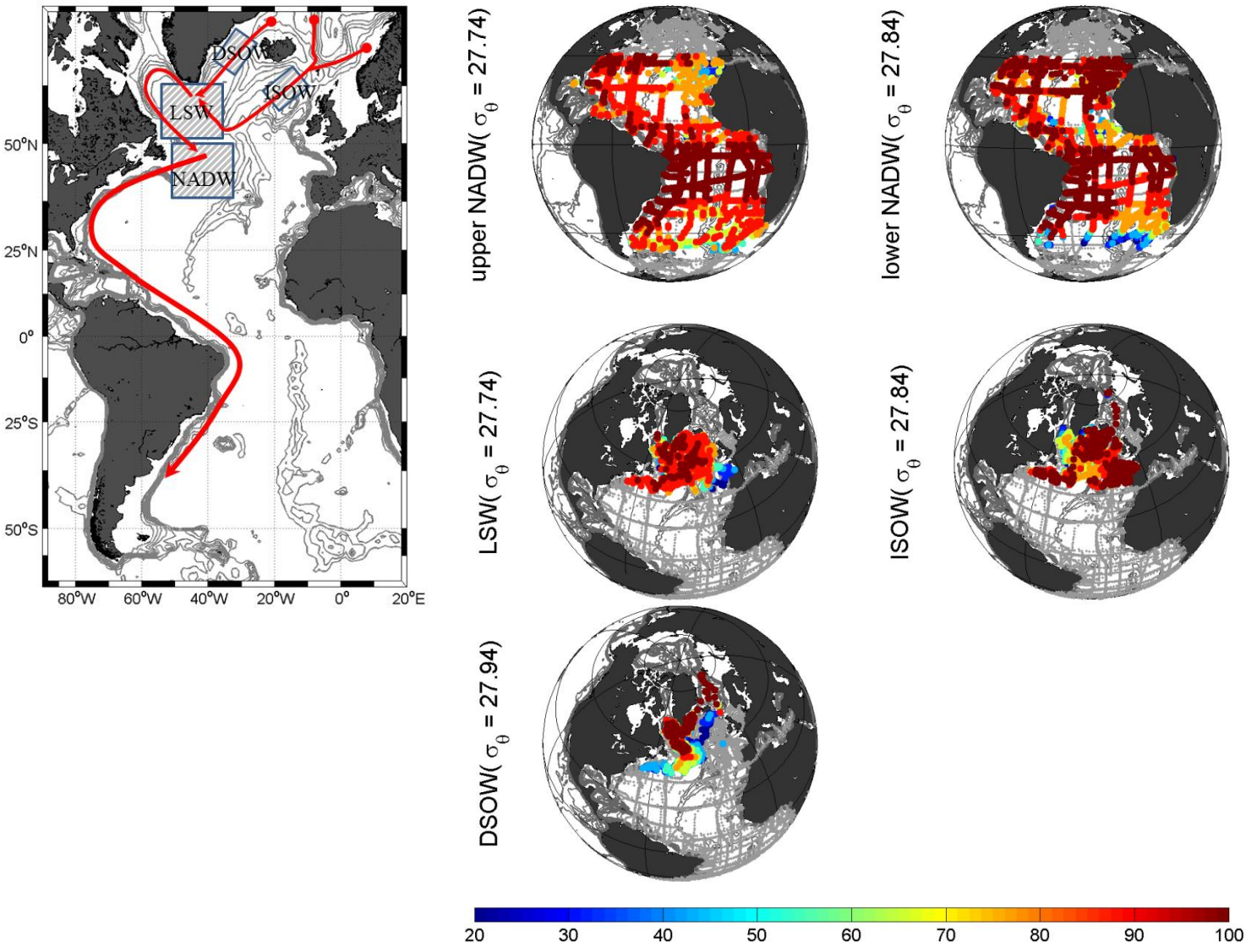

Fig.7 Currents (left) and Water Masses (right) in the Deep and Overflow Layer
Left: The arrows show the currents and rectangular shadow areas show the formation areas of water masses in the Deep and Overflow Layer.
Right: Color dots show fractions (from 20% to 100%) of water masses in each station around core potential density (kg/m^3). Stations with fractions less than 20% are marked by black dots while gray dots show the GLODAPv2 stations without specified water mass.

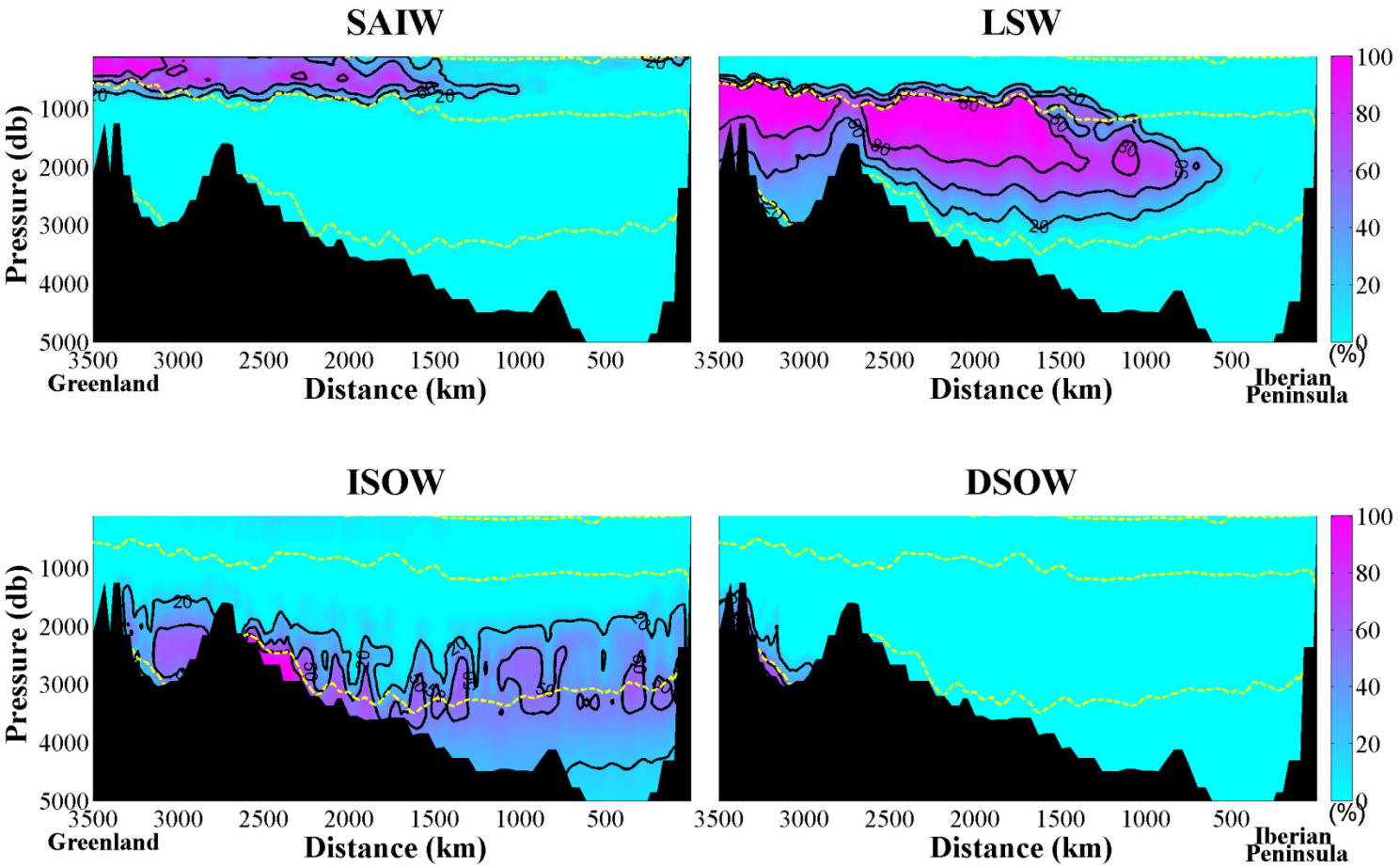

Fig. 8 Distribution of SAIW (upper left), LSW (upper right), ISOW (lower left) and DSOW (lower right) based on A25 cruise Contour lines show fractions of 20% 50% and 80%, blue lines show cross section of other cruises, yellow dashed lines show the boundaries of vertical water columns layers (potential density at 27, 27.7 and 27.88 kg/m^3)

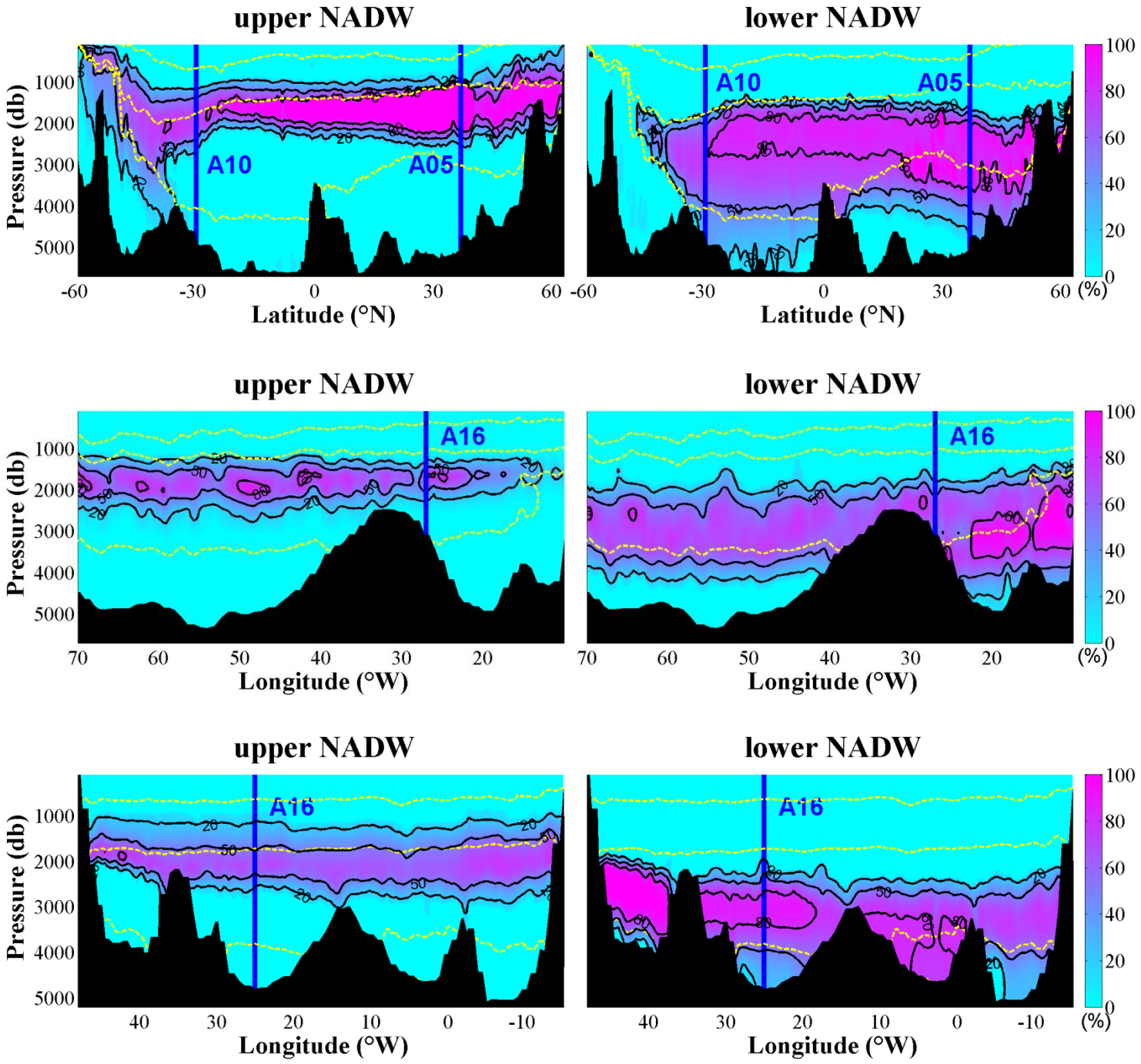

Fig. 9 Distribution of upper and lower NADW based on A16 (upper), A05 (middle) and A10 (lower) cruises
Contour lines show fractions of 20% 50% and 80%, blue lines show cross section of other cruises, yellow dashed lines show the boundaries of vertical water columns layers (potential density at 27, 27.7 and 27.88 kg/m^3)

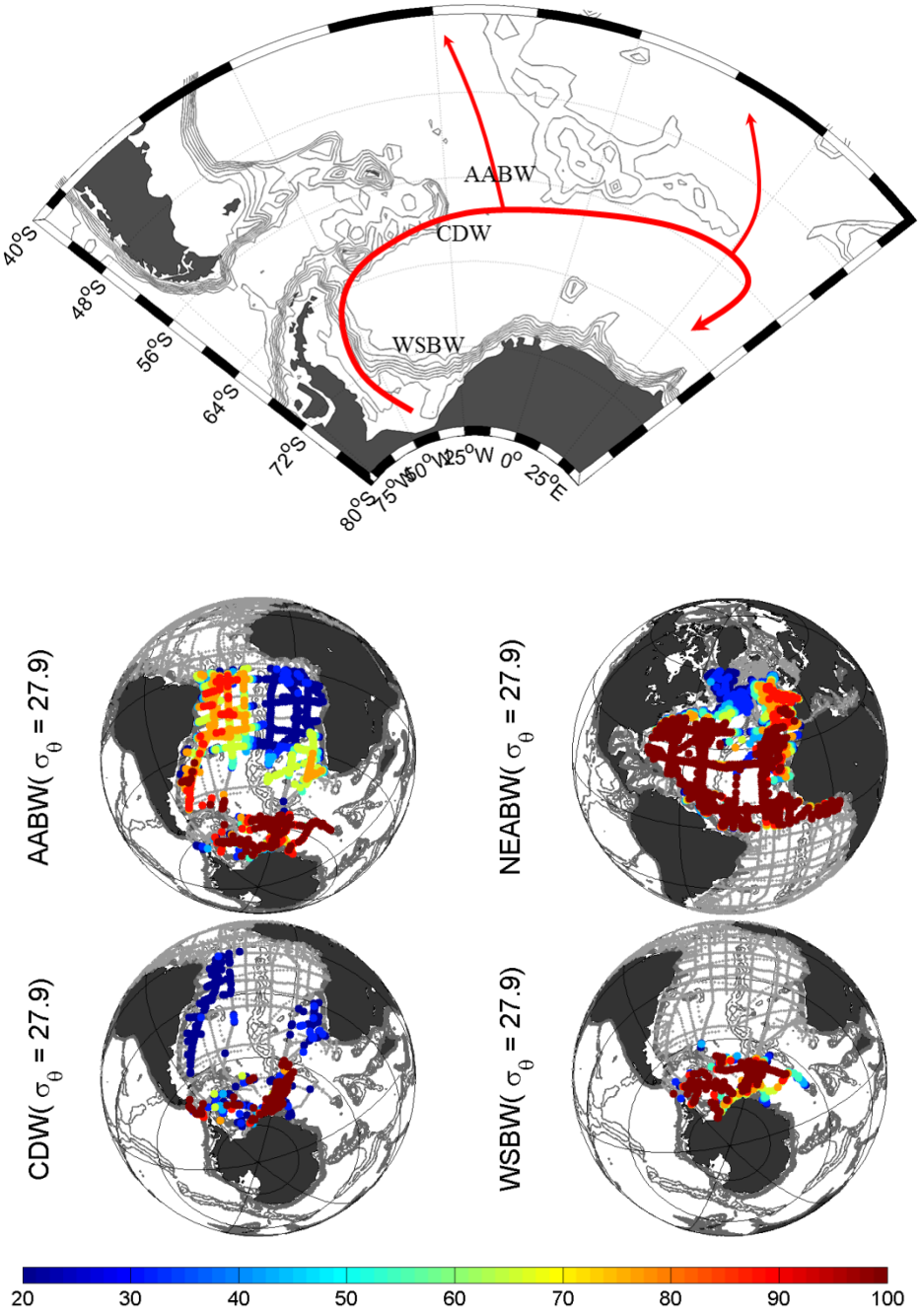

Fig.10 Currents (upper) and Water Masses (lower) in the Bottom Layer (AABW and NEABW) and the Southern Area (CDW and WSBW)
Upper: The arrows show the currents in the Southern Area.
Lower: Color dots show fractions (from 20% to 100%) of water masses in each station around core potential density (kg/m^3). Stations with fractions less than 20% are marked by black dots while gray dots show the GLODAPv2 stations without specified water mass.

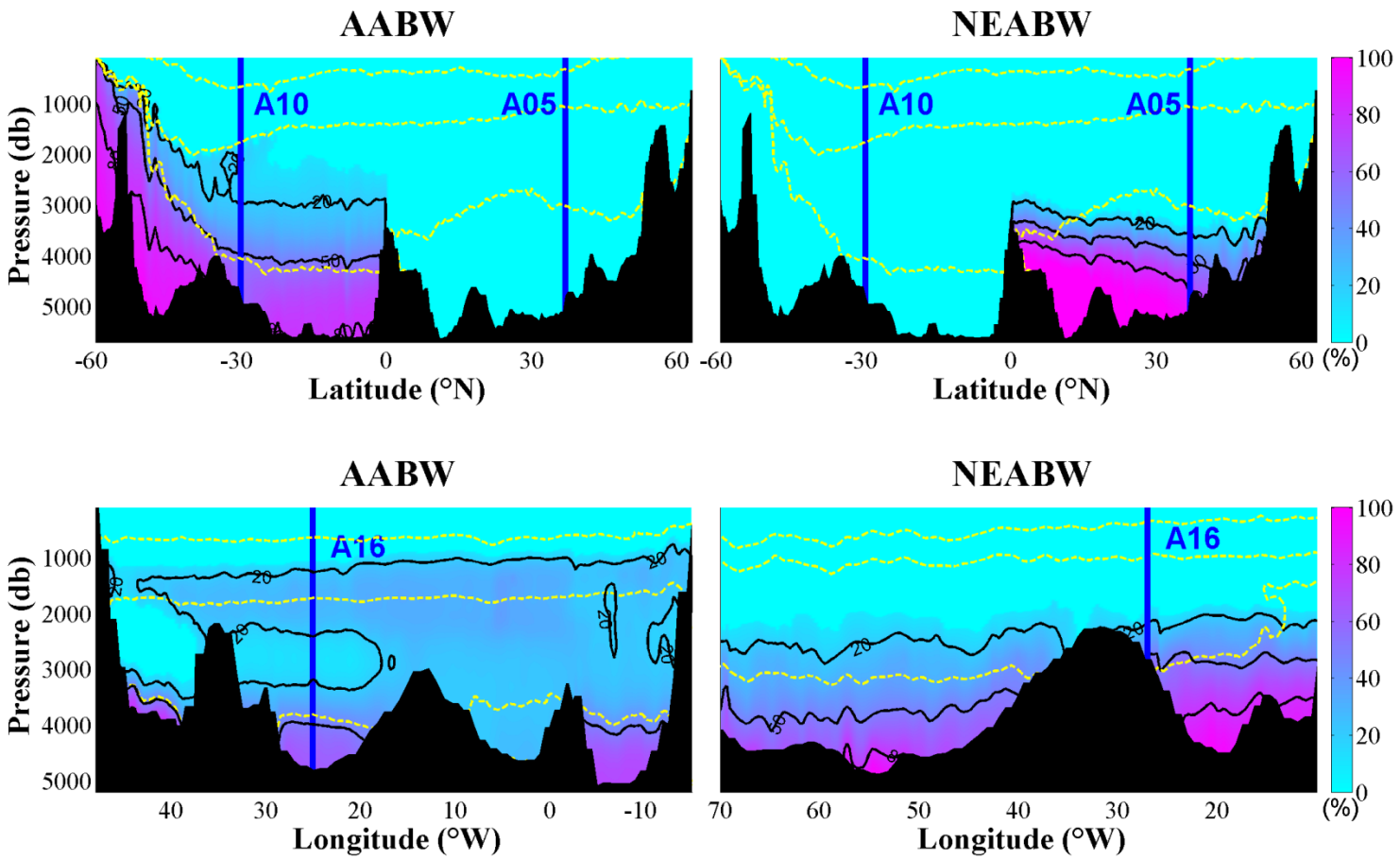

Fig. 11 Distribution of AABW and NEABW based on A16 (upper), A10 (lower left) and A05 (lower right) cruises
Contour lines show fractions of 20% 50% and 80%, blue lines show cross section of other cruises, yellow dashed lines show the boundaries of vertical water columns layers (potential density at 27, 27.7 and 27.88 kg/m^3)

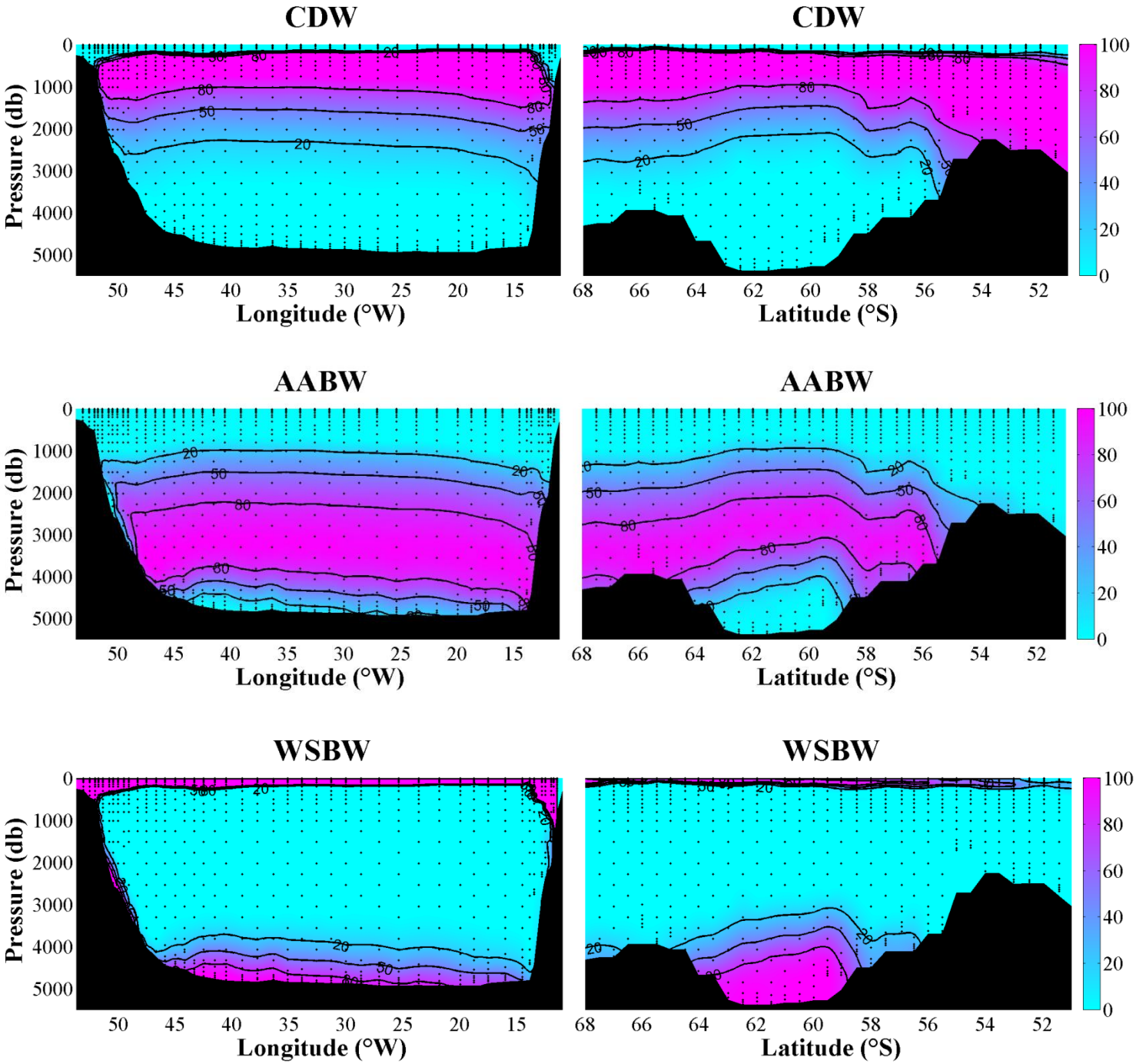

Fig. 12 Distribution of Southern Water Masses (CDW, AABW and WSBW) based on SR04 cruises
Left figures show the west (zonal) part and right figures show the east (meridional) part
Contour lines show fractions of 20% 50% and 80%, blue lines show cross section of other cruises

50 °S	Equator	40 °N	
#13 AAIW AABW CDW WSBW (σ_θ = 27 kg/m^3)	**#6** WSACW ESACW AAIW	**#5** WSACW WNACW ESACW ENACW AAIW	**#1** WNACW ENACW SAIW MOW
	#8 ESACW AAIW uNADW	**#7** ENACW ESACW AAIW MOW uNADW	**#2** ENACW SAIW MOW LSW
(σ_θ = 27.7 kg/m^3)			
	#10 AAIW uNADW lNADW CDW AABW	**#9** AAIW MOW uNADW lNADW NEABW	**#3** SAIW LSW ISOW DSOW NEABW
(σ_θ = 27.88 kg/m^3)			
	#12 lNADW AABW	**#11** lNADW NEABW	**#4** ISOW DSOW NEABW
50 °S	Equator	40 °N	

Table 1 schematic of OMP runs in this study

Chapter IV:

Ages of Water Masses in the Atlantic Ocean and the Estimation of mean Transport Velocities based on cruises from GLODAPv2 dataset

Abstract: Combining with the distributions of the main water masses in the Atlantic Ocean described in previous chapters (Chapter II and III), the mean ages of these water masses observed from meridional (A16) and zonal (A05 and A10) sections in the Atlantic Ocean are investigated based on transient tracers (CFC-12 and SF_6). The mean ages of water masses classified by four vertical layers and their transport time during the pathways are calculated and mapped out assuming with a standard mixing ratio ($\Delta/\Gamma = 1$) and a saturation of 100%. In general, mean ages increase with pressure and the central waters in the upper layer have the lowest mean ages within 50 years. In the intermediate layer, AAIW and MOW show gradients of mean ages in the meridional (south to north) and zonal (east to west) direction respectively. The transport time of AAIW is ~400 years from formation area to the north boundary at ~20 °N while it takes MOW ~300 years from the Strait of Gibraltar across the Mid-Atlantic-Ridge to the west basin of North Atlantic. As the main water mass in the deep and overflow layer, NADW (both upper and lower parts), which is formed in the high latitude region in the North Atlantic, sinks and transports to the south until ACC region at ~ 50 °S. During the pathway to the south, NADW also spreads westward and the whole process takes ~500 years. Bottom waters, including AABW and NEABW, have the same origin in the Antarctic region and take ~500 years to spread to the north boundary at ~50 °N. Velocities of upper NADW can be estimated with the mode ages and distances based on CFC-12 and SF_6. Result from three cruises along the DWBC shows a velocity of ~1.0 cm/s before upper NADW passes the equator while the velocity is difficult to be estimated in the south hemisphere due to the complex situation of eddies and hard mixing.

Key words: Water Mass, Atlantic Ocean, Transient Tracer, Mean Age, GLODAPv2

1 Introduction

Formations and transports of water masses in the Atlantic Ocean, as an indispensable branch of Atlantic Meridional Overturning Circulation (AMOC), has been widely concerned for decades due to its impacts on the Europe and even global climate (Bryden et al., 2005; Clark et al., 2012). Different from the general global situation, heat transport in the Atlantic Ocean shows a net northward direction instead of polarward. The heat transfer is mainly achieved through the transport of water masses. Warm surface water transports to the north in the shallow, while cold deep water spreads to the south (Ganachaud and Wunsch, 2000; Hall and Bryden, 1982; Trenberth and Caron, 2001). Meanwhile, transport of water masses in the Atlantic Ocean also plays a critical role in the carbon cycle. As the significant carrier/storage of carbon, the ocean contains 60 times as much carbon as in the atmosphere and the transport of water masses in the ocean influences the sea-air exchange directly or indirectly (Tanhua et al., 2006; Ziska et al., 2013).

As early as the beginning of 20th century, Bjerknes and Sandström proposed, both theoretically and experimentally, the existence of heat source into the deep Atlantic Ocean and opened up the large scale research on downward heat and water mass in the Atlantic Ocean (Bjerknes, 1964; Sandström, 1908, 1916). With the development of the research, the fact is gradually realized that mostly water masses in the Atlantic Ocean are included within the following four processes, or more specifically, a complete cycle that composed by four parts. 1. Central waters are transport by surface currents northward until high latitude in the North Atlantic; 2. Deep water (NADW) is formed and sinks near Labrador and Irminger Sea region, where surface water becomes dense and due to low temperature and high salinity. 3. The formed deep water (NADW) spreads southwards with Deep Western Boundary Currents; 4. Upwelling of deep water to the surface takes place in the Southern Ocean. This cycle also constitutes the main part of thermohaline circulation and AMOC (e.g. Bryden et al., 2005; Hall and Bryden, 1982; Kuhlbrodt et al., 2007). Simultaneously, this circulation does not remain constant but is affected by environmental factors such as wind stress (Rahmstorf, 2000; Rahmstorf et al., 2005). Many researches focus on specific areas or details (e.g. Toggweiler and Samuels, 1993; Toggweiler and Samuels, 1995) but less sketch out the overview of all the water masses in the Atlantic Ocean. A general introduction on movements of water masses is helpful and necessary to understand the thermohaline circulation and, furthermore, to speculate the impacts on climate (Kuhlbrodt et al., 2007).

In this chapter, main water masses are labeled with transient tracers (CFC-12 and SF_6) and their mean ages (consuming time during the pathway from formation area) are calculated based on GLODAPv2 dataset. Since concentrations of CFC-12 and SF_6 are not measured in many cruises especially early cruises, data of mean ages are insufficient to show an aerial view of distribution in the entire Atlantic Ocean, data from representative cruises are analyzed and present. Firstly, as the continuous work of previous chapters, the relevant criteria, including for vertical layer division of water columns and

distribution of water masses, is still used and transport time of water masses are investigated. Four central water masses, due to similar formation and transport processes, are considered as a whole part instead of listing the details of each water mass separately. In general, central water masses have the low mean ages within 50 years and increase with pressure and the distance from their formation areas. In the intermediate layer, AAIW and MOW are two conspicuous water masses and they travel from south to north (AAIW) and from east to west (MOW) respectively. As the dominant water mass in the deep and overflow layer, NADW, which is formed in the high latitude North Atlantic Ocean, sinks and spreads southward with deep western boundary current and further eastward with eddies. The whole process takes as long as ~500 years to cover the deep Atlantic Ocean. Upper and lower portions of NADW, during their southward transport, are generally similar but different in details. Similar as central waters, all water mass in the bottom layer are considered together. Bottom waters origins from south of ~50 °S (south of ACC) and take ~500 years spreads to the north.

2 Data and methods

2.1 Water Mass Analysis

The distribution of the main water masses in the Atlantic Ocean are based on investigation of the Optimal Multi-Parameter (OMP) analysis in previous chapters (Chapter II and III). The OMP analysis is to use six key properties in the water samples to find out the minimum of residual and finally to determine the contribution of each water mass in the GLODAP v2 observational data. Central waters, which are distinguished by high potential temperature and salinity and low nutrient concentrations, are the main water masses in the upper/central layer. In the intermediate layer, the Antarctic Intermediate Water (AAIW) with lowest salinity is formed in the south Atlantic sinks into ~1000m depth and spreads northward until ~30 °N. Mediterranean Overflow Water (MOW), identify by high salinity, flows from the Strait of Gibraltar and eastwards cross the Mid-Atlantic-Ridge. NADW, upper and lower, dominates the deep and overflow layer both in the North and South Atlantic. This water mass is formed in high latitude region in the North Atlantic and spreads southward at pressure ~ 2000m until meets AAIW and AABW at ~ 50 S. In the bottom layer, AABW is the only natural water mass (After passing the equator, AABW is redefined as NEABW) with high silicate signature spreading from the Antarctic to the North Atlantic in the bottom.

2.2 Measurement of Transient Tracers

Data of transient tracers (CFC-12 and SF_6) based on GLODAPv2 dataset were taken and measured throughout the pass decades. Electron capture-gas chromatography is in general used in the measurements of transient tracers and purge-and-trap techniques is the typically way to analyze the seawater samples (Bullister and Tanhua, 2010; Bullister and Weiss, 1988). Water samples are transferred from the sampling containers (syringes or ampoule) into the glass chamber are then purged with a flow of nitrogen in order to make dissolved tracers escape from water samples and collected in

a cryogenic trap. After the purging step, the trap is heated and the tracers swept into a chromatographic precolumn and main column and elute separately into the Electron Capture Detector (ECD). The peak areas displayed from the water samples will be compared with the peak areas of the standard gases (known concentration) and finally calculate the concentration of tracers in the water sample. Water samples are normally taken by syringes or ampoules and analyzed immediately on board and the rest samples are flame sealed and taken back to the lab.

2.3 Transit Time Distribution (TTD) and Inverse Gauss (IG) Distribution

Due to the mixing and diffusion in the ocean, it is difficult to measure the whole process in one timescale and the transit time distribution (TTD) is a required and composed by following parameters (Waugh et al., 2003):

Tracer age (c(t)) is the time that water mass takes from surface to the deeper layer.

$$\mathbf{c(t) = c_0(t - \tau);}$$

Mean age (Γ) shows the year in which the water mass is equilibrium to the atmosphere.

$$\mathbf{\Gamma = \int_0^\infty \xi G(\xi) d\xi;}$$

Width (Δ^2) describes the mixing and the diffusion in the ocean.

$$\mathbf{\Delta^2 = \frac{1}{2}\int_0^\infty (\xi - \Gamma)^2 G(\xi) d\xi;}$$

The relationship between all the above parameters is often assumed to follow an inverse Gauss distribution:

$$\mathbf{G(t) = \sqrt{\frac{\Gamma^3}{4\pi\Delta^2 t^3}}\, exp(\frac{-\Gamma(t-\Gamma)^2}{4\Delta^2 t});}$$

In this equation t, Γ and Δ describes the tracer age, mean age and the width of TTD. The mixing ratio (Δ/Γ) indicates the advective (low ratio) or diffusive (high ratio) situation in the ocean and the detail will be illustrated in the next section.

3 Involved Definitions in the Water Mass Age Investigation

Due to complexities and similarities between definitions during the investigation of the water mass age and in order to avoid confusions, it is necessary to explain firstly the following definitions and to clarify the relationships between them before displaying the results.

3.1 The Mixing Ratio (Δ/Γ):

As mentioned in the above section, another topic is placed in front of us due to the advective or diffusive situations in the ocean: the determination of mixing ratio (Δ/Γ), where low ratio reflects advective while high ratio reflects diffusive situation. The choice of mixing ratio has significant impacts on the calculation of the ages. However, in such a large scale calculation as in the whole Atlantic Ocean, the mixing ratios can be totally different in different areas (for instance, in the North Atlantic upper NADW spreads along the DWBC without much mixing while in the southern ocean area a hard mixing with AAIW and AABW exists), a standard ratio of 1 might sometimes not be applicable for the general calculation, and the age of water mass need to be calculated in each specific area. These situations are common in the oceans since most water masses do not appear alone but two or more water masses mix with each other. Under such circumstance, IG-TTD for only one water mass appears to be insufficient and a further approach is required to determine the mixing ratio with the linear combination of distributions from all the water involved water masses (Ebser et al., 2018; Stöven and Tanhua, 2014). A theoretical overall value of mixing follows:

$$\Gamma = \alpha_1 \cdot \Gamma_1 + \alpha_2 \cdot \Gamma_2 + \ldots\ldots + \alpha_n \cdot \Gamma_n$$

Where α means the fraction of each water mass and $\alpha_1 + \alpha_2 + \ldots\ldots + \alpha_n = 1$ and Γ_n is the mixing of each water mass.

When the details of specific sea areas in a small-scale calculation, or when the area is very diffusive or convective (mixing ratio is far from 1), a corresponding values of the ratio (Δ/Γ) according to the specific situation is required, to obtain a more accurate results on ages of water masses. In fact, in most cases we still need a standard mixing ratio during the large-scale calculations, when we are unable to determine the specific conditions of the sea area or the fractions of the water mass. And a typical standard mixing ratio is set to be 1, if further information about the TTD is not available (Schneider et al., 2014; Waugh et al., 2004). The calculation about the mean age of water mass can still follow the common assumption and the ratio of Δ/Γ is set to be 1.0 (e.g. Schneider et al., 2010; Stöven and Tanhua, 2014; Waugh et al., 2004) since such a ratio is considered to be in large parts of the world ocean as standard a ratio (e.g. Huhn et al., 2013; Schneider et al., 2014). In this chapter, a standard mixing ratio ($\Delta/\Gamma = 1$) is used.

3.2 Partial Pressure (ppt) and the Ages of Water Mass (Tracer Age, Mean Age and Mode Age)

After determining the mixing ratio, the calculation of ages can be started according to the equations in section 2. Firstly, the concentrations (μmol/kg) of tracers are measured from the observation and partial pressures in ppt can be calculated directly combining with potential temperature, salinity and the sampling year. And finally, the ages of water masses can be estimated from partial pressure. In other words, partial pressure is the first-hand data we can get directly, and the following estimations,

the ages of the water masses, are derived from it. Refer to the ages of the water mass, the most intuitive definition is the tracer age which shows the consuming time on the way from start to destination. However, the tracer age considers the ocean as a totally advective situation but ignores the diffusion in the ocean. As a result, the tracer age shows an ideal state rather than the actual state, and underestimates the actual age of the water mass. Therefore, we need to introduce two more concepts, the mean age and the mode age. From the mathematical definition, mode age is the value of t when G(t) researches the maximum while mean age is the mean value of t in the whole Inverse Gauss Distribution. (Details about Inverse Gauss Distribution and TTD of tracers are described in Chapter I.) From the physical perspective, the mean age refers to static states and the mode age refers to dynamic states. In other words, the mean age is used to show the mean state of water masses, while mode age is a better choice to show the signals or phenomena in the ocean, for instance the transfer velocity. Relationships between tracer age, mean age and mode age are shown in Fig 3.0.

The IG-TTD between mean ages and mode ages under a fixed partial pressure are shown in Fig 3.1 a) and b). The assumption is that the saturation is set to be 100% in the year 1990, the differences between partial pressures of CFC-12 from 250 and 300 ppt are displayed. In general, both mean age and mode age decrease with partial pressure since the concentration of CFC-12 increase monotonically in the atmosphere until late 1990s (detail in Chapter I). Under the same partial pressure, the mean age increases with mixing ration while the mode age decreases. This is because in the IG-TTD distribution, when the mixing ratio increases, the 'tail' becomes longer the mean age becomes higher, but on the other hand, the 'peak' appears earlier so the mode age becomes lower.

Under a fixed mixing ratio (for instance: Δ/Γ = 1), the mode ages increase with the mean ages (Fig 3.1 c). However, the mode ages are also affected by the mixing ratios (Δ/Γ) on the other hand. As shown in Fig 3.1 d), under the same mean age (for instance: 100 years) but depending on different mixing ratios (Δ/Γ), the mode ages can be very different. The general trend is that the mode ages decrease with mixing ratios.

In addition to the above theoretical description, the significance of mixing ratios can also be obviously seen in the calculations of actually cruises. The situation between mean ages and mode ages in the Atlantic Ocean is shown in the A16 section of Fig 3.2. Both mean ages and the mode ages are closely related to the choice of mixing ratio (Δ/Γ). However, the mean ages increase with the value of mixing ratio, while the mode ages decrease. In the relative advective case Δ/Γ = 0.5, mean ages and mode ages both range from 0 to 200 years. The situation become very different in the diffusive case with Δ/Γ = 1.5, the mean ages range from 0 to as high as 800 years, while the mode ages range from 0 to only 50 years. In our standard case (Δ/Γ = 1.0), mean ages are located between 0 and 500 years compared with mode ages between 0 and 100 years.

4 Results: Distribution of Transient Tracers and Mean Ages

Partial pressure of CFC-12 and SF_6 shows similar distributions and, as mentioned above, mean age is used to show the distributions. In general, partial pressures of both tracers have high values in shallow depth and increase with pressure while the situation of mean ages is just the opposite. In the upper/central layer and the shallow part of the intermediate layer close to the boundary, partial pressure of CFC-12 and SF_6 have highest values with ~500 and ~10 PPT. This indicates water masses have the lowest mean ages within ~50 years. In the deeper layers, where low partial pressures appear and even close to 0, mean ages reach values close to 500 years. In high latitude region in the North Atlantic, where NADW is formed and sinks, partial pressures show relative higher in deep and overflow layer compared with the same latitude in the southern hemisphere. This represents newly formed water mass (NADW) sinks with lower mean age. Combining with the previous work in Chapter III, mean ages of water masses can be clear at a glance.

4.1 The Upper Layer

WNACW, ENACW, WSACW, ESACW

As described in the previous two chapters, water masses in upper/central layer are formed by subduction from mixed layer water during winter convection and are in general distributed with core pressure at potential density (σ_θ) around 26.4 (west central waters) and 26.8 (east central waters) kg/m^3.

Compared to deeper water in other layers, mean ages of central waters have the lowest (within ~50 years) mean ages, since they did not experience complicate spreading processes during their formations and transports. In vertical scale, central waters are located only in shallow layer within ~1000m and their mean ages increase with pressure. In horizontal scale, mean ages show low values in the mid-latitude while high values in the tropical regions. Such distributions of mean ages are determined by formation areas and transports of central waters (SWTs and currents). In shallower pressure, where both WNACW and WSACW are distributed (σ_θ= ~26.4 kg/m^3), mean ages in mid-latitude region (near formation area) have low values (within 10 years) and in tropical region (spread with currents) are relative higher (between 30 and 40 years). In relative deeper pressure, where ENACW and ESACW are distributed (σ_θ= ~26.8 kg/m^3), the situation is similar but differences in mid-latitude region and in tropical region are more obvious.

This result shows the direction and transfer time of each water mass in the upper/central layer. After leaving their formation areas, WNACW and WSACW spread general in zonal region and towards the formation areas of ENACW and ESACW separately along Azores Current and South Atlantic Current. This process lasts for within 20 years. In relative deeper pressure, ENACW and ESACW start from their formation areas and spread along the currents towards the equator. In the north hemisphere,

ENACW spreads southward with Canaries Current while ESACW in the south hemisphere spreads northward with Benguela Current and South Equatorial Current. About 50 years are taken from their formation area until they reach the equatorial region.

4.2 The Intermediate Layer

AAIW

The north flow of AAIW is classified to the upper limb of AMOC (Kirchner et al., 2009) and Atlantic western boundary current system (Talley, 1996). In general, AAIW is transported northward along the path way of Gulf Stream -- North Atlantic Current and spreads also eastward during the way to the north (Piola and Gordon, 1989; Tsuchiya, 1989).

Compared to central waters, the northward transport of AAIW takes much longer time. Totally ~400 years are required from formation area to the north limit at ~40 °N. In the meridional investigation of A16 cruise in 2013, ~50 years are taken from formation area at surface until sinking to the core pressure (~1000m). This phase takes place between 60 and 40 °S. The process of spreading northward between 40 and 20 °S takes ~100-150 years (from the origin) and ~200-300 years to equator. In total, AAIW takes ~400 years from the origin (in formation area) until reaches the north limit. Zonal investigation of A10 and A05 cruise also provide supports to these results. A10 section at ~30 °S shows mean age ~100 years in the core of AAIW. AAIW can also be found with ~350 years mean ages in A05 cruise at ~27 °N.

Regarding to the north limit of transport, still no unified statement can be found in the relevant literatures but most show between them 20 °N and 60 °N (e.g. Tsuchiya, 1989). During the investigation of GLODAPv2 data set, the north limit of AAIW is ~40 °N based on all the observational data but for also different in each cruise. (For example: A16 cruise in 2005 shows AAIW reaches ~40 °N but in 2013 AAIW reaches only ~ 10 °N).

MOW

The mixture of three parts, pure Mediterranean Sea Water that overflows across the Strait of Gibraltar, Eastern North Atlantic Central Waters (ENACW) and Subarctic Intermediate Water (SAIW), is defined as the Mediterranean Overflow Water (MOW) in Chapter I. This water mass is formed in the east of the Gulf of Cadiz where Mediterranean Water exits the Strait of Gibraltar as a deep current and then turns into two branches after leaving the formation area. One branch spreads to the north into the West European Basin until ~50°N, the other branch spreads to the west and past the Mid-Atlantic-Ridge (Carracedo et al., 2016; Price et al., 1993). Distribution of this water mass can be seen in mostly the entire North Atlantic by recognizing its high salinity (Chapter II).

Westward transport of MOW, accompanied by spreading to the north and south at the same time, is a process that takes ~300 years. In zonal direction based on A05 cruise, original MOW is starts from Strait of Gibraltar, across the Mid-Atlantic-Ridge and enters the western North Atlantic. In meridional direction, MOW spread both north and southwards. Due to the influence of currents, the northward flow goes faster and takes within ~200 years until ~50 °N, while the southward flow takes a relative longer time, between ~300 and 400 years to the region near equator.

4.3 Deep and Overflow Layer

Upper and lower NADW

Upper and lower NADW are the main water masses in deep and overflow layer, meanwhile, southward transport of NADW constitutes the deep/cold limb of the AMOC. The main route of the southward transport of NADW is DWBC. And during the pathway to the south, NADW expands eastward by eddies and further cover the most of Atlantic Ocean in deep layer (σ_θ between 27.7 and 27.88 kg/m^3) (Dickson and Brown, 1994).

Southward transport of NADW is in general a long process with mean ages ~500 years. In meridional scale, upper and lower NADW are located at pressure ~1000 — 2000m and ~2000 — 4000m separately. Mean ages of NADW increase with the process of spreading south. After leaving formation area, ~100 years are takes from 60 to 40 °N, ~300 years (from the origin) from 40 to 20 °N and ~400 years 20 °N to 20 °S. In the region south of 20 °S, especially 40 °S, upper and lower NADW meet and mix with AABW, which has lower mean ages in this region, so the mean ages decrease slightly to ~300 years at their junction. In horizontal scale, mean ages show low values in the west basin near DWBC while high values in the east. In A05 section, 200 years in the west 400 years in the east. In A10 section, mean ages are ~300 years but the difference between west and east is not obvious.

Such a mean age distribution provides evidence for the southward transport of NADW. Upper and lower NADW spread general to the south from ~60 °N until ~ 40 °S with Deep Western Boundary Current. This process lasts ~400 years. In zonal direction, NADW spreads eastward by eddies.

4.4 Bottom Layer

AABW & NEABW

AABW, the main water masses in the bottom layer, receives extensive and sustained attentions. As early as in Wüst (1933), the bottom layer is noticed out as filled with water origins from the south. Sverdrup further pointed out the role of ACC plays in the formation and transport of AABW (Sverdrup, 1940). On this basis, Mantyla and Reid (1983) further elaborated that the most original dense bottom water is restricted near the Antarctic region by topography and the northward flow of bottom water is the mixture of original dense water and the overlying warm water. Gordon and Huber

(1990) and Orsi et al. (1999) illustrated the pathway of AABW to the north is through the Drake Passage sill into the Argentina and Brazilian Basin.

Northward transport of AABW, as well as southward NADW, is another large time scale process with mean ages ~500 years. In meridional direction based on A16 cruise, original dense AABW is mostly limited within 40 °S and the mean age is within 200 years. The mixture with overlying NADW to the north until equator has mean ages ~300 – 40 0years. After passing the equator, newly defined NEABW has mean ages ~400-500 years. In zonal direction, AABW has mean ages ~200 — 250 years at A10 section near 30 °S and the difference between the east and the west is not obvious. However, in the north hemisphere, NEABW in the west is obviously younger than the east.

5 Results: Mode Ages and Transport Velocities based on Transient Tracers

Understanding of the velocities and durations of water masses transport, as well as the AMOC in the whole Atlantic Ocean, is thus of importance for regional and global climate. The flow velocity in the horizontal direction is can be measured directly by the equipment, however such a result is a kind of snap-shoot velocity, that means a specific velocity during the specific measuring time but without universally representative. The measurement of a general transport velocity of a water mass during a relative long time requires transient tracers. In this chapter, the transport velocities of upper NADW, which origins from LSW, on the way to the south are estimated based on the investigation of CFC-12 and SF_6 and the mode ages are used instead of mean age in displaying the velocities because velocity is a ‘‘dynamic phenomenon’’.

As described in previous chapters, upper NADW is formed in the high latitude region near Labrador Sea in the North Atlantic and spreads southward through the most entire Atlantic Ocean along the Deep Western Boundary Current (DWBC). In this chapter, parts from three cruises are selected and spliced to display the transport velocity during the pathway in the region along DWBC to show the main transport of upper NADW to the south and estimate the transport velocity (Fig 5.1 a).

In the first part of the cruise from A22 section in 2000, the upper NADW spreads from ~40 °N to ~15 °N. During this stage, the mode age of our target water mass increases along the path to the south until ~25 years near the equator. This cruise starts near the formation area of NADW and shows the early stage of upper NADW from forming, sinking and spreading southward. The mode age increases with southward transmission (Fig 5.2 a1) with a transport velocity of ~0.83 cm/s (Fig 5.2 a2). Compared to the other two stages, mean ages in this stage is relatively low and the boundaries between other water masses (central water from the above and lower NADW from the bottom) are also relative clear. The linear distribution of mode age with distance shows that DWBC flows southward smoothly without much external interference or retard. However, the velocity might be under estimated due to the under estimation of transport distance. The A22 cruise went straightly southward while the DWBC

went approximately along the continental slope of eastern North American coast so that the actual transport distance (calculated according to the distance on the map) may be ~1.2 of the distance observed from A22 cruise. Therefore, the actual transport velocity could be ~1.0 cm/s.

The second part of the cruise from AR04 section in 2003 lasts from ~15 °N to ~20 °S and the mode ages during this stage/cruise maintains between ~20 and ~30 years. At the beginning of this stage, from ~15 °N to the equator (distance from 0 to ~2200 km), the upper NADW continues the smooth transmission as in the stage 1 with a similar velocity of ~ 0.94 cm/s and shows a linear distance -- mode age distribution, but this situation changes after upper NADW passes the equator (Fig 5.2 b). After passing the equator, the flow of DWBC which carries upper NADW becomes more complicated due to a change of sign in planetary vorticity and DWBC breaks up into anticyclonic coherent eddies (Dengler et al., 2004). As a result, the distribution of mode age shows an irregular distribution instead of the linear with distance before, so the transport velocity cannot be calculated as a whole process.

The third cruise (A17 section in 1994) takes place between equator and 50 °S. In this region, the upper NADW embeds into the space between AAIW and AABW. The mixture between these water masses is intense due to the Antarctic Circumpolar Current (Details refer to Chapter III and van Heuven et al. (2011)). The fraction of upper NADW involves in this cruise/stage goes lower to the south and is mixed with AAIW from the above and AABW from the bottom. The result shows a relative large range of mode ages from 0 to ~40 years and the velocity of upper NADW shows a negative value. This does not mean the upper NADW turns back to north, but because the hard mixing with newly formed AAIW and AABW leads to low mode ages in the south, the actual velocity cannot be calculated by transient tracers.

The selected three parts from different cruises are as close as possible to the region of DWBC, along which the upper NADW spreads to the south, but still cannot follow the pathway of DWBC strictly. Therefore, the result from the above calculation could be deviated from the actual transport velocity. Another difficulty in estimating the overall or average velocity of a water mass during a long transport process comes from the complex situations in the ocean (for instance: different mixing ratios or mixing with other water masses) so that the transport velocities of one water mass during the pathway can also be very different (for instance: the AR04 cruise in stage 2). In this case, we need to focus on the transmission in specific sea areas, or specific stages and a relatively complete transmission process can be spliced according to each stage.

6. Conclusion

In this chapter, ages, including mean ages and mode ages, of main water masses in the Atlantic Ocean and the mean transport velocity of upper NADW are investigated combining with the characteristics and distributions of water masses described in previous chapters. Based on the transient tracers (CFC-

12 and SF_6), mean ages of these water masses observed from meridional (A16) and zonal (A05 and A10) cruises in the Atlantic Ocean are estimated with the assumption that standard mixing ratio ($\Delta/\Gamma = 1$) and a saturation of 100%. In general, mean ages increase with pressure and the central waters have the lowest mean ages within 50 years. In the intermediate layer, AAIW and MOW show gradients of mean ages in the meridional (south to north) and zonal (east to west) direction respectively. The transport time of AAIW is ~400 years from formation area to the north boundary at ~20 °N while it takes MOW ~300 years from the Strait of Gibraltar across the Mid-Atlantic-Ridge to the west basin of North Atlantic. As the main water mass in the deep and overflow layer, NADW (both upper and lower), which is formed in the high latitude region in the North Atlantic, sinks and transports to the south until ACC region at ~ 50 °S. Bottom waters, including AABW and NEABW, have the same origin in the Antarctic region and take ~500 years to spread to the north boundary at ~50 °N.

Velocities of water masses can be estimated with mode ages based on CFC-12 and SF_6 and upper NADW is investigated as the example. The southward transport of upper NADW is formed by three stages. From ~40 °N to ~15 °N, which takes within 25 years, is the early stage and shows the forming, sinking and early south spreading of upper NADW. In the second stage from ~15 °N to ~20 °S, At the beginning of this stage, upper NADW continues the smooth transport until the equator, while the DWBC breaks into eddies from DWBC brings the upper NADW to the east. The last stage takes place between 20 °S and 60 °S and the fractions of NADW is mostly not higher than 50% in this region due to the hard mixing.

References

Bjerknes, J., 1964. Atlantic air-sea interaction, Advances in geophysics. Elsevier, pp. 1-82.

Bryden, H.L., Longworth, H.R., Cunningham, S.A., 2005. Slowing of the Atlantic meridional overturning circulation at 25 N. Nature 438, 655.

Bullister, J., Tanhua, T., 2010. Sampling and measurement of chlorofluorocarbons and sulfur hexafluoride in seawater.

Bullister, J., Weiss, R., 1988. Determination of CCl3F and CCl2F2 in seawater and air. Deep Sea Research Part A. Oceanographic Research Papers 35, 839-853.

Carracedo, L., Pardo, P.C., Flecha, S., Pérez, F.F., 2016. On the Mediterranean Water Composition. Journal of Physical Oceanography 46, 1339-1358.

Clark, P.U., Shakun, J.D., Baker, P.A., Bartlein, P.J., Brewer, S., Brook, E., Carlson, A.E., Cheng, H., Kaufman, D.S., Liu, Z., 2012. Global climate evolution during the last deglaciation. Proceedings of the National Academy of Sciences 109, E1134-E1142.

Dengler, M., Schott, F.A., Eden, C., Brandt, P., Fischer, J., Zantopp, R.J., 2004. Break-up of the Atlantic deep western boundary current into eddies at 8° S. Nature 432, 1018.

Dickson, R.R., Brown, J., 1994. The Production of North-Atlantic Deep-Water - Sources, Rates, and Pathways. J Geophys Res-Oceans 99, 12319-12341.

Ebser, S., Kersting, A., Stöven, T., Feng, Z., Ringena, L., Schmidt, M., Tanhua, T., Aeschbach, W., Oberthaler, M., 2018. $^{39} $ Ar dating with small samples resolves ocean ventilation. arXiv preprint arXiv:1807.11146.

Ganachaud, A., Wunsch, C., 2000. Improved estimates of global ocean circulation, heat transport and mixing from hydrographic data. Nature 408, 453.

Gordon, A.L., Huber, B.A., 1990. Southern Ocean winter mixed layer. Journal of Geophysical Research: Oceans 95, 11655-11672.

Hall, M.M., Bryden, H.L., 1982. Direct estimates and mechanisms of ocean heat transport. Deep Sea Research Part A. Oceanographic Research Papers 29, 339-359.

Huhn, O., Rhein, M., Hoppema, M., van Heuven, S., 2013. Decline of deep and bottom water ventilation and slowing down of anthropogenic carbon storage in the Weddell Sea, 1984–2011. Deep Sea Research Part I: Oceanographic Research Papers 76, 66-84.

Kirchner, K., Rhein, M., Huttl-Kabus, S., Boning, C.W., 2009. On the spreading of South Atlantic Water into the Northern Hemisphere. J Geophys Res-Oceans 114.

Kuhlbrodt, T., Griesel, A., Montoya, M., Levermann, A., Hofmann, M., Rahmstorf, S., 2007. On the driving processes of the Atlantic meridional overturning circulation. Reviews of Geophysics 45.

Mantyla, A.W., Reid, J.L., 1983. Abyssal characteristics of the World Ocean waters. Deep Sea Research Part A. Oceanographic Research Papers 30, 805-833.

Orsi, A.H., Johnson, G.C., Bullister, J.L., 1999. Circulation, mixing, and production of Antarctic Bottom Water. Prog Oceanogr 43, 55-109.

Piola, A.R., Gordon, A.L., 1989. Intermediate Waters in the Southwest South-Atlantic. Deep-Sea Research Part a-Oceanographic Research Papers 36, 1-16.

Price, J.F., Baringer, M.O., Lueck, R.G., Johnson, G.C., Ambar, I., Parrilla, G., Cantos, A., Kennelly, M.A., Sanford, T.B., 1993. Mediterranean outflow mixing and dynamics. Science 259, 1277-1282.

Rahmstorf, S., 2000. The thermohaline ocean circulation: A system with dangerous thresholds? Climatic Change 46, 247-256.

Rahmstorf, S., Crucifix, M., Ganopolski, A., Goosse, H., Kamenkovich, I., Knutti, R., Lohmann, G., Marsh, R., Mysak, L.A., Wang, Z., 2005. Thermohaline circulation hysteresis: A model intercomparison. Geophysical Research Letters 32.

Sandström, J.W., 1908. Dynamische versuche mit meerwasser.

Sandström, J.W., 1916. The hydrodynamics of Canadian Atlantic waters.

Schneider, A., Tanhua, T., Körtzinger, A., Wallace, D.W., 2010. High anthropogenic carbon content in the eastern Mediterranean. Journal of Geophysical Research: Oceans 115.

Schneider, A., Tanhua, T., Roether, W., Steinfeldt, R., 2014. Changes in ventilation of the Mediterranean Sea during the past 25 year. Ocean Science 10, 1-16.

Stöven, T., Tanhua, T., 2014. Ventilation of the Mediterranean Sea constrained by multiple transient tracer measurements. Ocean Science 10, 439-457.

Sverdrup, H., 1940. The currents of the Pacific Ocean and their bearing on the climates of the coasts. Science 91, 273-282.

Talley, L., 1996. Antarctic intermediate water in the South Atlantic, The South Atlantic. Springer, pp. 219-238.

Tanhua, T., Biastoch, A., Körtzinger, A., Lüger, H., Böning, C., Wallace, D.W., 2006. Changes of anthropogenic CO2 and CFCs in the North Atlantic between 1981 and 2004. Global biogeochemical cycles 20.

Toggweiler, J., Samuels, B., 1993. Is the magnitude of the deep outflow from the Atlantic Ocean actually governed by Southern Hemisphere winds?, The Global Carbon Cycle. Springer, pp. 303-331.

Toggweiler, J., Samuels, B., 1995. Effect of Drake Passage on the global thermohaline circulation. Deep Sea Research Part I: Oceanographic Research Papers 42, 477-500.

Trenberth, K.E., Caron, J.M., 2001. Estimates of meridional atmosphere and ocean heat transports. Journal of Climate 14, 3433-3443.

Tsuchiya, M., 1989. Circulation of the Antarctic Intermediate Water in the North-Atlantic Ocean. J Mar Res 47, 747-755.

van Heuven, S.M.A.C., Hoppema, M., Huhn, O., Slagter, H.A., de Baar, H.J.W., 2011. Direct observation of increasing CO2 in the Weddell Gyre along the Prime Meridian during 1973–2008. Deep Sea Research Part II: Topical Studies in Oceanography 58, 2613-2635.

Waugh, D.W., Haine, T.W., Hall, T.M., 2004. Transport times and anthropogenic carbon in the subpolar North Atlantic Ocean. Deep Sea Research Part I: Oceanographic Research Papers 51, 1475-1491.

Waugh, D.W., Hall, T.M., Haine, T.W., 2003. Relationships among tracer ages. Journal of Geophysical Research: Oceans 108.

Wüst, G., 1933. Das Bodenwasser und die Gliederung der atlantischen Tiefsee. W. de Gruyter.

Ziska, F., Quack, B., Abrahamsson, K., Archer, S., Atlas, E., Bell, T., Butler, J., Carpenter, L., Jones, C., Harris, N., 2013. Global sea-to-air flux climatology for bromoform, dibromomethane and methyl iodide. Atmospheric Chemistry and Physics 13, 8915-8934.

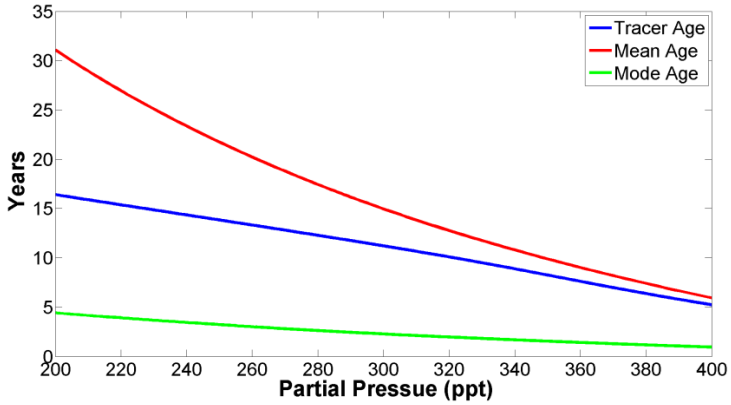

Fig 3.0 Concept of relationships between Tracer ages, Mean ages, Mode ages and Mixing ratios based on partial pressure of CFC-12 = 300 ppt under the assumption in the north hemisphere in the year 1990 and the saturation is 100%

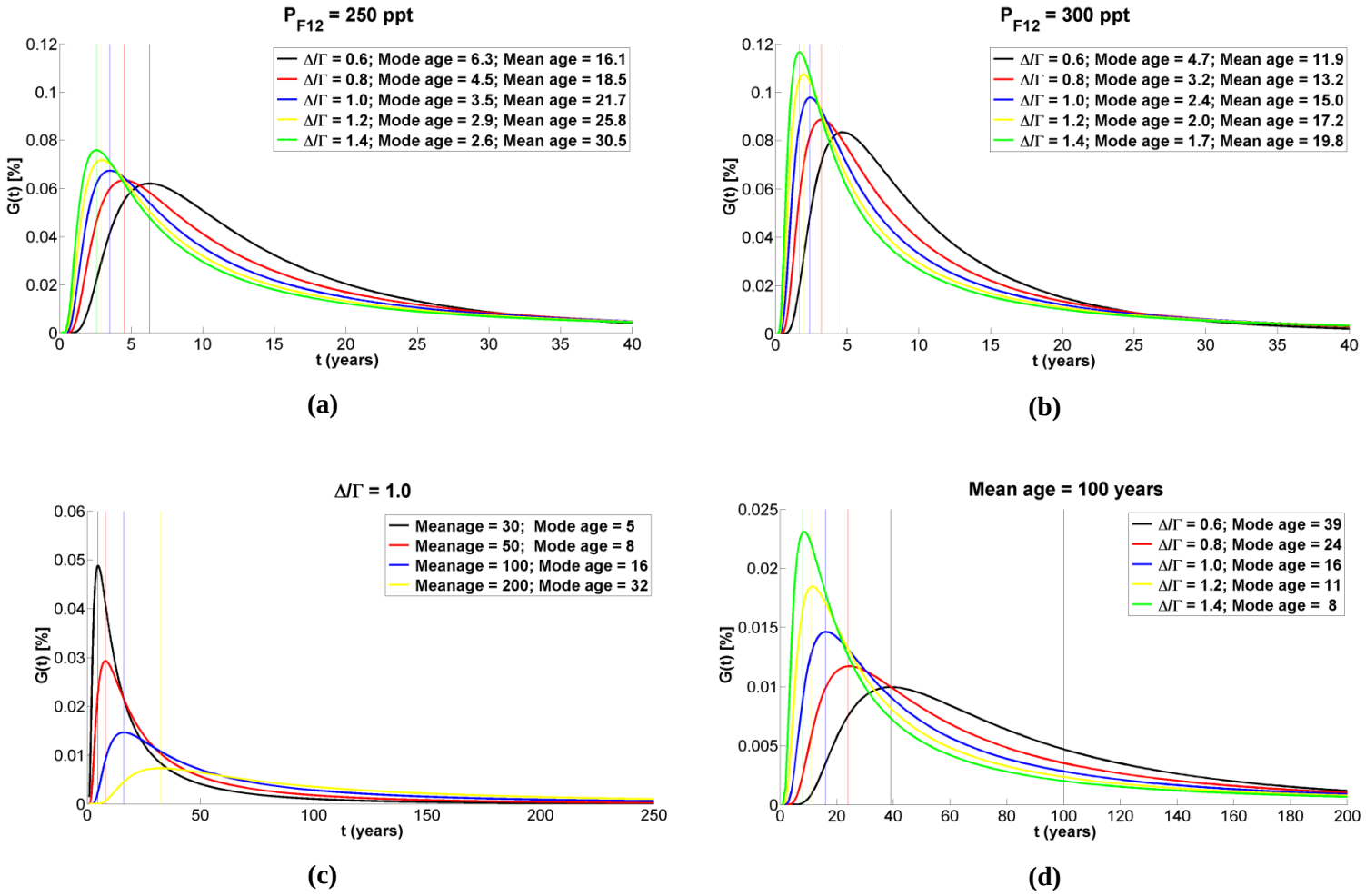

Fig 3.1 Concept of relationships between Tracers, Mean ages, Mode ages and Mixing ratios
(a) and (b)Relationship between Mode ages and Mean ages with the same tracer partial pressure (CFC-12 = 250 and 300 ppt) but different mixing ratio;
(c) Relationship between different Mode ages and Mean ages with the same Mixing ratio ($\Delta/\Gamma = 1$);
(d) Relationship between different Mode ages and Mixing rations with the same Mean age ($\Gamma = 100$ years);
The colored Inverse Gaussian lines show the TTD and the vertical lines show the Mode ages.

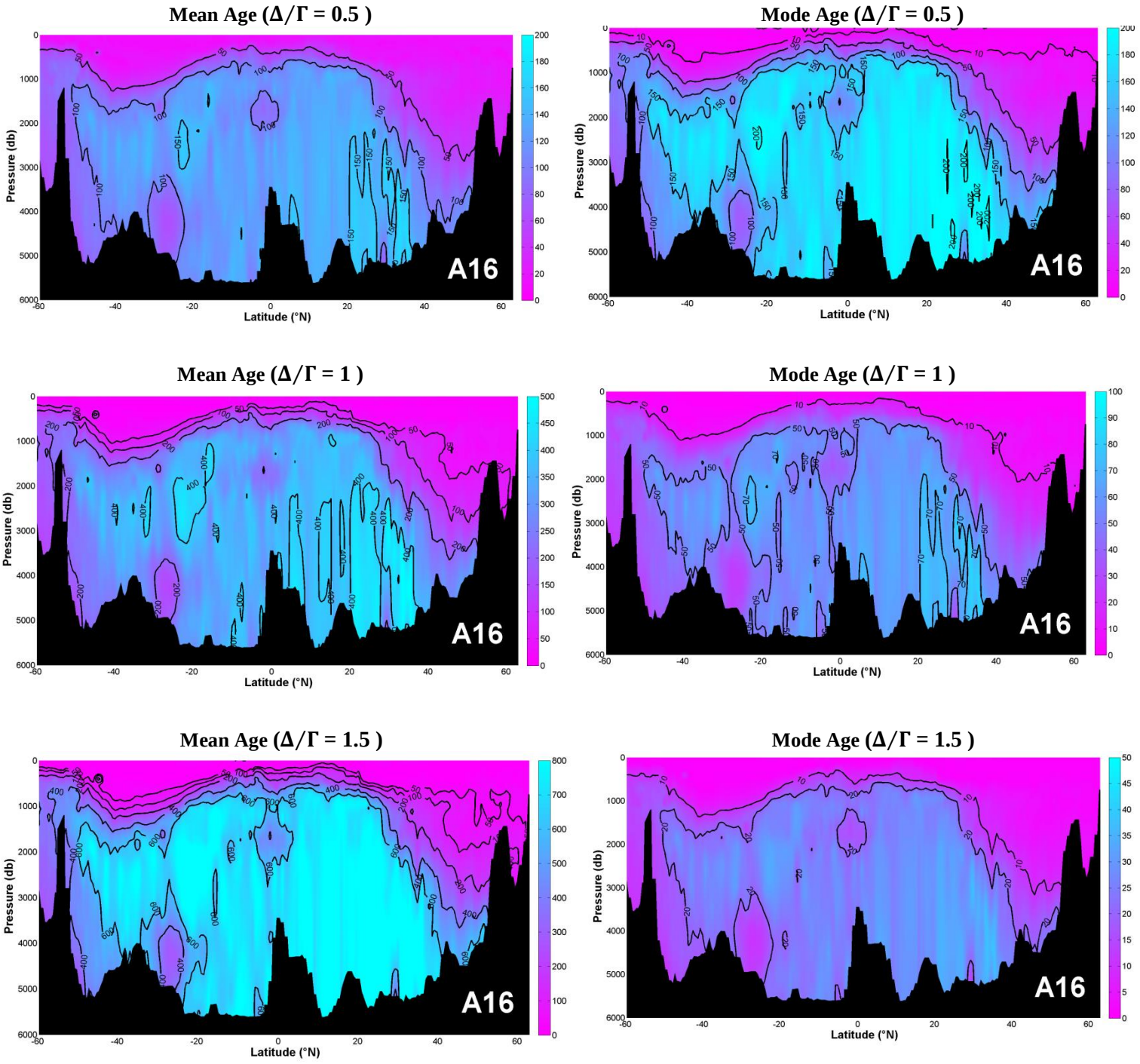

Fig 3.2 Mean Ages and Mode Ages with different mixing ratios (Δ/Γ) based on A16 cruise

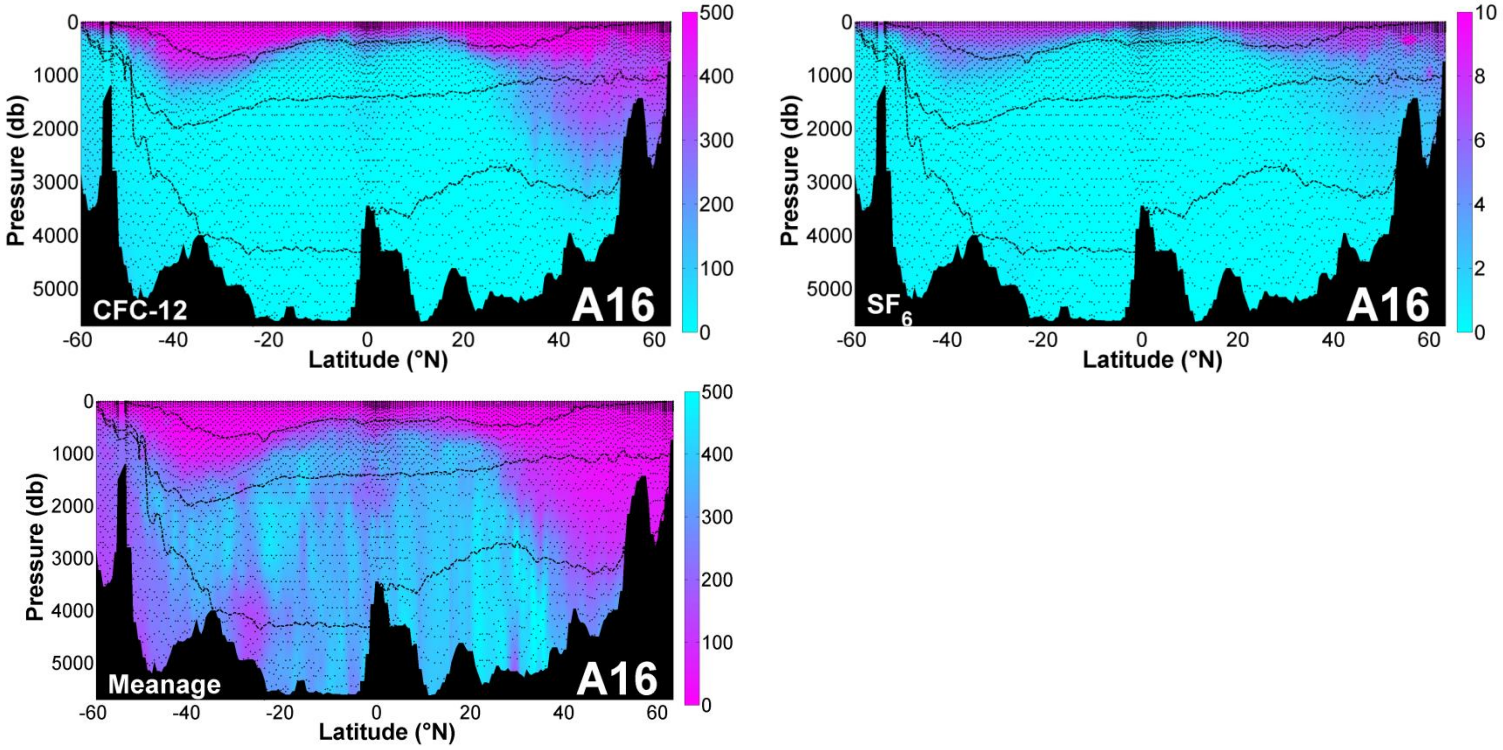

Fig 4.0 Partial pressure of CFC-12 and SF_6 (ppt) and Mean age (year) based on A16 cruise in 2013. Mean age is calculated from CFC-12 in 'old' water samples (partial pressure of CFC-12 < 450 ppt) and from SF_6 in 'young' water samples (partial pressure of CFC-12 > 450 ppt). The dached lines show four vertical layers of water columns and the black dots show sampling points.

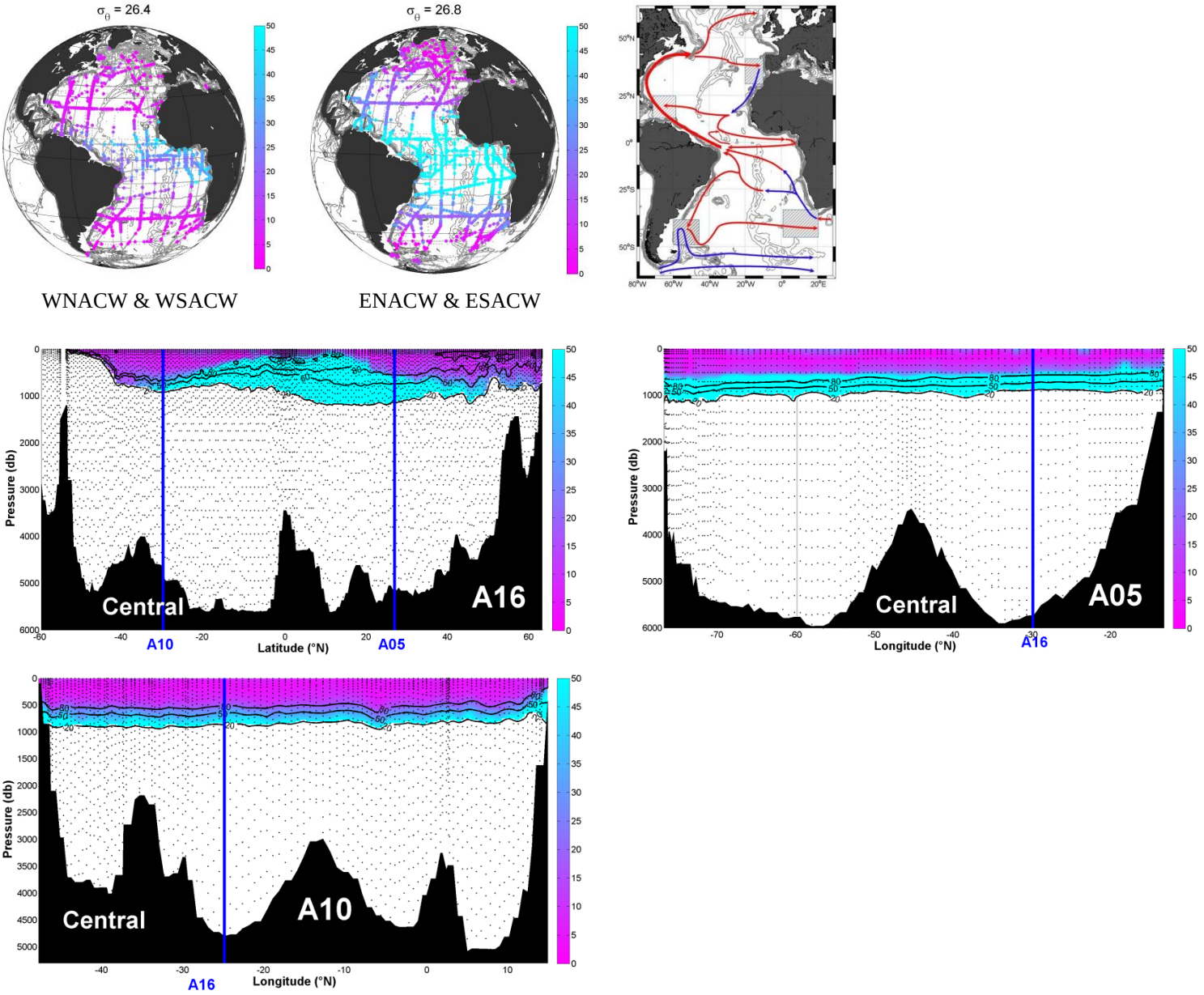

Fig 4.1 Mean ages of Central Water

Maps (upper plots) show mean ages of water masses and currents in their core potential density layer. Section plots (lower plots) show mean ages based on meridional (A16 cruise in 2013) and zonal cruises (A05 in 2008 and A10 in 2010).Blue lines show position of other cruises. Solid black contour lines show fraction of water masses with 20%, 50% and 80% and black dots show sampling points.

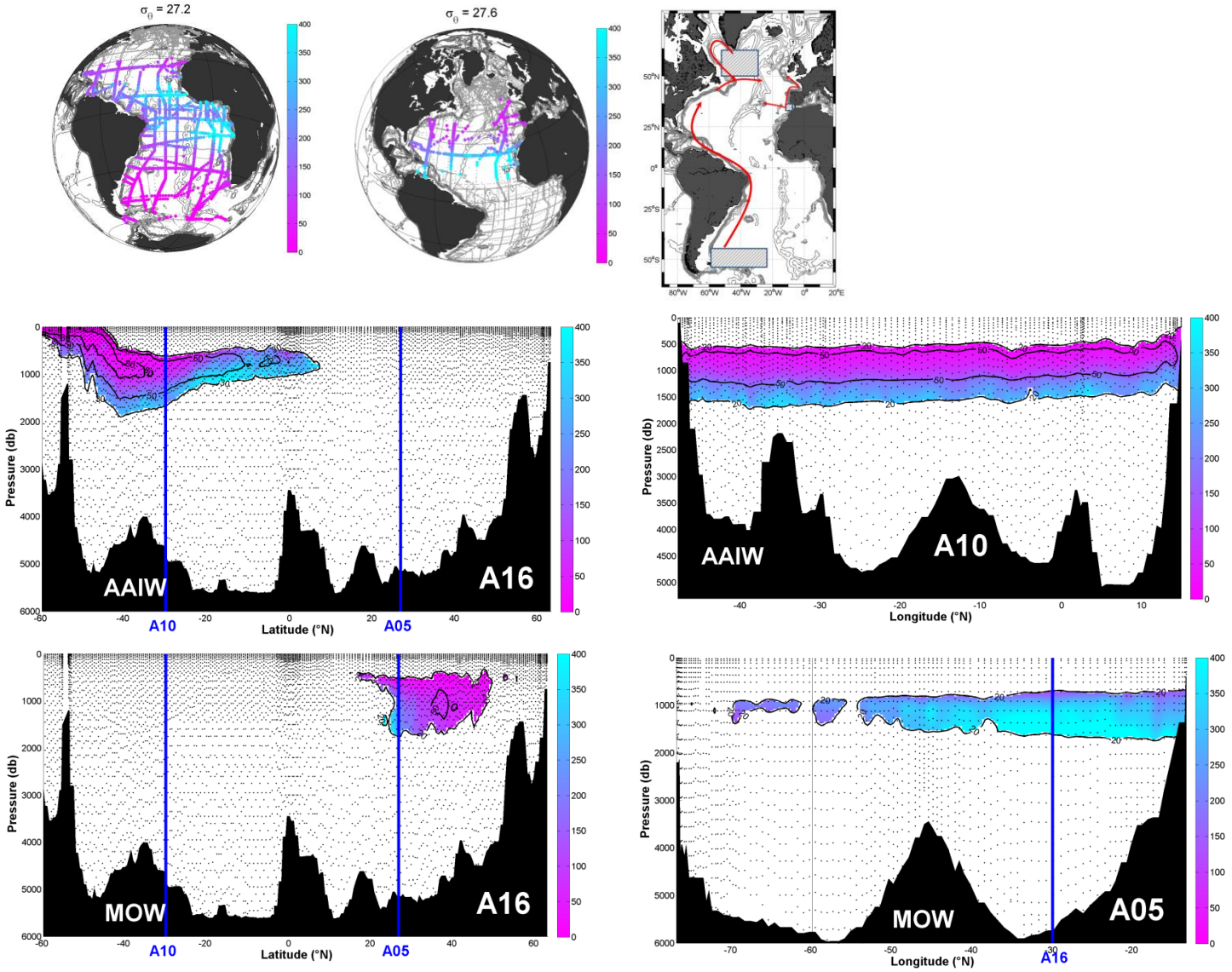

Fig 4.2 Mean ages of Water masses in the intermediate layer (AAIW and MOW)
Maps (upper plots) show mean ages of water masses and currents in their core potential density layer. Section plots (lower plots) show mean ages based on meridional (A16 cruise in 2013) and zonal cruises (A05 in 2008 and A10 in 2010).Blue lines show position of other cruises. Solid black contour lines show fraction of water masses with 20%, 50% and 80% and black dots show sampling points.

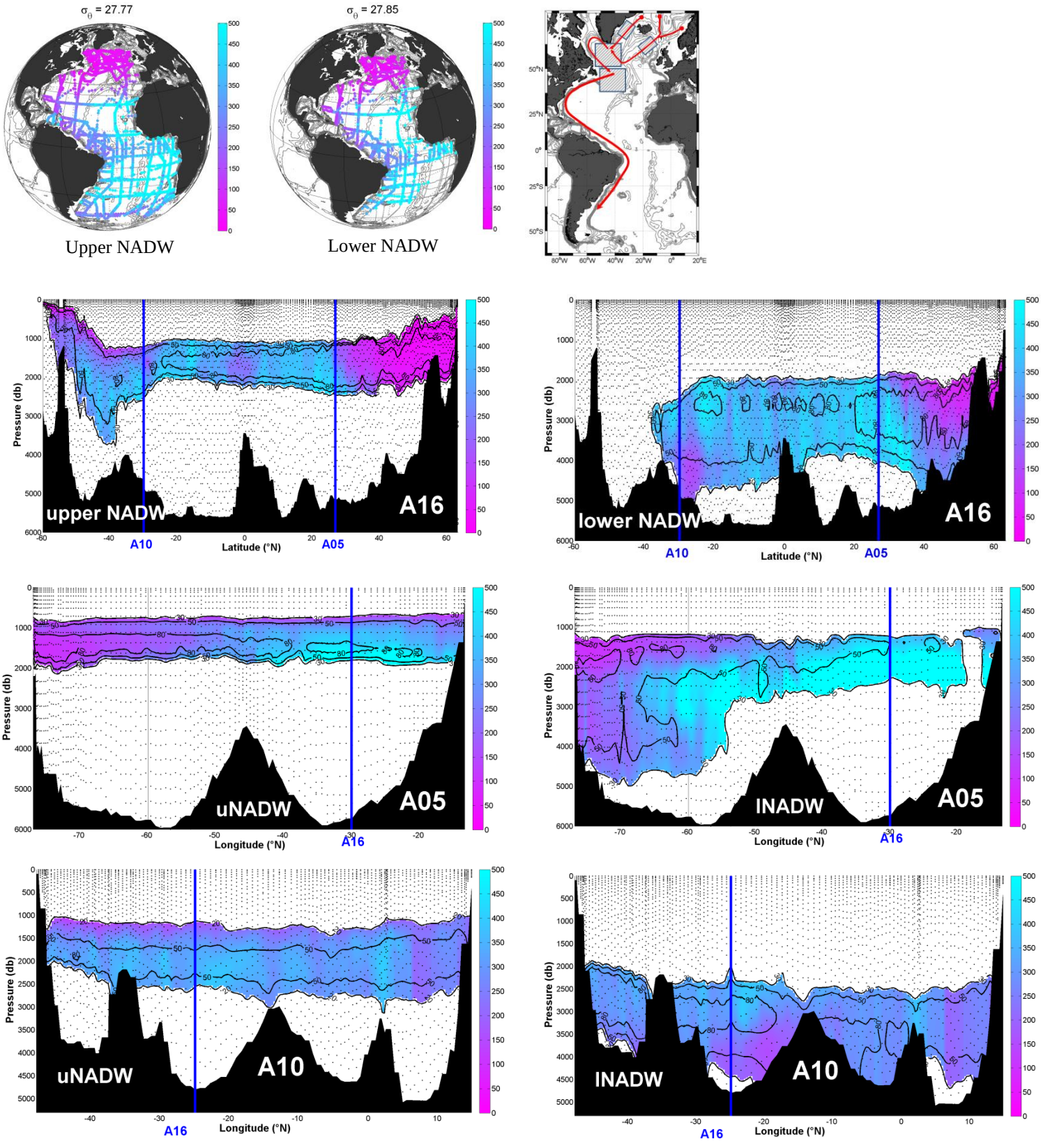

Fig 4.3 Mean ages of water masses in the deep and overflow layer (upper and lower NADW)
Maps (upper plots) show mean ages of water masses and currents in their core potential density layer. Section plots (lower plots) show mean ages based on meridional (A16 cruise in 2013) and zonal cruises (A05 in 2008 and A10 in 2010).Blue lines show position of other cruises. Solid black contour lines show fraction of water masses with 20%, 50% and 80% and black dots show sampling points.

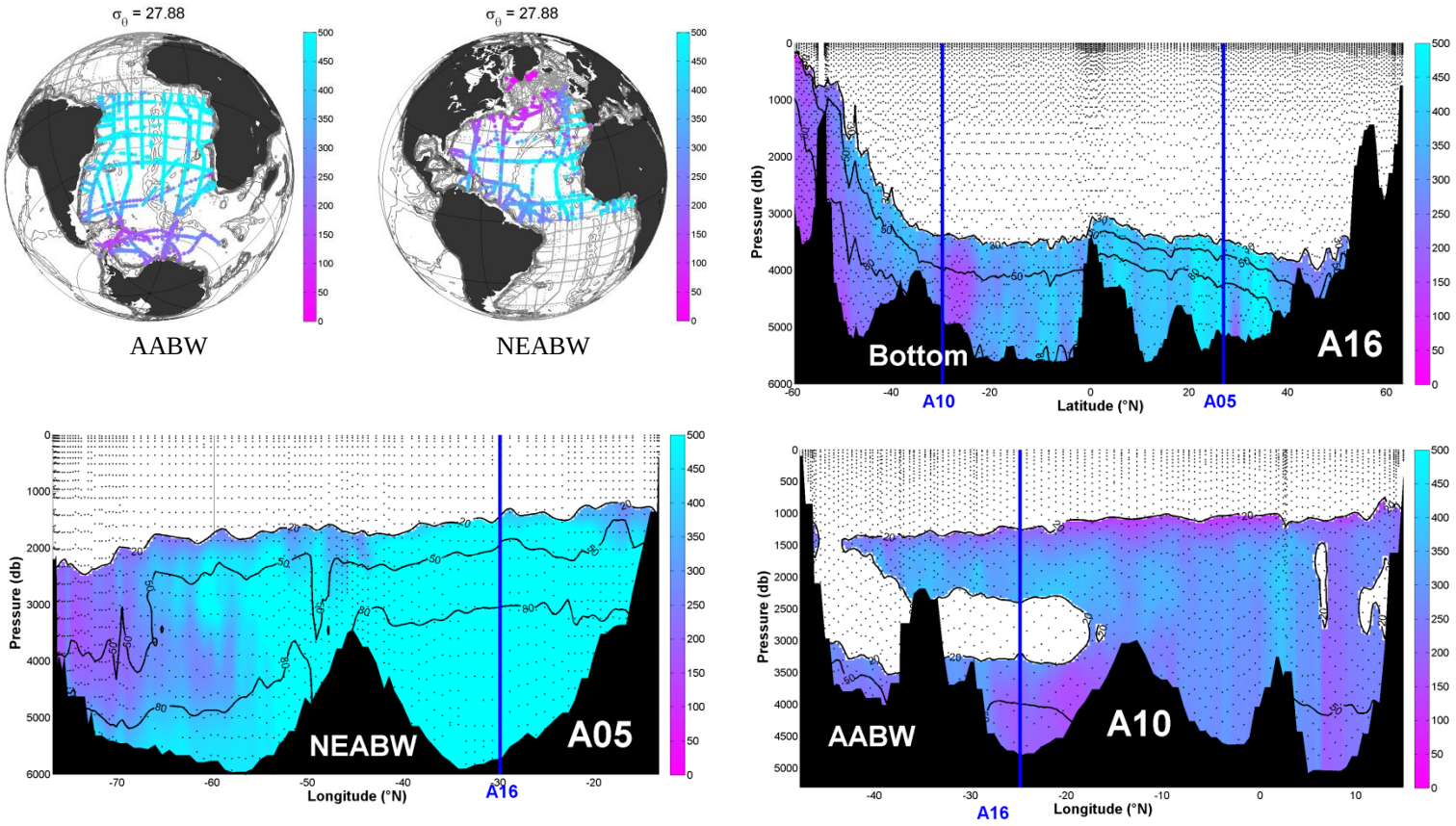

Fig 4.4Mean ages of Bottom Water (AABW and NEABW)
Maps (upper plots) show mean ages of water masses and currents in their core potential density layer. Section plots (lower plots) show mean ages based on meridional (A16 cruise in 2013) and zonal cruises (A05 in 2008 and A10 in 2010).Blue lines show position of other cruises. Solid black contour lines show fraction of water masses with 20%, 50% and 80% and black dots show sampling points.

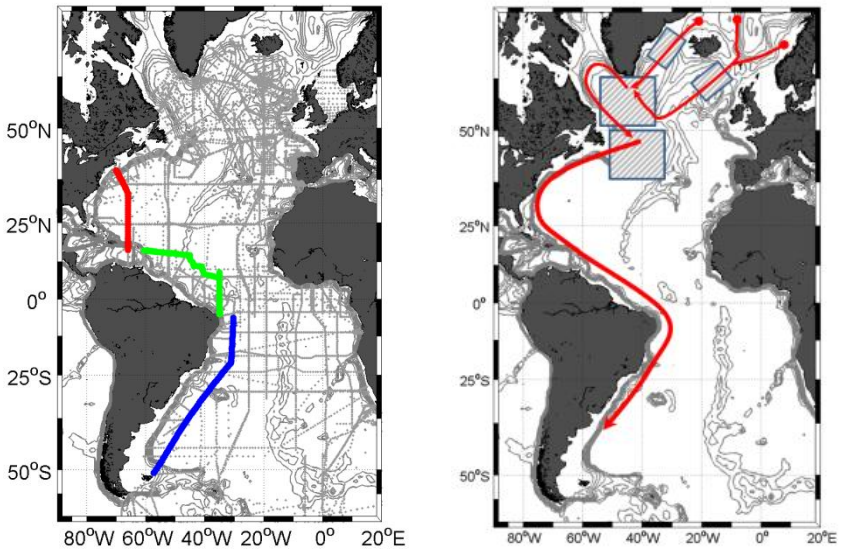

Fig 5.1 Map of three cruises in DWBC region (left) and the schematic of pathway of upper NADW to the south (right). The colored lines show A22 section in 2000 (red) AR07section in 2003(green) and A17 section in 2000 (blue).The grad dots show all the GLODAP samplidsng stations.

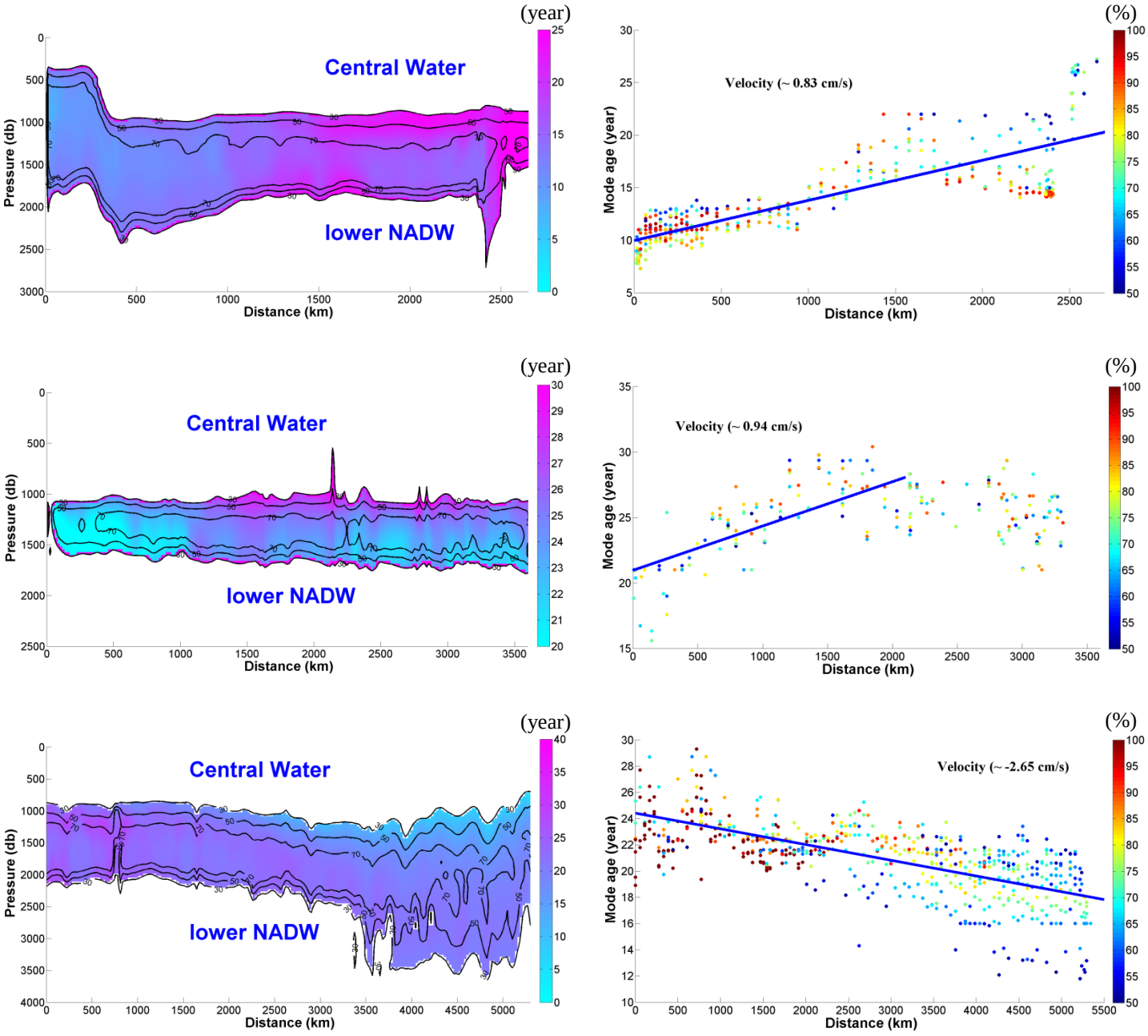

Fig 5.2 Plots of southward spreading of upper NADW (left) and Distance--Mean age distribution (right)
Left: The colorbar shows mean ages of upper NADW in each cruise and the contour lines show fraction of water masses with 30%, 50% and 70% and black dots show sampling points. The distance in X-Axis shows the distance from the first station of each cruise in the north.
Right: The color dots show the fractions of water mass in each water sample and the colorbar shows fraction of each water mass from 50-100% and the blue lines show linear fits calculated from fractions higher than 50%. The numbers show the average transport velocity in meters per day (cm/s) based on the linear fit.